Slope Stability Assessment on a Critical Rock Slope Section around Alem Ketema, North Shoa, Ethiopia

Dawit Asmare Manderso

A Thesis Submitted to

School of Earth Sciences

Presented in Partial Fulfillment of the Requirements for the Degree of Master of Science (Engineering Geology)

ADDIS ABABA UNIVERSITY
Addis Ababa, Ethiopia
MAY, 2018

Slope Stability Assessment on a Critical Rock Slope Section around Alem Ketema, North Shoa, Ethiopia

Dawit Asmare Manderso

A Thesis Submitted to

School of Earth Sciences

Presented in Partial Fulfillment of the Requirements for the Degree of Master of Science (Engineering Geology)

ADDIS ABABA UNIVERSITY

Addis Ababa, Ethiopia

MAY, 2018

Signature Page

Addis Ababa University

School of Graduate Studies

This is to certify that the thesis prepared by Dawit Asmare entitled: *Slope Stability Assessment on a Critical Rock Slope Section around Alem Ketema, North Shoa, Ethiopia* and submitted in partial fulfillment of the requirements for the Degree of Master of Science (Engineering Geology) complies with the regulations of the University and meets the accepted standards with respect to originality and quality.

Signed by the Examining Committee:

Examiner _____ Signature _____ Date _____

Examiner _____ Signature _____ Date _____

Advisor _____ Signature _____ Date _____

Co-Advisor _____ Signature _____ Date _____

_____

Chair of School or Graduate Program Coordinator

Abstract

Slope Stability Assessment on a Critical Rock Slope Section around Alem Ketema, North Shoa, Ethiopia.

Dawit Asmare Manderso

Addis Ababa University, 2017

The present research was carried out in an area around Alem ketema town, North Showa, central Ethiopia; with a general objective of conducting a rock slope stability assessment on the selected natural rock slope sections. To achieve this objective, slope stability probability classification and geological strength index approaches were followed to determine the stability probability conditions of slope rock mass in the study area. These classification systems mainly depend on the primary data collected from field works. As a reason, systematic and extensive field work was conducted. However, secondary data was also required in order to characterize the general conditions of the study area and to have a deep understanding on the subject matter. In SSPC system, ratings for degree of weathering, intact rock strength, method of excavation, roughness condition and infill material were given according to standards.

The SSPC system uses three step classification systems (exposure rock mass, reference rock mass and slope rock mass). Following these steps, slope rock mass stability probability classifications have been carried out for 92 natural slope sections. The stability of slope rock mass were determined by two different approaches namely orientation dependent and orientation independent stability. Orientation dependent stability related to orientation of the discontinuities and characterized by toppling and sliding criteria, while orientation independent stability related to the strength of slope rock mass. Accordingly, overall assessment indicated that 80.4% of slope sections showed less than 5% stability probability, 10.9% of slope sections showed from 5 to 49%, 6.5% showed from 50 to 95% and the rest 2.2% of slope sections showed greater than 95% stability probability. According to GSI system, the slope rock mass quality obtained falls in to three classes; 63.1% of slope sections showed fair quality, 21.7% showed good quality and 15.2% showed poor quality. All these result were also compared with the visual stability assessment results. Moreover, different stability probability maps were produced for all assessment approaches. Finally, on the basis of findings of the present research, recommendations are forwarded.

Key words/phrases: slope stability probability classification (SSPC), geological strength index (GSI), exposure rock mass (EMR), reference rock mass (RRM), slope rock mass (SRM), orientation dependent failure and orientation independent failure.

*****

Acknowledgement

I don't have adequate words to express my feeling of gratitude to my advisor Dr.Trufat Hailemariam whose benevolent guidance and constant encouragement during the present investigation could help me to complete my work. He is the person who has always helped me and his constant encouragement made me strong enough to face every ups and down with confidence during the present research study.

I would also like to express my deepest gratitude to Head and staff of School of Earth Sciences, College of Natural Science, and Addis Ababa University for providing a nice working environment and its entire supportive staff who helped me by providing support what I needed on time.

I would like to express my appreciation to all organizations and individuals who contributed directly or indirectly to this thesis and provided the necessary materials and support for realization of this thesis.

I would like to forward my appreciation to Ethiopian Institute of Geological Survey and National Metrological Agency for providing me necessary data for this research.

It is with great love when I express my warmest gratitude to my mother W/ro Enetensh Abeje and my father Ato Asmare Manderso. Even if you are not with me, I'll never forget what you have done in my life. I would like to thank you for everything you have given to me and I say rest in peace.

Last but certainly not the least; words cannot express my feelings which I have for my beloved wife Lakech Lulie and her family, the lovely daughter of me, Betelihem Dawit, my brother Enyew Asmare and his wife W/ro Woyineshet, I am highly indebted to them for their blessing, guidance, advice, encouragement and support.

Contents page

List of Tables

List of Figures

List of plates

Annex

Abbreviations

AP	Apparent angle of the dip of discontinuity plane
CD	Exposure overall weighted discontinuity condition
Coh' mass	Exposure rock mass cohesion
DS	Discontinuty spacing
ERM	Exposure rock mass
FRI / ϕ 'mass	Exposure rock mass internal friction
GSI	Geological strength index
Hmax	Maximum slope height
Hslope	Slope height
IRS	Exposure intact rock strength
Ja	Joint alteration factor
Jc	Joint condition
Js	Small scale smoothness
Jv	Volumetric count
Jw	Large scale wavinnes
Lm	Infill material
MSMR	Modified slope mass rating
RCD	Reference overall weighted discontinuity condition
RCOH	Reference cohesion
Rf	Infill rating
RFRI	Reference internal friction
RIRS	Reference intact rock strength
Rl	Large scale roughness
Rr	Roughness rating
RRM	Reference rock mass
Rs	Small scale roughness
Rw	Weathering rating
RSPA	Reference discontinuity spacing parameter
RTC	Reference condition of discontinuity parameter
SCR	Surface condition rating
SR	Structural rating
SIRS	Slope rock massinternal friction
SCOH	Slope rock mass cohesion
SME	Slope rock mass excavation
SMR	Slope mass rating
SPA	Exposure discontinuity spacing parameter
SRM	Slope rock mass

SSPA	Slope rock mass discontinuity spacing parameter
SSPC	Slope stability probability classification
STC	Slope rock mass condition of discontinuity parameter
SWE	Slope rock mass weathering
TC	Exposure condition of discontinuity parameter
USC	Unconfied compressive strength
Vb	Block volume
WE	Degree of weathering

*****

Chapter I Introduction

1.1 Background

Rock slope failure is one of the most frequently happening natural phenomena in mountainous parts of Ethiopia. These events are controlled by natural physical processes and cause immediate economic losses, property damages and maintenance costs as well as injuries or fatalities (Pantelidis, 2009). The cost of slope failures is greatest in urbanized areas with high population densities where even small slides may destroy houses and block transportation routes (Ali et al., 2015). Most of the engineering projects in highland areas require excavation of rock to trigger slope failure problems. Therefore, rock slope stability assessment is the most important aspect relating to any infrastructure in the mountainous and rugged terrains.

Rock slope stability assessment has a paramount importance for planning and construction of infrastructures. Identifying potential instability mechanisms and ensuring that the most problematic mechanisms are considered is an especially important stage of slope stability analysis where rock masses are involved in the failed slope system (Smith and Arnhardt, 2016). Rock slope stability assessment is performed routinely and directed towards assessing the safe and effective design of an excavated slope and to assess the equilibrium condition of a natural slope. This assessment requires the detailed information on the geometry of the exposed rock face and definition and assessment of discontinuity properties of the rock mass because these determine, largely the mechanical behavior (Bieniawski, 1989 as cited in Pernito, 2008). Therefore, stability assessment of rock slopes requires knowledge of different conditions, patterns, distributions, geometry, and engineering properties of the discontinuities within the rock mass.

According to Pathak et al. (2006), the rock slope stability assessment is influenced by the random parameters such as active friction angle, water pressure, and seismic acceleration, which cannot be properly represented by a single value as input parameters in slope stability assessments. Furthermore, pre-requisite in slope stability assessment is that the internal structure and the mechanical properties of the soil or rock mass of the slope, are known or can be estimated with a reasonable degree of certainty (Hoek et al., 2000).

Alem Ketema town is one of the Ethiopian highland towns that is defined by extremely rugged mountainous terrains. It is characterized by complex geological set-up and formations. It is also known for previous landslides and rock slope instability problems (Birhanu Ermias et al., 2017). It is reported that rock slope instabilities are common in different parts of the study area resulting household damages, road blockages, loss of life (animals and human beings), crop destruction, and disruption of agricultural lands. Moreover, external processes such as erosion play a big role in the formation of the present regional physiographical setting of the study area.

Any natural slopes modification for the purpose of infrastructure development should need prior detail investigations. Accordingly, general rock slope stability assessment study is essential in the study area. However, previous researches around Alem Ketema were focused on medium scaled landslides hazards zonation (Birhanu Ermias et al., 2017; Tsion Aragaw., 2017) . Because of this reason the present research is targeting rock slope stability assessments in reducing the associated damages caused by different magnitudes and mechanisms of rock failure problems. A detailed slope stability assessment will give the opportunity to analyze slopes individually, and to understand the characteristics of critical rock slope sections. This will be helpful to recommend possible remedial measures and to create awareness of peoples live nearby prone areas so as to minimize the rock slope failure hazards and associate risks. Therefore, the present study will focus on detailed slope stability assessment on a critical rock slope section of prone areas.

1.2 Problem Statement

Around Alem Ketema, rock slope failure is a common problem during rainy seasons. That is frequently observed on steep rocky slopes, road cuts, valleys and cliffs. These instabilities interact with people, settlements, infrastructures, properties and farmlands. Roads from Fetera to Alem Ketema, Alem Ketema to Meranya and other roads linked to Alem Ketema was constructed on and sides of hills and mountainous terrains are highly prone to rock slope failure problems. These results in loss of life, hindering traffics ,injury or other health impacts, property damage, loss of livelihoods and services. Moreover, rapid urbanization and population growth forced the people to construct their houses near to the toe of steep slopes, on the top of slope and valleys to expose themselves for the dangers associated with the rock slope instabilities in the study area.

1.3 Research Objective

1.3.1 General Objectives

The general objective of this study is to conduct a rock slope stability assessment on selected rock slopes around Alem Ketema using rock slope stability probability classification (SSPC) and GSI classification approaches.

1.3.2 Specific objectives

To attain the general objective the following specific objectives are required.

1. To define the geometric features and rock slope mass characterization
2. To map active sign such as tension cracks, discontinuities properties and weathering
3. To assess the possible rock slope failure mechanisms in the study area
4. To classify the slope rock mass in the study area
5. To determine causative factors for rock slope failures in the study area
6. To define the rock slope stability condition in the study area

1.4 Significance of the research

The findings of this research are believed to contribute for understanding of rock slope stability condition, engineering properties of rock slopes, mechanism of failure and delineate triggering factors of the study area. It is also important for decision makers to use the results as part of disaster management in the study area. Moreover, it is used as a source of information to design infrastructures, to specify method of excavation, to know rock strength etc. It serves as an input for town planners and land managers of Alem Ketema to plan sustainable development.

The research will help to forward possible remedial measure that helps to overcome the rock slope failure problems in the study area. It may also be used as a source of information for later researchers who intend to work on the same subject or in the same study area.

1.5 Methodology

The following systematic and organized methodology has been employed to achieve the objectives of the present study. The main activities are discussed as follow:

- Literature review on geology, geomorphology, structure, hydrogeology, engineering geology of the study area from both published and unpublished reports, maps, journals and books pertaining to geophysical investigation and rock mass classification. This was essential to have overall background knowledge on the subject matter. It was also used to get the priority information about the study area and techniques that were used in related researches.
- Preparation of different types of maps including geological map, topographic map and regional seismic map of the study area
- Secondary data collection: includes all required data associated with the present research. Secondary data has also been procured from governmental organizations such as Ethiopian geological survey and meteorology agency. The data includes geological map, topographic map, landslide hazard zonation map, DEM (resolution of the DEM is 30m and 90m), satellite images, meteorology data and other related secondary data which is valuable for the specific research topic.
- Primary data collection: was focused in collecting field observations, mapping, parameter measurements, descriptions, close observations and field judgments of the required slope rock mass parameters. During field work the following activities have been performed.
  - ✓ Delineation of rock slopes which are suitable for the present research
  - ✓ Identify discontinuities location and number of joint sets, joint spacing, joint orientations, joint continuity, joint material, joint patters
  - ✓ Assess degree of weathering
  - ✓ Measuring slope and joint orientations
  - ✓ In-situ rock hammering strength tests
  - ✓ Identify possible triggering factors responsible for slope failure
  - ✓ Assess topographic parameters (relief, elevation, aspect)
  - ✓ Understand possible failure mechanisms, general slope morphology, geology of rock slopes
- Data analysis and interpretation of results: has been done in view of the objective of the present research. Rock mass classification such as SSPC and GSI system were applied to classify the rock stability condition as well as the strength of the slope. SSPC system is a three step classification system and it was dominantly practiced in this study to estimate

slope stability probability condition of selected slope section. Based on results, slope stability maps were prepared. Finally, conclusion and recommendations has been given.

- Different software were used as assisting tool such as Arc GIS, ERDAS IMAGINE 2015, Global Mapper 16, Surfer 13, CorelDraw 12, Google Earth pro, QuikGrid and Stereo 32.

1.6 Limitations of the research

The major limitations that were faced in present research are listed as follow:

- ✓ It was conducted in selected slope section of the study area. This is due to accessibility, time and financial constraints.
- ✓ There was also limited data.
- ✓ Lack of sufficient secondary data related to the present study.
- ✓ There are no exited researches related to deterministic or probabilistic rock slope conducted in the study area.

1.7 Thesis organization

The content of the present research is organized in to seven chapters.

Chapter one deals with the general background about the research and slope rock mass failure, problem statement, objectives, methodology, significance and limitations of the research.

Chapter two briefly describes the study area including location and accessibility, geology, geological structures, climate condition, physiography, land use land cover, drainage pattern and seismicity, status of slope rock masses etc.

Chapter 3 discusses about literature review including types of rock slope failure, mode of slope rock mass failure, factors influencing rock slope stability, slope rock mass assessment methods, previous works and genesis of methodology.

Chapter four discusses about the methods, data collections and parameters.

Chapter five presents data analysis, parameter determination and assessments of slope stabilities.

Chapter six presents the results obtained from the assessments, interpretation and discussion of slope stability probability and estimation rock strength of the slope sections.

Chapter sever gives briefly conclusions and recommendations.

****

Chapter II Description of the Study Area

2.1 Preamble

This chapter describes the study area. It discusses the geology, geological structures, climate condition, physiography, land use land cover, drainage pattern and seismicity, which can influence the stability of rock slopes in the study area (Zare et al., 2011).

2.2 Location

The present study area is located in the eastern central part of the North-western Ethiopian Plateau (NWP), in the North Showa district of the Amhara Regional State, which is roughly about 185 Km from capital city Addis Ababa. Geographically, it is located between 1109850-1113700m latitude and 495980-501930m longitude (Fig.2.1). It is bounded by Wenchit River to the north direction and Jema River to the south direction. The study area covers an area around 22km^2. The study was conducted along the natural slope escarpments around Alem Ketema.

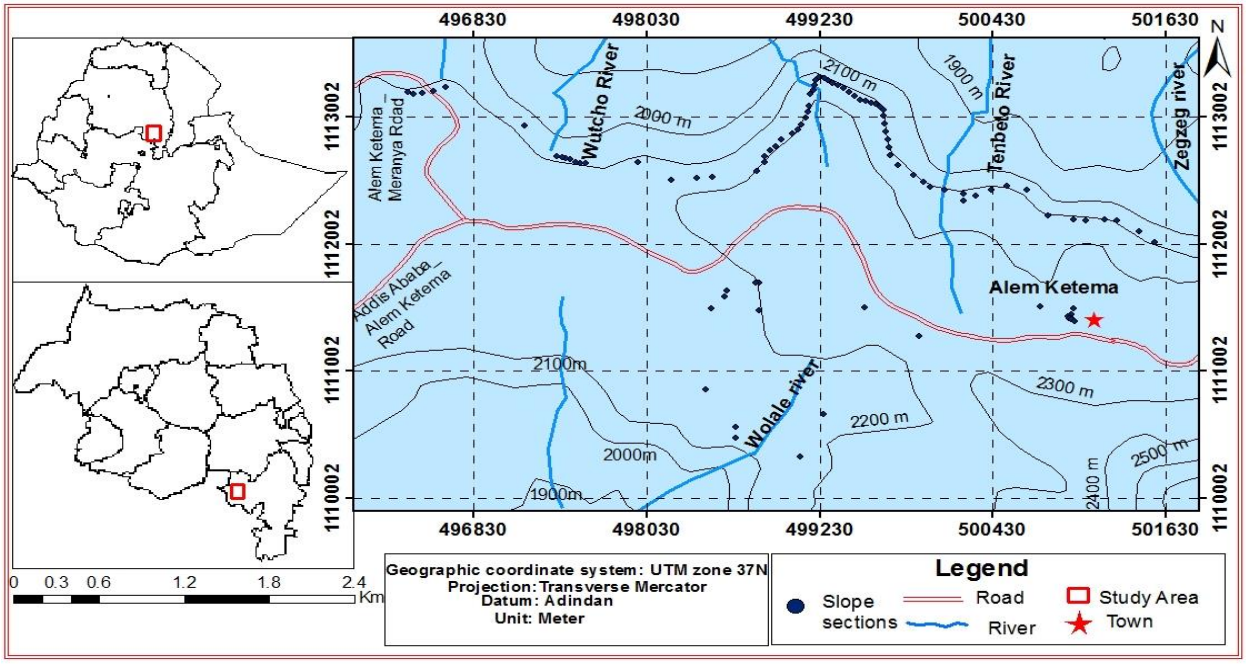

Fig 2.1 Map of the study area

2.3 Accessibility

The study area can be accessed via Addis Ababa to Muke Turi main Asphalt road which is about 85 Km and then from Muke Turi town to Alem Ketema via gravel road which is about 100 Km. Generally, the area is not easily accessible by vehicles and has no standard routes to reach in all parts of the study area. The physiographic condition at the Alem Ketema town and the surrounding area is characterized by highly variable topographic features with rugged and complex geology.

2.4 Climate

Climate includes average temperature and precipitation condition of an area. There are different distributions of rainfalls in Ethiopia. Lowland areas has little precipitation records and highland areas has more than 70% of the annual rainfalls (Lulseged Ayelew, 1999). According to Lulseged Ayalew (1999) presentation, there are two known climate components which are the amount and distribution of precipitation and temperature conditions.

In Ethiopia, there are five climatic zones. According to Daniel (1977) presentation, "Wirch" mean sea level above 3300m and mean annual temperature is below 10°c, "Dega" mean sea level 2300m to 3300m and mean annual temperature is between 10°c and15°c, "Weina Dega"(Subtropical) mean sea level 1500m to 2300m and mean annual temperature is between 15°c and 20°c, "Kolla" (Tropical) mean sea level 500m to 1500m and mean annual temperature is between 20°c and 30°c, "Bereha" (Desert) below 500m and mean annual temperature is between 30°c and 40°c.

Accordingly, the climate of the study area falls under warm subtropical climate conditions which is characterized by mean sea level 1500m to 2300m and mean annual temperature between 15°c and 20°c. Generally, the area receives rainfall twice in a year. These are heavy precipitation from June to September and light to moderate precipitation from mid-February to mid-March. However, there are also unseasonal or unexpected rainfalls in the area.

2.4.1 Rainfall

Based on Ethiopian meteorology agency rainfall records, the study area is defined by heavy precipitation from June to September, moderate precipitation from April to May and light precipitation from February to March. The remaining months receives low precipitation as compared to other months (Table 2.1).

Table 2.1 Long-term monthly rainfalls at Alemketema [mm] (fully recorded years only)

Year	Jan	Feb	Mar	Apr	May	Jun	Jul	Aug	Sep	Oct	Nov	Dec	Total
1992	14.1	48.6	33.2	56.1	15.9	24.8	204.4	326.7	133.9	50.1	112.9	0	1020.7
1993	0	23.5	11.7	123.3	111.4	48.3	345.5	256.6	194.6	23.6	0	0	1138.5
1994	0	0	44	26.2	8.3	98.6	290.7	320.5	170.5	0	2.2	0	961
1995	0	3.4	53.9	43.9	50.1	26	229.2	342	83.3	0	0	12.8	844.6
1996	25.9	6.7	101.6	11.5	79	191.1	319.9	338.5	104	0	16	0	1194.2
1997	20.3	0	49.3	37.1	40.3	190	344.2	252.5	85	76	46.3	2.1	1143.1
1998	17.4	17.6	28.3	25	73.4	66.8	247.2	355.5	87.1	113.9	23.15	0	1055.4
1999	7.2	0	0	1.5	10	39.3	297.4	514.6	66.3	151.8	0	1.3	1089.4
2000	0	0	36.1	103.7	88.1	58.6	449.1	311.5	122.1	7.2	32.2	0.4	1209
2001	0	5	45.7	20.5	29.9	96	373.5	266.5	90.9	0.3	0	6.1	934.4
2002	41.6	38.2	44.8	40.8	9.3	39.3	283.9	282.2	121.1	0	0	13.4	914.6
2003	9	54	53.4	61.3	1.5	90.5	308.8	254	139	2.5	0.5	31.2	1005.7
2004	9.2	6.1	21.9	71.5	23.2	96.4	206.8	258.9	142.8	32.6	1.1	0	870.5
2005	18.9	0	53.6	47	97.9	91.1	273.8	328.7	142	15.4	7.4	0	1075.8
2006	12.6	13	96.4	27.8	31.2	103.7	388.9	355.6	166.1	5.4	6.2	0	1206.9
2007	2.4	37	34.5	57.4	24.3	138.7	373.4	299.4	201.7	8	0	0	1176.8
2008	0	0	0	37.8	46.3	96.5	301	313	106.2	13	47.2	0	961
2009	17.7	2.6	25.2	18.1	52	24.6	371.8	285.3	71.6	23.1	1	55.7	948.7
2010	0	37.5	22.1	38.3	57.7	13.5	252.5	369.8	156	1.1	13.2	18.4	980.1
2013	1	0.6	21.7	43.8	30.8	91.1	314.7	325.1	114	82.1	0	3.95	1028.9

2.4.2 Temperature

In the study area, based on Ethiopian meteorology agency records, the maximum mean annual temperature was recorded from February up to Jun, especially. Besides, the mean annual temperature becomes increases from year to year. The mean annual temperature of the area is between 19.32°c and 20.03°c (Table 2.2).

Table 2.2 Long-term monthly temperatures [0C] at Alem Ketema (fully recorded years only)

Temp.	Year	Jan	Feb	Mar	Apr	May	Jun	Jul	Aug	Sep	Oct	Nov	Dec
max	2001	25.5	27.3	25.7	28.2	27.6	25.4	21.2	20.5	23.3	25.7	25.3	25.7
min	2001	13.3	14.4	14.5	16.1	15.9	14.6	13	13.7	13.8	13.9	12.6	13
Mean		19.4	20.85	20.1	22.15	21.75	20	17.1	17.1	18.55	19.8	18.95	19.35
max	2003	26.7	28.1	27.5	27.7	29.5	26.9	21	20.8	22.4	25.7	25.7	25.4
min	2003	14.1	15.1	15.2	15.8	18	15.7	13.4	13.7	13.5	13.4	13	12.5
Mean		20.4	21.6	21.35	21.75	23.75	21.3	17.2	17.25	17.95	19.55	19.35	18.95
max	2005	25.6	27.9	28.3	27.7	26	26.5	21	20.8	23.1	25.3	24.9	24.9
min	2005	12.9	14.4	14.9	14.7	15.2	15.2	12.8	13	13.2	12.8	11.9	10.7
Mean		19.25	21.15	21.6	21.2	20.6	20.85	16.9	16.9	18.15	19.05	18.4	17.8
max	2006	26.4	28	27.2	26.7	28	27.3	22	20.5	22.3	25.6	24.5	25.6
min	2006	12.4	14.3	14.8	15.1	16.1	15.4	13.1	12.7	13.3	14.6	13	13.4
Mean		19.4	21.15	21	20.9	22.05	21.35	17.55	16.6	17.8	20.1	18.75	19.5
max	2007	26.4	26.8	28.4	27.9	28.8	25.4	20.8	20.6	22.5	24.6	25.5	25.1
min	2007	14.3	14.6	15.4	15.9	16.9	15.2	12.8	12.8	16.7	13.5	12.7	11.9
Mean		20.35	20.7	21.9	21.9	22.85	20.3	16.8	16.7	19.6	19.05	19.1	18.5
max	2008	26.5	27.3	29.2	27.8	28.1	26.3	22.4	20.9	23.3	25.3	24.3	25.6
min	2008	14.1	14.1	15.4	16.2	16.7	14.9	13.1	12.6	13.7	14	12.2	13.1
Mean		20.3	20.7	22.3	22	22.4	20.6	17.75	16.75	18.5	19.65	18.25	19.35
max	2011	26.5	28.6	27	29.1	28.3	27.7	22.6	21.2	23.2	25.9	25.7	26.3
min	2011	14.2	14.1	14.7	16	16.1	15.9	13.3	13.1	13.6	13.7	13.3	12.40
Mean		20.35	21.35	20.85	22.55	22.2	21.8	17.95	17.15	18.4	19.8	19.5	19.35

2.5 Physiography

Physiography is closely associated with the geological setting and the geomorphological history of a rock wall (erosion) and also effectively influence the geomechanical setting (Fischer and

Huggel, 2008). According to Fischer and Huggel (2008) discussion, the physiographic condition of an area has a significant contribution on the stability of rock slope masses.

The physiography of the study area is characterized by forming steepest cliffs associated with benches on basalt units; while gentle slopes and topographic breaks in soft rocks such as mudstone and chert units (Fig.2.4). Besides, most slopes are characterized by steep slopes. Accordingly, gravity plays a significant role on the stability of steep slopes in the study area. As a result, during field work, several slope rock mass failures were observed.

2.5.1 Slope

In the study area, the slope is characterized by changing its steepness along faces from bottom to the top. It also defined by rugged features which is very steep at the toe of the slope and becomes gentler towards the top slope sections. In general, steep slopes are more susceptible to instability as compared to gentle slopes (Hamza and Raghuvanshi, 2017).

The slope map was initially produced from DEM. This was very helpful to characterize the slope geometry during practical field work. Because, it was challenging to characterize the angle and height in the field accurately due to rugged slope features. Based on Anbalagan's (1992, as cited in Raghuvanshi et al., 2014) slope classification, the present study area slope map was produced by classifying the slope angle in to five classes (Fig.2.2). Accordingly, the classes are; very gentle slope (<15°), gentle slope (16–25°), moderately steep slope (26–35°), steep slope (36–45°) and escarpment /cliff (>45°) (Fig. 2.2).

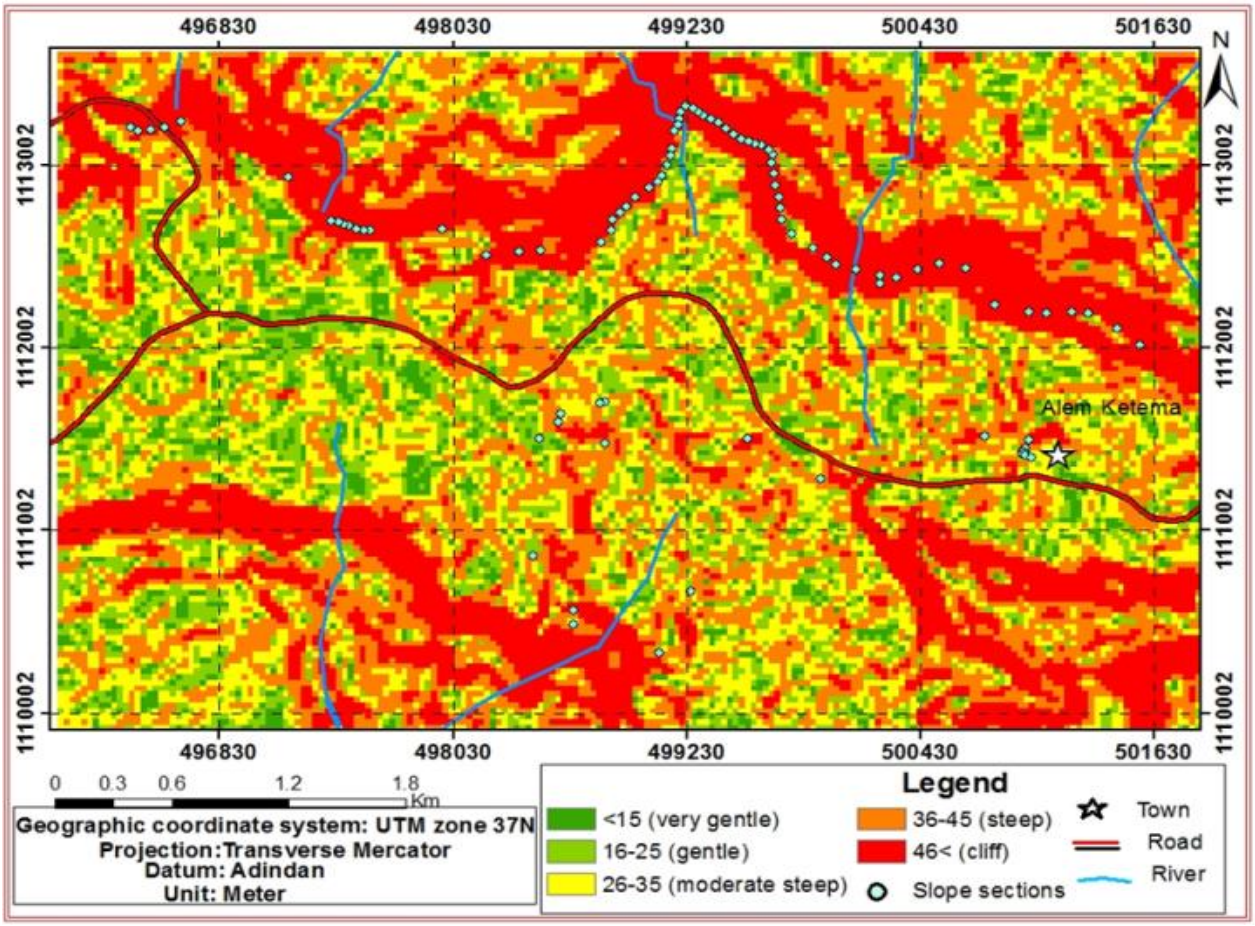

Fig. 2.2 Slope map of the study area

2.5.2 Aspect

Slope aspect refers to the direction in which the slope is facing. Accordingly, it has a major contribution for slope rock mas weathering (Huisman, 2006).

The aspect of slopes in the present study area was derived from the DEM and it was classified into 10 classes. The aspect classes were adopted from Hamza and Raghuvanshi, (2017). Accordingly, the classes are; Flat (-1°), North (0–22.5°), Northeast (22.5–67.5°), East (67.5–112.5°), Southeast (112.5–157.5°), South (157.5–202.5°), Southwest (202.5–247.5°), West (247.5–292.5°), Northwest (292.5–337.5°) and North (337.5-360) (Fig.2.3).

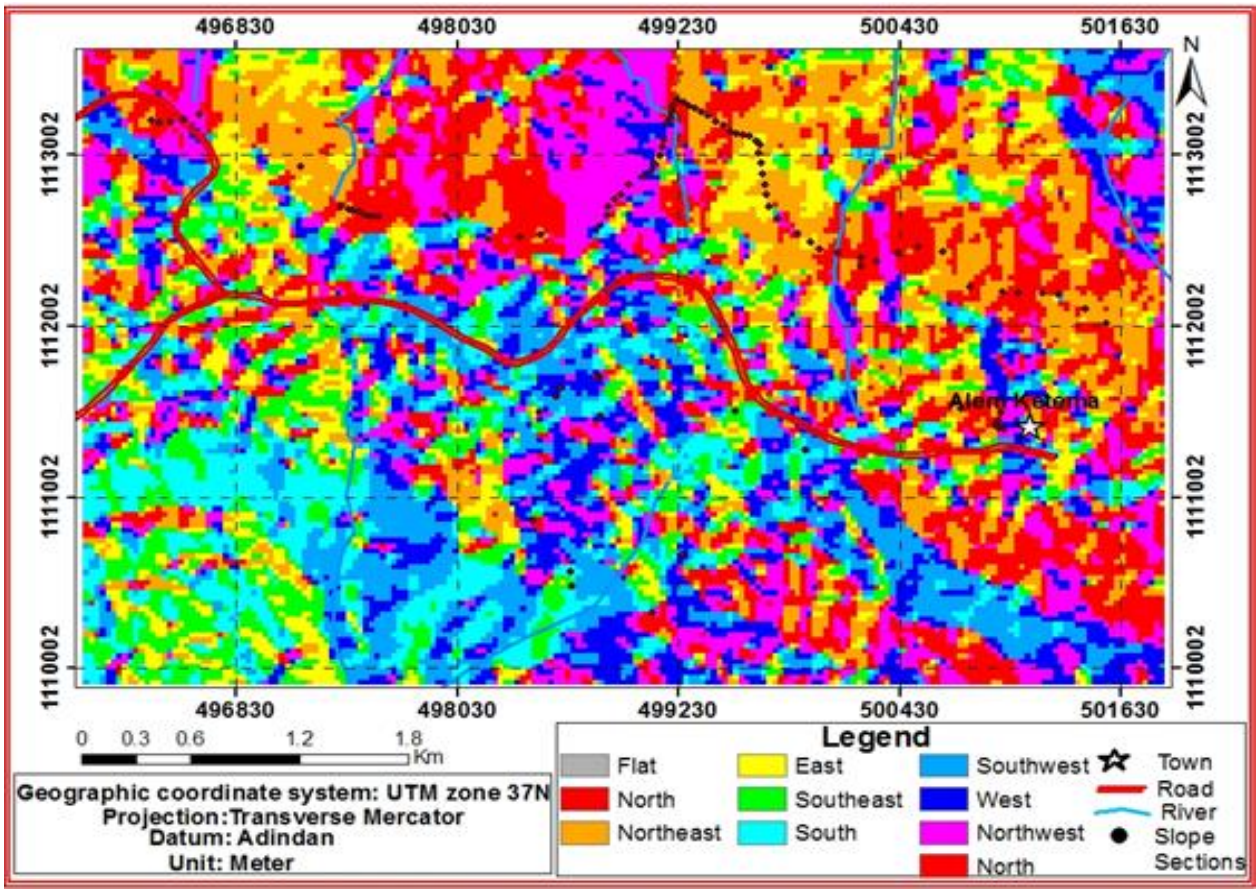

Fig.2.3 Aspect of the study area

2.5.3 Elevation

The study area is a part of central Ethiopian highlands and its elevation ranges from 1,783m-2,613m as shown in Fig.2.4. This elevation was subdivided into 10 classes: 1,783-1,878m, 1,878-1,944m, 1,944-2,010m, 2,010-2,087m, 2,087-2,159m, 2,159-2,210m, 2,210-2,271m, 2,271-2,347m, 2,347-2,468m, and 2,468-2,643m, respectively.

The elevation difference between the maximum and minimum elevations with in this specific area is about 830m. In the present research, the delineated slope sections are located from elevation 2,087- 2,271m. However, most of the delineated slope sections are located from 2,087-2,210m elevations.

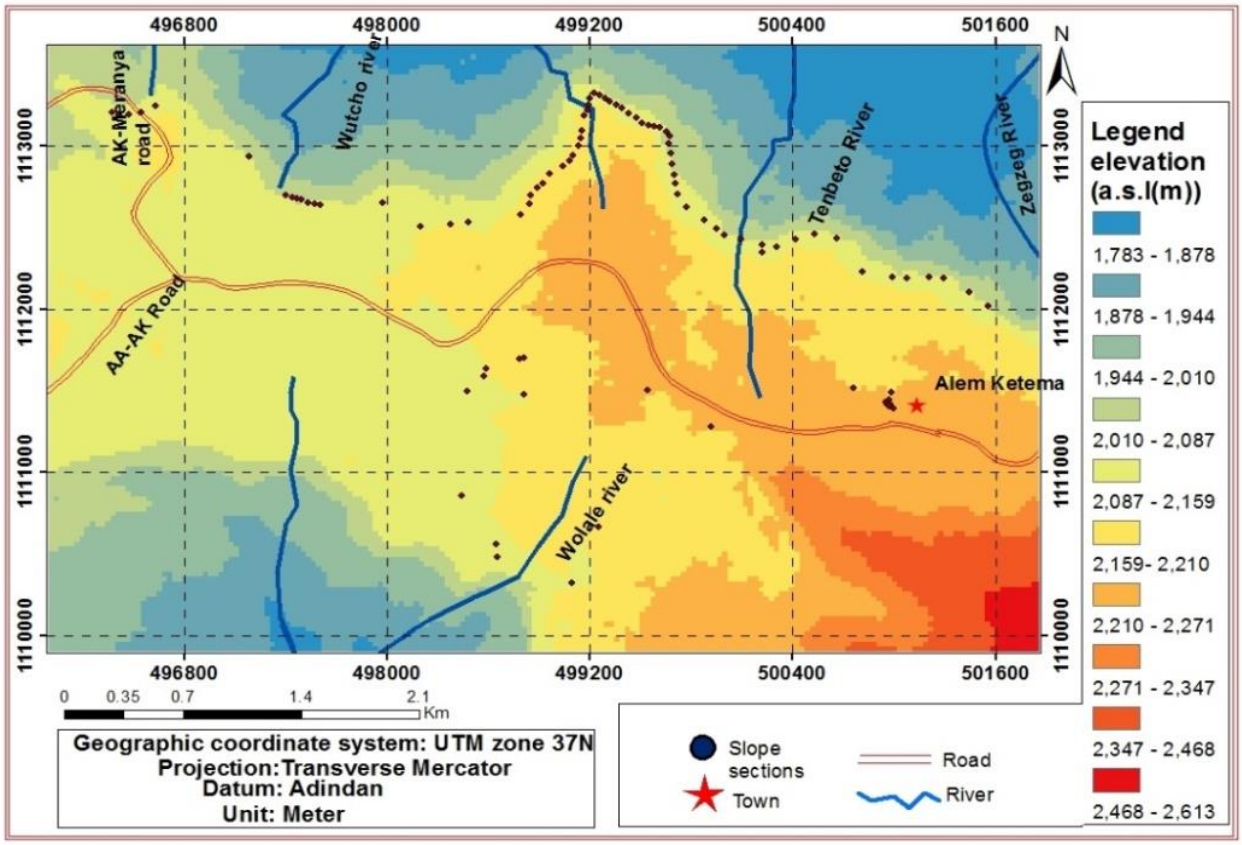

Fig.2.4 Elevation of the study area

2.6 Drainage pattern

In a drainage system, streams or rivers always link together to form networks. The drainage system is highly influenced by many variables including human intervention, vegetation, topography, geology, climate conditions, transport of sediment and water (Zhang and Guilbert, 2016).

Number of small tributary streams are passing through the study area and intersecting at various locations. The drainage network of the study area is characterized as dendritic, parallel and sub-parallel. Jemma and Wonchit River are the main drainage networks in the study area (Fig.2.5). These river basins are major tributaries for the Blue Nile River. Jemma and Wonchit River also have their own sub tributaries which are dominantly flows during rain seasons and dry out in dry seasons. The drainage systems of the study area are mainly controlled by the topographic features.

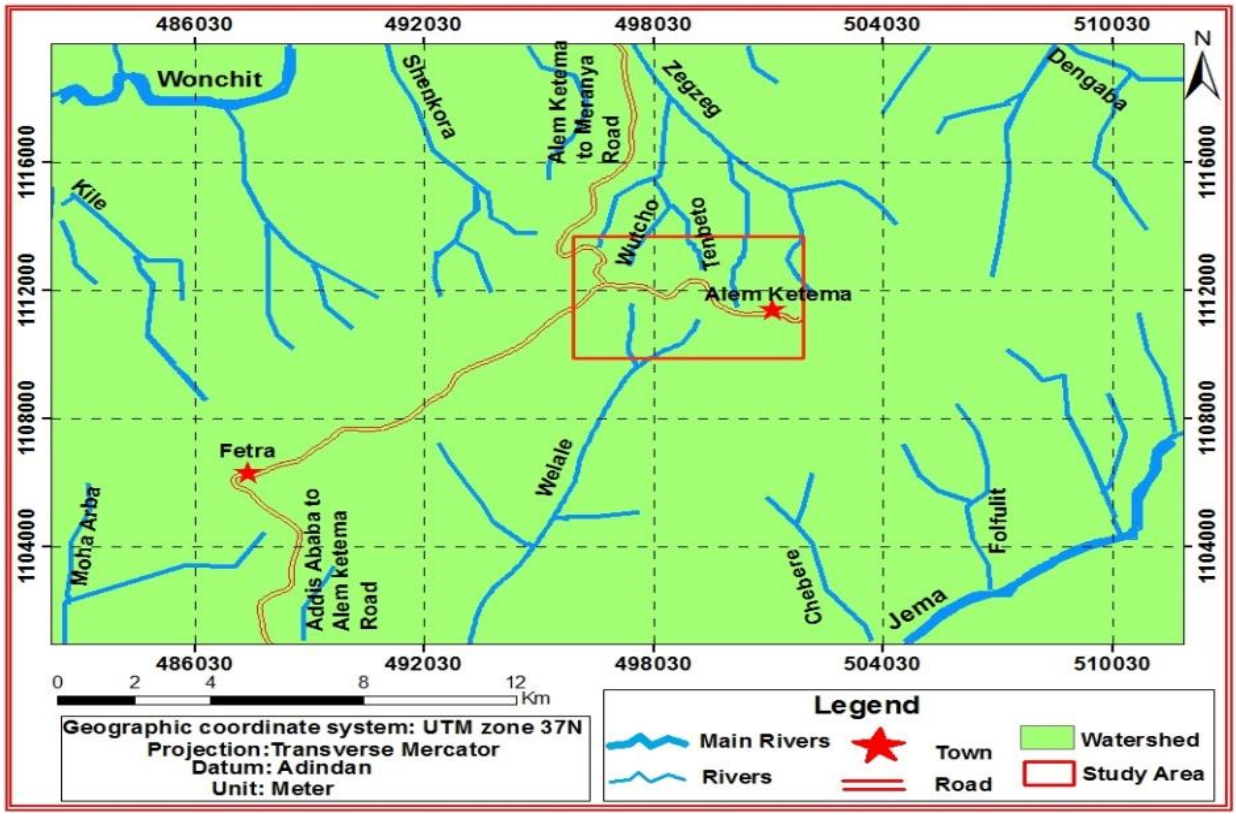

Fig.2.5 Drainage patterns of the study area

2.7 Land use Land Cover

In Ethiopia, land use land cover (LULC) shows a significant changes from year to year. Most of these changes were from the natural forest to agricultural land and was due to human intervention. Human intervention changes one land cover class to another land cover class. The first one was the deliberate and direct conversion of many LULC classes to cultivated land (Hagos Gebreslassie, 2014).

In the present study area, most of the settlements, including Alem Ketema are located on the top of the slopes escarpments and some at the toe of the slopes. There are also localities which are free from population settlement and are sparsely settled peoples. Moreover, during field work, it has been observed that the area is scarcely covered by Eucalyptus and short bushes in different surroundings.

Very gentle slope areas which are characterized by mud units and completely weathered basalt units are covered by crops. Commonly practiced crop types are Teff, Maize, Pea, Legume, Sorghum, and Vegetables (Fig.2.6). Besides to agricultural activities, a number of surface drainage ditches were constructed by farmers to protect farm land erosions. However, these ditches were constructed in the wrong ways that drains towards the cliff slopes. These improper surface drainage practices in combination with springs that throw down from the top of the cliff towards the toe erode the toes of unstable slopes and activate the slope failure process. Moreover, the steeper parts of the area including steep slopes and valley sides are sparsely vegetated and mainly comprise bushes and grasses. There are also bare land which are completely covered by slightly to moderately weathered basalts.

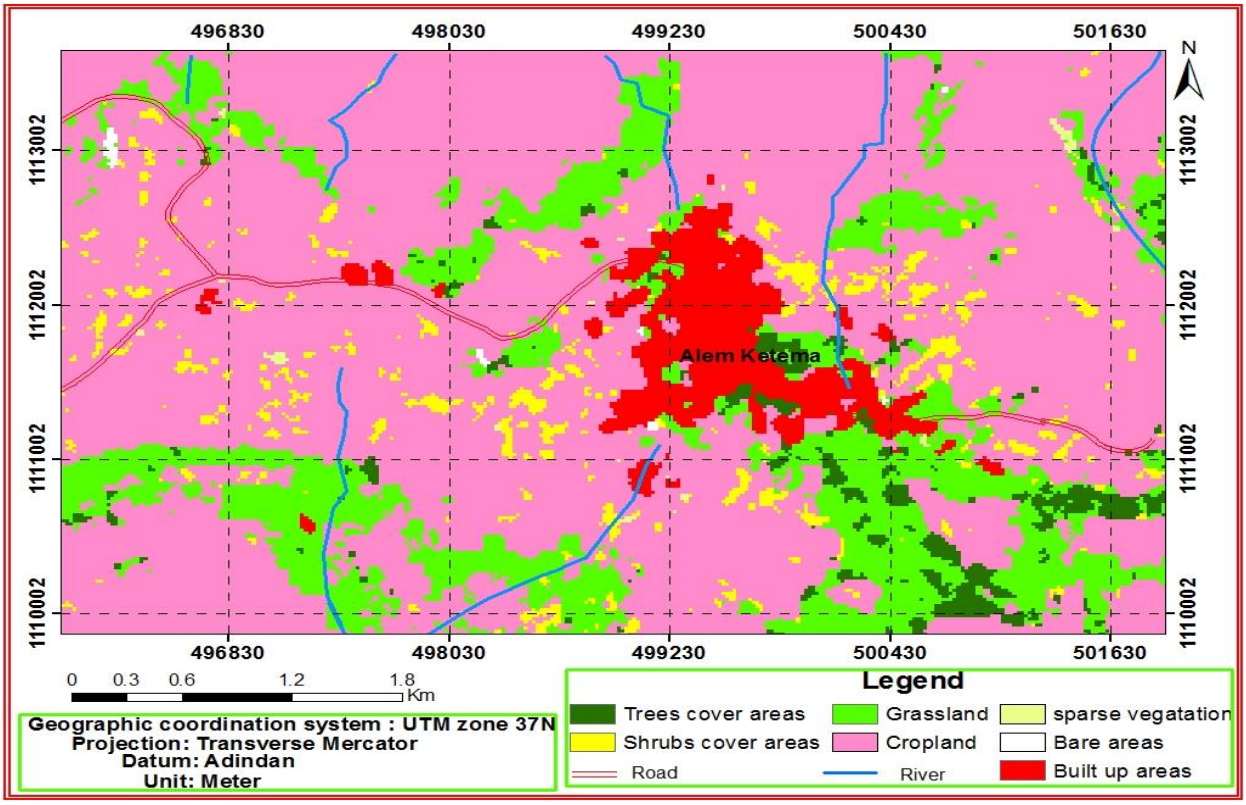

Figure 2.6 Land use land cover map of the study area

2.8 Seismicity

Earthquake is a natural hazard producing seismic waves that can damage all natural and man mad structures. There are three main distinct seismic zones in Ethiopia (Samuel Kinde et al., 2009). These seismic zones are Afar triangle seismic zone (which consists of the triple junctions Red Sea, Gulf of Aden and Main Ethiopian Rift), the escarpment seismic zone (characterized by N-S running faults), and the Ethiopian Rift System seismic zone (which links the Red Sea, Gulf of Aden with the East African Rift System through the Afar Triangle) (Samuel Kinde et al., 2009). These seismic wave propagation can affect the rock slope strength by widening or opening of structural discontinuities (Raghuvanshi et al., 2014).The effect of earthquake can be manifested on the surface as landslide, differential settlement, ground cracking, subsidence, and rock mass fracturing.

The seismic risk map of Ethiopia produced by Laikemariam Asfaw (1986) for a hundred year return period and 0.99 probability shows that the present study area falls within 8 M.M scale as shown in Fig.2.7. Based on the Modified Mercalli intensity scale the estimated earthquake acceleration comes out to be 0.1–0.5g, as determined from the MM intensity graph as shown Fig.2.8 (Hays, 1980). Accordingly, the present study area was falls under high seismic zones. Therefore, the study area has a big chance to have slope stability problems which can be triggered by seismic activities.

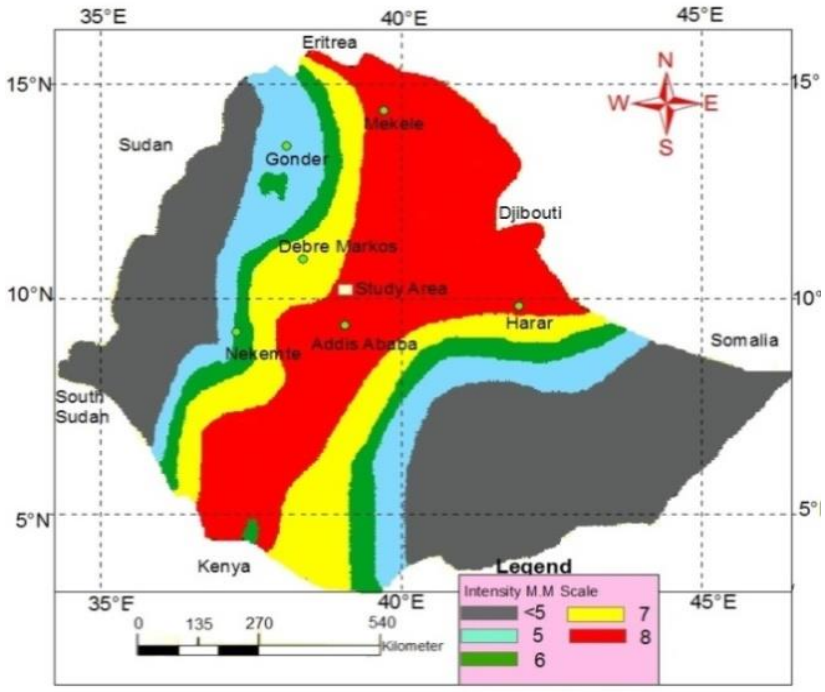

Fig. 2.7 Seismic risk map of Ethiopia 100 year return period, 0.99 probability (Modified after Laike Mariam Asfaw, 1986)

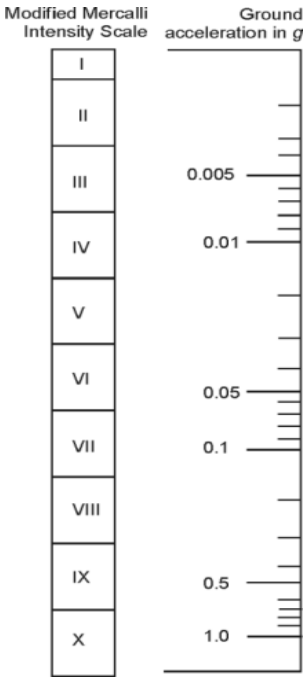

Fig.2.8 Relationship between intensity of earthquake and ground acceleration (Hays, 1980)

2.9 Regional geology

The study area is located in the central part of the Northwestern plateau which is characterized by the geology of the Blue Nile basin. The northwestern Plateau of Ethiopia is almost entirely covered with extensive Tertiary continental flood basalts that mask the underlying formations (Hautot et al., 2006). The Blue Nile basin is a major geological formation in the northwestern Plateau.

The basin consists of Precambrian basement, Palaeozoic and Mesozoic sedimentary rocks, Tertiary to Quaternary volcanic rocks and Quaternary deposits (Getaneh Assefa, 1991; Russo et al.,1994; Dawit Lebenie and Bussert, 2009; Dawit Lebenie, 2010; Gani et al, 2008; Wolela Ahmed, 2008, 2009, 2010; Gani et al,2008; Mogessie et al., 2002; Ismail and Abdelsalam, 2012). These formations are described as follows.

2.9.1 Precambrian basement rock

The age of the basement rocks is considered to be Neoproterozoic, ranging from 850 to 550 Ma ((Dereje Ayalew et al.,1990 as cited in Gani et al.,2008). It is rocks composed of metamorphic rocks including highly deformed and sheared gneisses, schists, migmatites, granites and igneous intrusions (Gani and Abdelsalam, 2006 ; Gani et al.,2008; Worku 1996; Stern and Abdelsalam 1998, Tadesse et al. 2000; Braathen et al. 2001; Yiabas et al. 2002; Miller et al. 2003; Dawit Lebenie, 2010).

Neoproterozoic basement rocks form the base of the Blue Nile Basin and crop out within rugged topography at an altitude of 900–1500m along the entire NW-flowing segment of the Blue Nile (Gani et al., 2008). This rock underlie the Mesozoic sedimentary rocks and are encountered along the Gorge of the Nile as the Blue Nile flows NW towards the lowlands of Sudan (Gani and Abdelsalam, 2006). The river exposes Neoproterozoic basement rocks as it flows NW towards the lowlands of Sudan (Gani and Abdelsalam, 2006). The Neoproterozoic basement rocks are affected by normal faults with throws ranging between 5 cm and 5m (Gani et al.,2008).

2.9.2 Paleozoic and Mesozoic sediments

Palaeozoic and Mesozoic sediments in the Blue Nile Basin is buried under up to 1100m thick Cenozoic volcanics (Wolela Ahmed, 2009). The Blue Nile Basin consists of a 3000m thick Palaeozoic and Mesozoic sedimentary succession, which is well exposed in the Blue Nile River canyon (Dawit Lebenie and Bussert, 2009). The typical sedimentary succession of the basin includes from bottom to top five formations; which are Adigrat Sandstone, Gohatsion Formation, Antalo Limestone, Debre Libanos Sandstone and Muger Mudstone,. These formations are briefly described below.

2.9.2.1 Adigrat sandstone

The age of Adigrat sandstone in Blue Nile Basin indicate an age 237-197 Ma years (Barsisa Bekele, 2011). In the Blue Nile Basin, the formation was deposited in alluvial fan, fluviatile and lacustrine depositional environments (Wolela Ahmed, 2010).

This unit overlies the Precambrian basement rocks unconformably with the exception of some places where it overlies unconformably the Paleozoic continental sediments (Wolela Ahmed, 2008; Russo et al., 1994).

The Adigrat sandstone formation, in the Blue Nile basin attains a thickness of 100-300m in the Jemma river section (Mohr, 1962 as cited in Zelalem Shiferaw, 2005; Russo, 1994). The formation is well exposed in the Blue Nile Basin, Ogaden Basin and the Mekele Outlier (Wolela Ahmed, 2008). According to Wolela Ahmed (2008), Mogessie et al.(2002) presentations, Adigrat sandstone forms vertical cliff exposures in Dejen, Gohatsion, Amuru-Jarty, Fincha, Gendbret-Jeldu and Ejere (near Jimma River Bridge). The formation is dominantly composed of continental clastics which are conglomerates, gravely sandstones, siltstones, mudstones and carbonaceous materials (Wolela Ahmed, 2008).

2.9.2.2 Gohatsion formation

The Gohatsion formation has thickness that reaches up to 450 m (Russo et al., 1994; Gani et al., 2008). It is exposed along the SW-flowing segment of the Blue Nile where it is underlain by the glauconitic sandy mudstone unit or the Triassic–Early Jurassic Sandstone and overlain by a Middle–Late Jurassic Upper Limestone unit (Gani et al., 2008).

Gohatsion formation comprises an association of mudstone, claystone, limestones, dolostones, shale and gypsum, variously alternating with beds of siltstone, sandstone and the whole comprising a thick and well defined lithostratigraphical unit (Getaneh Assefa ,1981; Russo et al.,1994; Wolela Ahmed ,2009; Mogessie et al., 2002). The Lower Limestone is cross-cut by NW-trending normal faults, NE- and NW-trending dilational fractures and less-frequent NE-trending normal faults (Gani et al., 2008).

2.9.2.3 Antalo limestone

In the Blue Nile Basin, the Antalo limestone formation reaches a maximum thickness of 720 m (bottom unexposed) (Wolela Ahmed, 2009).

It is found in the SW-flowing segment of the Blue Nile sandwiched between the Early–Middle Jurassic Lower Limestone unit, and either the Late Jurassic–Early Cretaceous Upper Sandstone unit or Early–Late Oligocene volcanic rocks (Gani et al., 2008). The Upper Limestone is affected by NW- and NE-trending normal faults (Gani et al., 2008). The Antalo limestone extended to the limestone unit of the Blue Nile basin (Dawit Lebenie, 2010). It conformably overlies the Gohatsion formation and can be subdivided into lower part, middle part and upper parts (Russo et al., 1994; Mogessie et al., 2002). It is exposed in the Jema River, Debre Libanoes, Gendeberet-Jeldu, Mugher and Dejen-Gohatshion (Wolela Ahmed, 2004).

2.9.2.4 Debre libanose sandstone

According to Getaneh Assefa (1991), the formation has 172 m thick but the variation in thickness west to east is extreme as it ranges from few meters to up to 280 m near Lemi and lithologically it comprises of pebbly sandstone, conglomerate and claystone. This unit is determined to be of Late Jurassic–Early Cretaceous age based on its stratigraphic relationship with overlying and underlying units.

Debre Libanose sandstone is well exposed at the areas of Lemi, Zega Wodem Stream, Mugher River, Jema River and Wenchit Stream and their tributaries and reaches a maximum thickness of 280 m near Lemi (Wolela Ahmed, 2009). It is encountered in the S-flowing segment of the Blue Nile below the Early–Late Oligocene volcanic rocks (Gani et al., 2008). It comprises thickly to thinly bedded sandstones, with bed thickness ranging from 1 to 40 cm (Gani et al., 2008).

2.9.2.5 Mugher mudstone

The 260m thick Mugher Mudstone unit (Getaneh Assefa, 1991). It is the result of withdrawal of the sea from east African Craton during late Late Jurassic (Getaneh Assefa, 1991). It consists of 15 m thick gypsum, dolomite, and shale alternations at the base, overlain by 240m thick mudstone intercalated with fine- to medium-grained sandstone (Getaneh Asefa, 1991). Mugher mudstone is exposed in the Mugher valley, Zega Wedom, Wencit, Wesena Adabai and Jemma river section (Russo et al., 1994; Getaneh Assefa, 1991).

2.9.3 Tertiary to quaternary volcanic rocks

Quaternary volcanic events resulted in the eruption of 300m thick basaltic rocks (Gani et al., 2008). No normal faults are observed in the Quaternary volcanic unit; however, this unit is characterized by the presence of NW- and NE-trending fractures (Gani et al., 2008).

The Tertiary to Quaternary volcanic rocks un-conformably rests on the Mesozoic sedimentary rocks (Mogessie et al., 2002). According to Mohr (1962, 1983 as cited in Birhanu Ermias et al., 2017), the Tertiary to Quaternary volcanic rock including basaltic to felsic flows, tuffs, ignimbrites, rhyolites and scoria together with inter-volcanic, clastic and evaporitic sedimentary rocks. Tertiary–Quaternary shield volcanoes whose accumulation might have contributed to the formation of the Gorge of the Nile and the Blue Nile Bend (Gani and Abdelsalam, 2006).

2.9.4 Quaternary deposits

The Quaternary sediments are the youngest sediments which are composed of alluvial, colluvial and lacustrine deposits (Poppe et al., 2013; Tenalem Ayenew, 2005; Mogessie et al., 2002).
Alluvial and colluvial deposits generated from fluvial processes are locally mixed with slope colluvium (Poppe et al., 2013). Quaternary lacustrine and fluvio-colluvial sediments and superficial deposits occur intermittently covering the basement and filling river channels (Seifu Kebede et al., 2005).

The alluvial deposits are mainly existed along the Wenchit and Jema sub basins and their tributary streams. The poorly sorted, crudely bedded conglomerates and gravely sandstones are explained as alluvial fan deposits (Wolela Ahmed, 2008). The alluvial fan sedimentation passes up vertically into channel, point bars and flood-plain fines Quartz, quartzite, orthoquartzite, granodiorite gneisses, metavolcanic boulders and pebbles indicate Precambrian basement rocks possibly derived from the North-western Ethiopian highlands (Wolela Ahmed, 2008).

2.9.5 Regional structures

The Blue Nile Basin is situated in the Northwestern Ethiopian Plateau and it is bounded by the uplifted tectonic escarpments on the western flanks of the Afar Depression and the Main Ethiopian Rift in the east and southeast, respectively, and in the west by the erosional Tana escarpment (Gani et al., 2008). The complex history of local uplift, deformation and volcanism of the Lake Tana region and Blue Nile basin has been associated to the influence of the Afar plume (Corti, 2009).

The Afar Mantle Plume resulted in extrusion of Early–Late Oligocene volcanic rocks that covered much of the Mesozoic sedimentary section. This volcanic event was followed by NW–SE-directed extension resulting in the opening of the NE-trending Main Ethiopian Rift and superimposition of NE-trending faults on rocks within the Blue Nile Basin (Gani et al., 2008).

The Main Ethiopian Rift was subsequently affected by Quaternary E–W and NNE–SSW-directed extensions related to oblique opening of the Main Ethiopian Rift and development of E-trending transverse faults, as well as NE–SW-directed extension in southern Afar and E–W-directed extensions in western Afar (Fig.2.9 A and B) (Gani et al., 2008; Acocella & Korme, 2002; Bonini et al., 2005; Wolfenden et al., 2004; Keir et al., 2015). These Quaternary stress regimes resulted in the development of N-, ESE- and NW-trending extensional structures within the Blue Nile Basin (Gani et al., 2008; Corti, 2009) . These faults are normally long, widely spaced and characterized by large vertical offsets (Corti, 2009). This formed NW-trending Mesozoic rift basins including the Muglad, the Melut, the Blue Nile and the Anza rift basins.

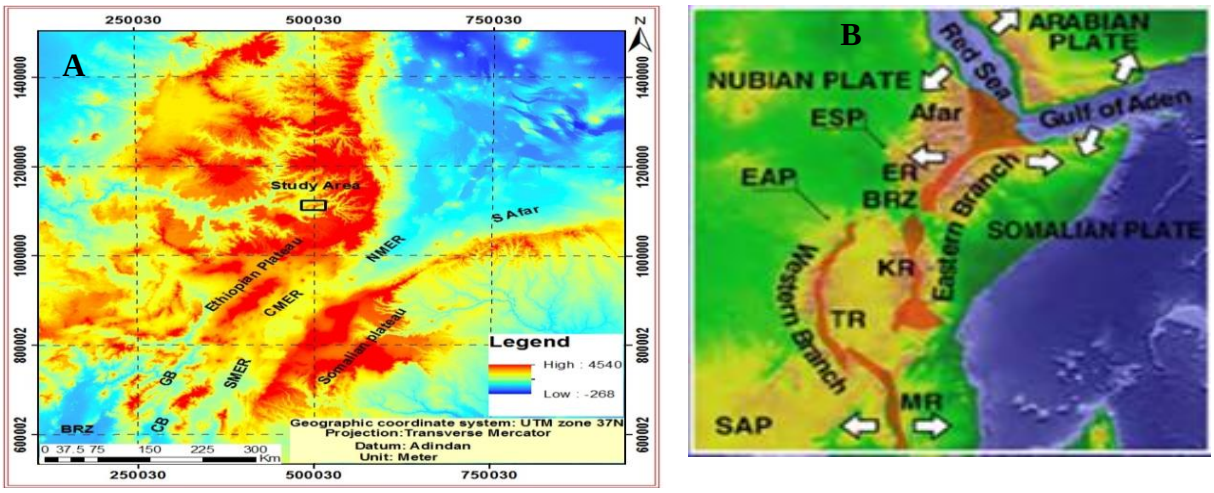

Fig 2.9 (A) Digital elevation model of the Ethiopian Rift showing the main rift segments: Northern Main Ethiopian Rift (NMER), Central Main Ethiopian Rift (CMER) and Southern Main Ethiopian Rift (SMER). BRZ: Broadly Rifted Zone; CB: Chow Bahir Rift; GB: Gofa Basin and Range (B) East African Rift System: BRZ: Broadly Rifted Zone; EAP: East African Plateau; ER: Ethiopian Rift; ESP: Ethiopian–Somalian plateaus; KR: Kenya Rift; MR: Malawi Rift; SAP: Southern African Plateau; TR: Tanganyika Rift (modified after Corti, 2009)

2.10 Local geology

The study area is mainly covered by Mesozoic sedimentary rocks, Cenozoic volcanic rocks and quaternary superficial deposit (Mengesha Tefera et al., 1996). Accordingly, the area comprises of three geologic units namely Alage formation (PNa), Ashangi formation (P2a) and Ambaradom formation (Ka) (Fig.2.10). Moreover, there are also chert and mud units which are not map-able in regional scales. These minor units are mostly well exposed along stream gorges.

2.10.1 Alage formation (PNa)

The Alage formation comprises transitional sub alkaline basalts with minor rhyolite and trachyte eruptive (Tigel Belay et al., 2009; Mengesha Tefera et al., 1996). It forms cliff slopes along the escarpment and flat topped topography in different parts of the study area (Mengesha Tefera et al., 1996). The Alage basalt is dominantly represented by association of different basalts, and subordinate pyroclastic rocks.

The basalts composed of olivine-pyroxene phyric, olivine-phyric and aphanitic varieties, and the pyroclastics are composed of rhyolitic tuff, rhyolitic obsidian and ignimbrites (Tigel Belay et al., 2009).

During field work, it was observed that, the exposures of the Alage formation is characterized by escarpments or cliff features. Most of the delineated rock mass sections also found in this formations (Fig.2.10). Moreover, the columnar basalts were also situated in this formation.

2.10.2 Ashangi formation (P2a)

Cenozoic volcanism in the northwestern Ethiopian plateau was started by eruption of Ashangi basalt (Tigel Belay et al., 2009). The Ashangie basalts are characterized by strong weathering, tilted basalt, columnar jointing, friable, intense fracturing and crushing. It is highly dominated by by inclined columnar joints (Tigel Belay et al., 2009). It is dominantly composed of basalt with minor interlayering of pyroclastic towards the top part of the succession (Tigel Belay et al., 2009).

During field work, it was observed that, the formation is relatively characterized by flat to gentler slopes as compared to Alage formations. The exposure covers large area including the town Alem ketema as shown in Fig.2.10.

2.10.3 Amba Aradom formation (Ka)

The Amba Aradam formation is the former upper sandstone and name was introduced by Blandford (1870) to define the upper sandstone unit (Tigel Belay et al., 2009; Getaneh Assefa, 1991). Getaneh Assefa (1991) divides the formation into two units Muger Mudstone after its type section at Muger, and DLS after its type section at Debre Libanose. It comprises of sandstone, shale and marl of probably Late Cretaceous age (Tigel Belay et al., 2009; Mengesha Tefera et al., 1996). Amba Aradom formation is not well exposed in the present study area.

During the field work, it was observed that, this formation is characterized by flat to gentler slopes as compared to other formation. However, for the present work, slope rock mass sections were not selected in this formation (Fig.2.10).

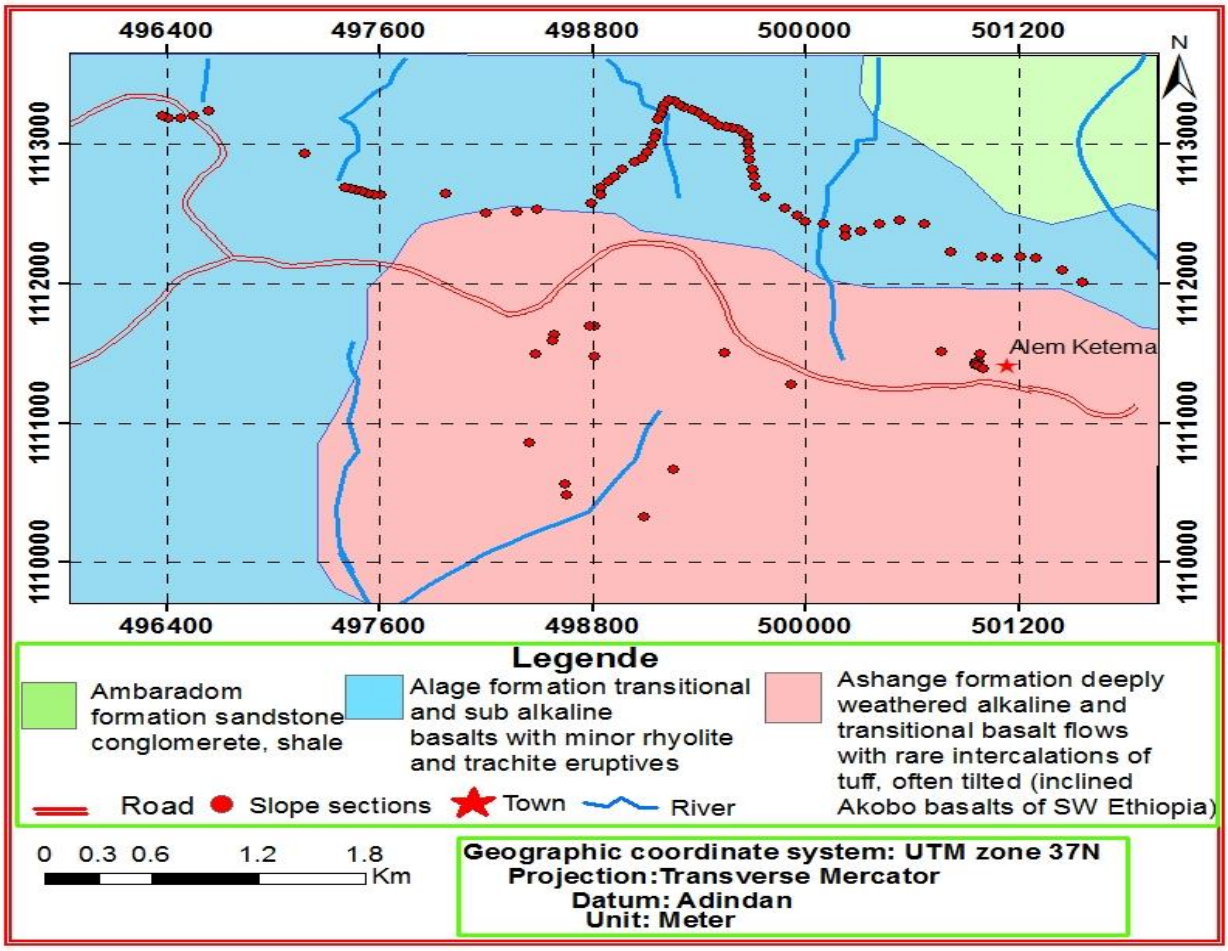

Fig. 2.10 local geology map (after Mengesha Tefera et.al 1996, Ethiopian Institute of Geological Survey)

2.10.4 Quaternary deposits

The alluvial deposits area mostly recent and are deposited as a result of transport of sediments from down wash of sloppy area. The patchy, poorly sorted, massive to crudely bedded sandy conglomerates and gravelly sandstones are interpreted as alluvial fan sedimentation (Wolela Ahmed, 2009). Alluvial fans are developed or accumulated at the edge of uplands often along fault line scarp (Wolela Ahmed, 2008; 2009). It is also transported and deposited by the river water and mainly found along Wonchit and Jemmar river tributaries.

The study area is predominantly covered by residual, colluvial and alluvial materials. However, most of the study area is covered by colluvial deposits.

Colluvials deposits are transported from their original location of formation by the action of gravitational forces. These thick materials are deposited at the toe or in front of the steep slopes as shown Plate 2.1. It is mainly consists of gravel, cobble, and boulder size fragments of basalts.

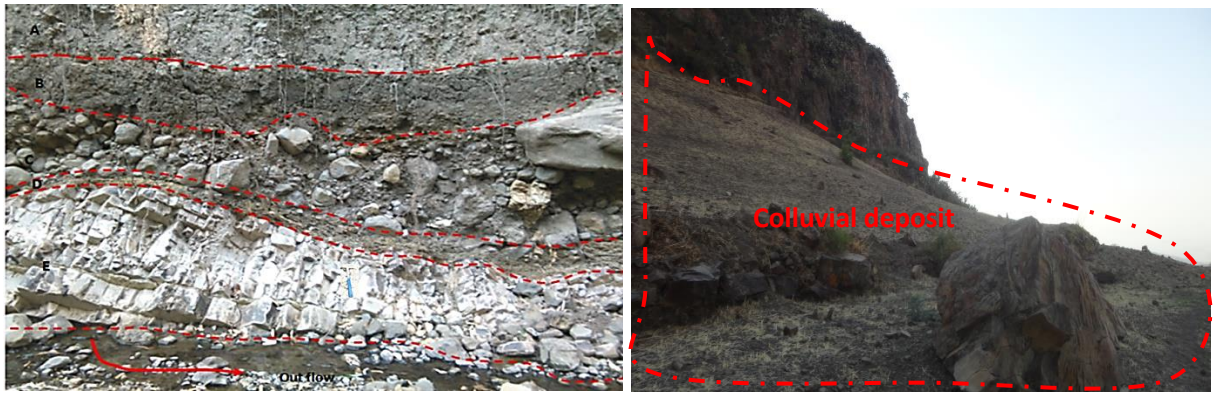

Plate 2.1Thick colluvial deposits

2.10.5 Local geological structures

Rock slope failures are frequently controlled by a complex combination of discontinuities that facilitate kinematic release (Brideau et al., 2009). The presence of geological structures has been frequently associated with rock slope failures (Brideau et al., 2009). Rock slope stability is thus highly dependent on the large-scale mechanical behavior and strength of the rock mass, in which the number and persistence of preexisting fracture zones plays a significant role (Bois et al., 2008). In the study area, the rocks mass exposed on the critical slope sections are dominantly affected by structural discontinuities. These discontinuities mainly include faults, joints, bedding planes and fractures.

2.10.5.1 Faults

Faults are zone of high joint density and rock mass weakening (Brideau et al., 2009; Kim et al., 2004). It is common to influence rock slope stability and gravitational deformation (Bois et al.,2008).

Progressive failure within a rock slope can initiate and propagate in zones preferentially weakened by faults (Bois et al.,2008).

The reduction in rock mass strength was attributed to different processes in a fault zone. These processes includes groundwater infiltration, geochemical alteration in clay-rich fault zones and fracturing related to thrusting were noted as important factors (Brideau et al., 2009).

In the study area fault escarpments were observed with a great extent and stepped appearances. All existing faults in the area are normal faults. The general structural orientations of these faults are striking from NNW to SSE and SSW to NNE. The fault escarpment/cliff also shows an undulating nature as shown in Plate 2.2.

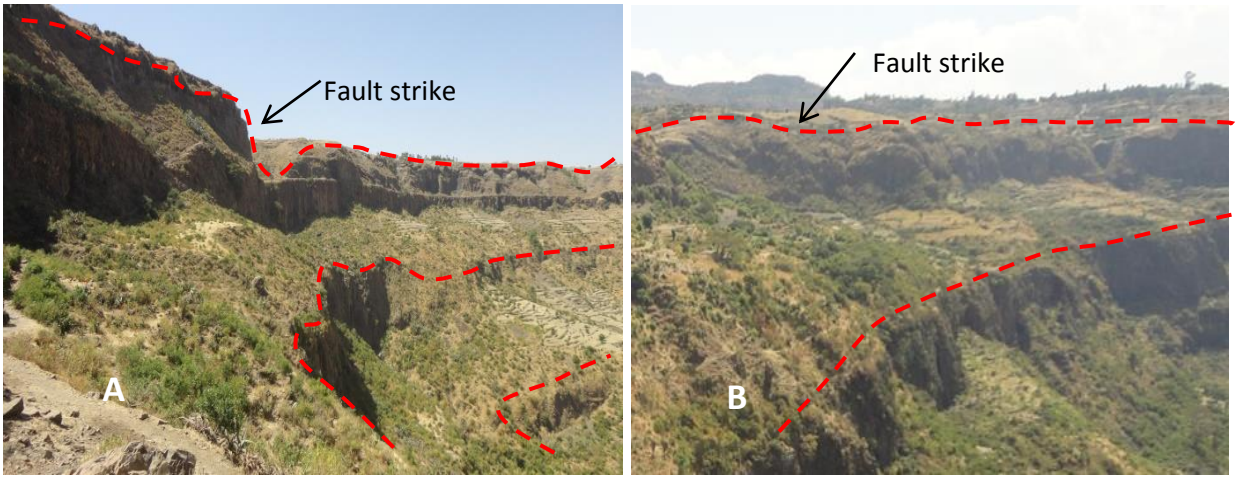

Plate 2.2 Normal faults in the study area (A) NNW-SSE, (B) SSW-NNE striking

2.10.5.2 Joints

Joint set conditions are one of the most significant parameters to characterize the slope rock mass stability conditions (Barton, 1976a; Mauldon, 1994; Agliardi et al. , 2001; Palmström, 1995; 1982; Cai et al., 2004; Akin, 2013; Hack et al, 2003; Brideau et al., 2009).

In the study area, slope rock masses were dominantly affected by numerous joints sets. These joins characterized by different geotechnical and geometrical properties. The overall rock mass quality at the area was degraded by the presence of joints.

During the field work, it was observed that, most of the slope sections were characterized by both systematic and non-systematic joint sets and most of them daylights on the slope faces.

Columnar joints are the one which are frequently observed joint types in the area. Selected slope sections joint set with various properties are shown in Plate 2.3.

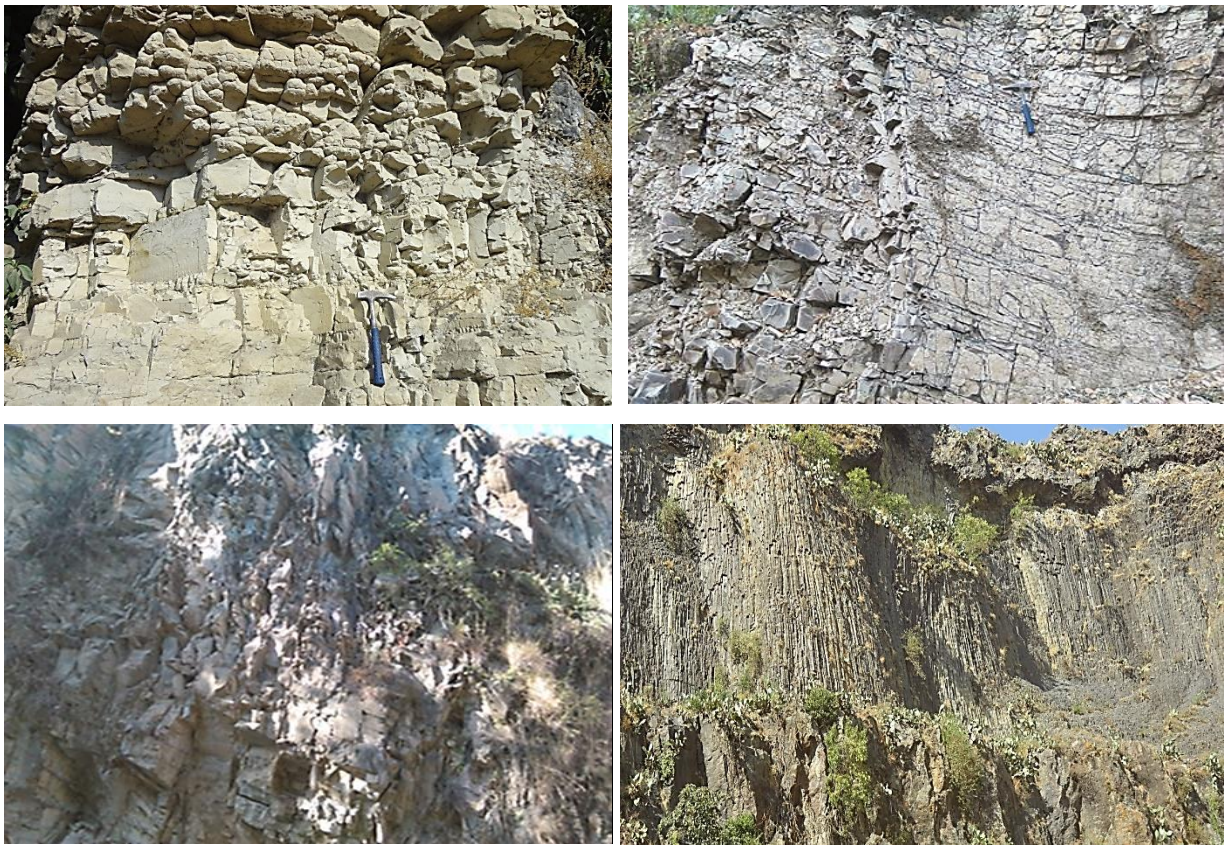

Plate 2.3 selected joint sets with different orientation in the study area

2.10.5.3 Bedding plane

Bedding rock slope stability dominantly controlled by groundwater, bedding inclination, slope height and presence of weak intercalated layers (Kun et al., 2015; Wang et al., 2016). Plane sliding is the most common instability failure mechanism of the bedding rock slope (Liuet al., 2018).

In the study area, bedding planes are mainly observed along the stream cuts (Plate 2.4). Most of investigated bedding planes showed relatively low inclinations as compared to the basaltic cliffs. The bedding planes are more or less perpendicular to the natural hill slopes and are gentler in dip angle. Moreover, the contact between the two lithological units is also strong and dry.

Plate 2.4 Bedding plane

2.10.5.4 Fracture

Natural slope rock mass fracturing is a result of deep weathering of slope rock masses and enhanced by fluid circulation (Zhu et al., 2017; Bachmann et al., 2004). Weathering is manifested in the breakup of material due to development of cracks, disintegration and in surface dissolution in contact with water (Miščević and Vlastelica, 2014). These are the weakened rock surfaces in which the detachment of fragments is most likely to occur, and are at the same time most susceptible to external influences, i.e. to the action of water which penetrates into the rock (Miščević and Vlastelica, 2014).

In the study area, due to highly fractured nature of the slope rock mass, the rock can easily detach from the slope rock mass even with single geological hammer blow. Basaltic rocks found in the study area are characterized by massive, slightly and highly degree of fracturing. Fracturing are dominantly observed on Ashange basalts; however they are not persistent and also showed random orientations (Plate 2.5).

Intensively fractured and weathered rocks have poor quality and shows high degree of slope stability problems. In addition, the stability of fractured rocks is significantly influenced by moisture content and nature of fracture filling materials.

Plate 2.5 Concoidal and irregular fractured basalt rocks

2.11 Status of slope rock masses in the study area

As discussed in the previous section, the slope rock mass observed in the study area are characterized by highly jointed, and have a joint orientation which leads to rock slope failure problems. In the study area, degree of weathering and physiographic features has a significant influence on the stability of slope rock mass. Accordingly, several slope sections are affected by slight to high degree of weathering and weakening of slope rock masses in study area.

During field work, several slope rock mass failures were observed along the slope escarpments. Some of slope rock mass failures cover extensive areas. As a result, farmlands nearby the toe of rock slopes are frequently affected. These slope failures buried and damage the crop as well as finally make the land challenging to plough. Besides, rock slide and rock fall can also block the gully or streams and which diverts the floods towards the farm lands. This is highly responsible for the wear away of corps as well as fertile soils. Moreover, animals are also highly injured by rapid rock falls and rock slide accidents in the study area. There are also a number of houses or infrastructures constructed at the toe, on the slope faces or on the top of unstable slope escarpments.

These uncontrolled buildings near to steep rock slopes or valleys without proper site investigation lead to extreme rock slope failure problems such as house destruction, foot street hindering etc. Some problems which were observed during field work are given Plate 2.6.

Plate 2.6 slope failure problems in the study area :A and B shows problems on G+1 Buildings constructed at the top of unstable chert slope located at the center of Alem ketema (10°03'21.6" northing and 038°59'44.9" easting); (C) Houses constructed at the top of the valley (D) Houses constructed at the toe of the steep slope (E) Road side problems (Alem ketema to meranya road side exposure) (F) Water tanker constructed at the toe of the slope

*****

Chapter III Literature Review

3.1 Preamble

Rock slope failures are geological activities which are controlled by natural physical processes (Hoek et al., 2000). These failures are strongly responsible for huge economic losses, property damage and maintenance costs, as well as injuries or fatalities (Pantelidis, 2010). Specially, rock block falls into an area where there are human activities or construction causes a considerable damages and loss of life (Li et al., 2009). According to Smith and Arnhardt (2016) explanation, rock mass failure hazards are usually defined by the orientation of discontinuities and associated mechanisms of slope failure. The orientation of discontinuities in relation with the orientation of the slope has a marked and often decisive effect on the stability of a slope (Hack, 2002). The type of hazard resulting from the pattern of discontinuities will vary according to the angle and direction of the slope face (Smith and Arnhardt, 2016). Sudden failure of slope material such as debris, rocks and earth can cause extreme damage to life, properties, environment as well as infrastructures.

Rock slope failures can occur when driving forces exceeds the resisting forces (Raghuvanshi, 2017). The main driving and resisting forces are gravity and shear strength, respectively. According to (Hack, 2002) the shear strength along discontinuities is unfavorably affected because water pressure reduces the normal pressure on the discontinuity and reduces the shear strength. Besides, the presence of water may lower the shear strength of the infill material and of the discontinuity wall (Hack, 2002). The detachment of rock block from the steep slope or cliff with a minimum shear leads to drop, bounce, roll or slide along the slope surface at a high speed (Li et al., 2009).

Rock slope failure mechanisms like shear displacement and the resulting different failure modes includes plane sliding, wedge failure, partial toppling and buckling are discontinuity related and depend on the orientations of the slope and discontinuity properties (Hack et al., 2002). These modes of failure are highly influenced by several factors including weathering, geological structures, hydrology, gravity, geology, geomorphology, anthropogenic, vegetation and dynamic forces (Jiewen et al., 2013).

The hilly and mountainous terrains which are dominantly characterized by variable topographical, geological, hydrological (surface and groundwater) and land use conditions, are frequently affected by rainfall triggered slope failures (Kifle Woldearegay, 2013).

Discontinuity conditions play a significant role on the stability and behavior of both natural and engineered slope rock masses. These discontinuities condition including material friction, roughness, discontinuity wall strength and infill material determines the shear and tensile strength characteristics of the discontinuities (Hack, 2002). Slope failures propagation depends on the extent, pattern and types of discontinuity present in the rock mass. Under natural conditions, a rock mass having complicated discontinuities can be influenced by natural and artificial factors (Li and Xu, 2015).

According to Hoek et al. (2000), geological-geotechnical models are important to understand and analyze rock slope failure processes. This includes structural data as well as information on lithology, mineralization and alteration, weathering, hydrogeology and rock mass characteristics such as joint persistence and the condition of joints. The critical initial step in any rock slope stability assessment is a detailed evaluation of the rock mass discontinuity properties.

According to Alzo'ubi (2016), rock slopes susceptible to instability could be divided into two main categories, the structurally controlled slopes and the complex rock slopes. In rock slope stability assessment, the failure surface is often assumed to be structurally controlled and predefined as a continuous plane or series of interconnected planes (Eberhardt et al., 2004). Under natural conditions, a rock mass having complicated discontinuities will be affected by several natural and artificial factors, such as long-term weathering, rain, and construction (Xu, 2015).

Generally, this chapter deals with the description of types of slope, types of rock slope failure, factors influencing rock slope stability, rock slope assessment methods, previous works and genesis of methodology for the present study.

3.2 Types of slopes

Based on the process of formation slopes can be classified as natural and manmade or cut slopes (Mulenga, 2015).

Natural slopes are slopes occur naturally by natural processes of internal (volcanic activities, tectonic activities, earthquake etc.) and external processes (weathering). Therefore, natural slopes include valleys, stream bank, hillside etc. On the other hand, cut slopes are slopes formed through human activities by excavating the natural slope surfaces for different reason such as infrastructures construction (road) and building construction. Their stability is strongly governed by the state of rock mass geometry and strength of discontinuities (Mulenga, 2015).

3.3 Mode of slope failure

Slope can fail in different modes depending on the conditions of slope rock mass structures. These failures may be gradual with very slow movement of the sliding mass/block or instantaneous without warning. There are many different types of mass movement ranging from simple rock falls from a cliff to very large complex movements (Price, 2009). Depending on the geometrical and mechanical nature of the discontinuity and the condition of rock mass, rock slope failure mechanisms can be categorized into four types which are circular, planar, wedge, and toppling failures (Youssef et al., 2012).

3.3.1 Plane failure

Planar failure refers to the sliding of a rock block(s) along one or a set of parallel failure planes oriented unfavorably with respect to the slope face (Pantelidis, 2010). It occurs when a discontinuity strikes parallel or nearly parallel to the slope face and dips into the excavation or valley at an angle smaller than the slope angle and greater than the angle of friction of the discontinuity surface (Raghuvanshi, 2017) (Fig. 3.1). The failure surfaces are usually structural discontinuities such as bedding planes, faults, joints or the interface between bedrock and an overlying layer of weathered rock.

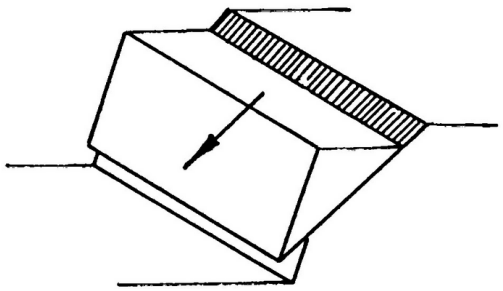

Fig. 3.11 plane mode of failure (after Alzo'ubi, 2016)

3.3.2 Toppling failure

Rock toppling is the most common type of slope failure along highway and they possess very high damaging effect. It is the forward overturning out of slope rock mass (Deep et al., 2014; Alzo'ubi, 2016). Jointed rock mass closely spaced and steeply dipping discontinuity sets that dip away from the slope surface are necessary prerequisites for toppling failure (Fig. 3.2). Toppling failure involves rotation of columns or blocks of rock about a fixed base. The two types of toppling are Flexural and block toppling. Flexural toppling occurs where a series of beds are steeply inclined away from a rock face. In rocks such as slates, schist, inter-bedded limestone and mudstones etc., at the rock face, each layer tends to bend downwards under its own weight. In such a situation, flexural cracks develop in the outer face of the cutting (Pantelidis, 2009). Block toppling occurring where there are frequent close joints in the rock mass such that the weight centroid falls outside the base of the column/block. As a consequence, the blocks tend to tilt forward as rigid columns (Pantelidis, 2009).

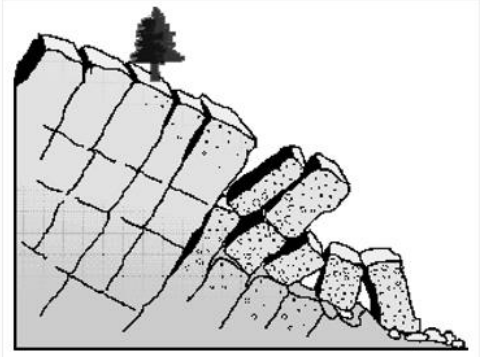

Fig. 3.12 Toppling mode of failure (Deep et al., 2014)

3.3.3 Wedge failure

Wedge failure refers to the sliding of a rock block(s) along two intersecting failure planes oriented unfavorably with respect to the slope face (Pantelidis, 2010). Wedge failure of rock slope occurs when two weak planes intersect to form a wedge. The lines of intersection for both discontinuities are approximately perpendicular to the strike of the slope and dip towards the plane of the slope (Fig. 3.3).

This mode of failure requires that the dip angle of at least one joint intersect is greater than the friction angle of the joint surfaces and that the line of joint intersection intersects the plane of the slope. Wedge type failures are more common occurrence in rock slopes.

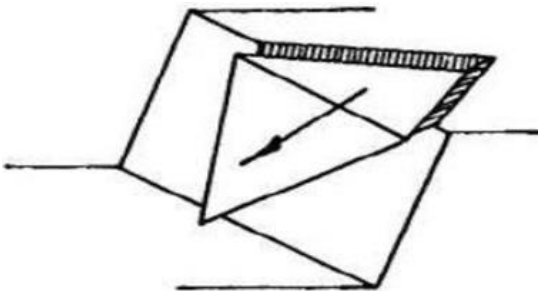

Fig. 3.13 Wedge mode of failure (after Alzo'ubi, 2016)

3.3.4 Circular failure

Circular failure is generally observed in slope of completely weathered rocks, highly disturbed rock with many intersecting weak planes / joints sliding along a curved surface forming a circular arc (Taheri, 2012) (Fig. 3.4). It is essential that all the joints are oriented favorably so that large-scale plane or wedge failure is not possible (Taheri, 2012).

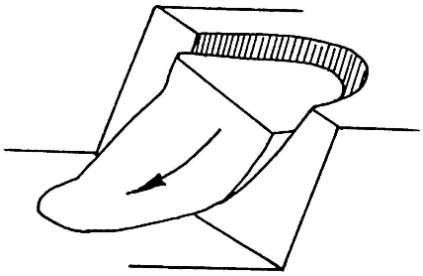

Fig. 3.14 circular mode failure(after Alzo'ubi, 2016)

3.3.5 Rock Fall

Rock fall is a rapid free falling, jumping, leaping, bouncing, or rolling of rock fragments or blocks without a continuous contact with failure plane (Alzo'ubi, 2016) (Fig. 3.5). It is dominantly occurs in steep rock slopes and triggered by water pressure or seismic activity.

Several factors control the behavior of rocks after they have begun traveling from their points of origin such as slope height, slope angle, slope roughness, vegetation, slope geology, natural or

manmade topography, rock soundness, rock size, rock angularity, rock elasticity etc. Rock fall may involve a single rock or a mass of rocks and the falling rocks can dislodge other rocks as they collide with the cliff. It is a major hazard in rock slopes for highways and railways in mountainous regions.

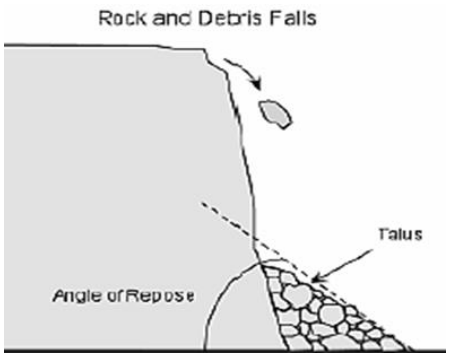

Fig. 3.15 Rock fall (after Alzo'ubi, 2016)

3.4 Factors influencing slope rock mass stability

Rock slope instabilities occur in areas that are subject to several types of external and internal forces. Rock slops stability can be influenced by more than one factor. Most of rock slope instability in the past has been caused by the influence of natural factors (El-Aal and Ansari, 2016).There are different influencing factors which makes rock slope unstable. These factors are briefly described as follows.

3.4.1 Weathering of slope rock mass

Weathering is the mechanical, chemical and biological disintegration and decomposition of slope rock masses (Zare et al., 2011; Mulenga, 2015; Patel, 2017; Pantelidis, 2010; Miscevic and Vlastelica, 2014). These decrease mechanical properties along discontinuity surfaces and increasing the instability potential of the slope (Zare et al., 2011). Physical weathering leads to the opening and propagation of discontinuities by intact rock fracturing, and progressively breaking down the original rock mass to residual material (Mulenga, 2015). Weathering of discontinuities through the passage of water can also strongly reduce the shear strength (Hack, 2002). Therefore, weathering has a great influence on the stability of slope rock mass, because it can reduces the strength and bearing capacity of rocks (Patel, 2017).

The temperature fluctuation is highly responsible for the development of cracks (Gruberet al.,2004). Under the influence of high temperatures in the rock, thermal stress appears which gives rise to several micro-cracks, which then gradually expand as the temperature rises (Sygała et al., 2014).

As a result of the thermal expansion and decomposition of minerals, dehydration, de-hydroxylation and an increase in thermal stresses, considerable changes in the internal structure of rocks take place (Sygała et al., 2014). This results in the reduction of the values of geomechanical parameters of rocks, including the reduction of uniaxial compressive strength (Sygała et al., 2014). Accordingly, weakening of the rocks strength due temperature fluctuation and intensity leads to gradual destruction, i.e. mechanical weathering. In conclusion, temperature has a significant contribution in weathering processes (mechanical, chemical weathering).

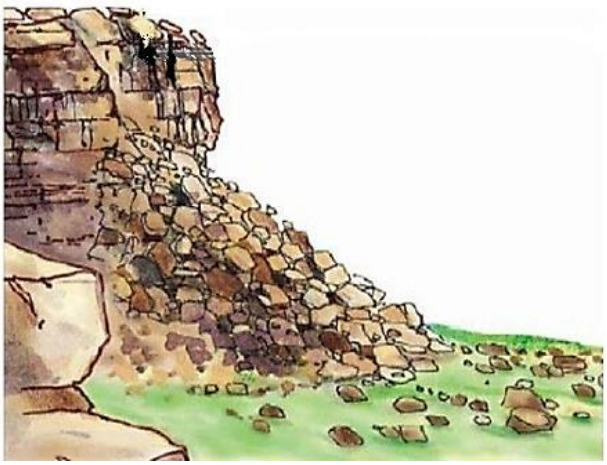

Fig. 3.16 Weathering effects of rock slopes (after Mulenga, 2015)

3.4.2 Geological discontinuities

Discontinuity strength and orientation are the most important properties for rock slope stability assessments (Zare et al., 2011; Hack, 1998). Moreover, stability of the rock slope depends on discontinuity spacing, persistence (continuity), surface characteristics, separation of discontinuity surface and thickness and nature of filling material within the discontinuity surfaces (Price, 2009; Youssef et al., 2012; Hack, 2002; Johnson and Graff, 1991 as cited in Raghuvanshi et al., 2014). According to Salmi and Hosseinzadeh (2014), slope failures in rock masses are mostly controlled by the pattern of discontinuities.

Slope failure mechanisms and their different modes are discontinuity related (Hack and Price, 1995). Accordingly, the orientation of discontinuities together with the shear strength along discontinuities determines the possibility of movement along discontinuities and thus has a major influence on the mechanical behavior of a rock mass (Hack et al., 2002). Among the internal influencing factors of slope stability, the shear characteristics of the discontinuity in the rock mass are important. Because, the discontinuity controls the deformation and destruction of the entire rock slope (Zhaoet al., 2015). Discontinuity persistence has a significant effect on rock mass resistance or strength but persistence is a difficult parameter to measure (Einstein et al., 1983). Non-persistent discontinuity sets do not have the same influence on the stability of a rock mass as persistent discontinuities have (Hack, 2002).

3.4.3 Hydrologic factor

Hydrology is one of the most important external influencing factors of rock slope stability. The principal effect of groundwater in a rock slope is to reduce the stability as a consequence of the resulting reduction in effective stress within discontinuities, which also reduces shear strength along discontinuities (Zare et al., 2011). Factors that increase the shear stresses or decrease the shear strength increase the chances of failure of a slope. Besides, hydraulic distribution form and flow activities of underground water can affect the stability of rock slopes (Zhao et al., 2015).

Ground water (rainfall) is one of the main triggering factors of slope instabilities (Raghuvanshi et al., 2014; Birhanu Ermias et al., 2017; Fischer and Huggel, 2008; Ahmed et al., 2016; Price, 2009). Hydraulic properties, infiltration patterns and amount of rainfall infiltrate have significant influence on the slope stability conditions (Ahmed et al., 2016; Suradi and Fourie, 2014). The influence of rainfall on slope failure mechanisms is mainly governed by the amount of rainwater infiltrate into the slope (Suradi and Fourie, 2014). Rain water infiltration can also increase the pore water pressure inside the rocks and fractures and weaken the rock strength parameters as well as it increases weight of the slope rock mass (Chen et al., 2008; Ahmadi and Eslami, 2011; Chen et al., 2004; Hack, 1998; Zhao et al., 2015; Ahmed et al., 2016; Hack, 2002; Zare et al., 2011).

These excess pore water pressure is certainly the triggering factor for the largest rockslide (Jaboyedoff et al., 2004). Reduced groundwater pressure within a discontinuity increases the shear strength of the infill material (resisting force), whereas lowering the groundwater level within tension cracks reduces the driving force on a rock block (Hack, 2002). Moreover, rainfall facilitates the slope movement by lubricating the sliding plane or it decreases the shear resistance of the slope (Ahmed et al., 2016). Later, this leads to several slope failure problems. Rainfall of extremely high intensity and short duration is usually results a numerous slope failures (Suradi and Fourie, 2014).

Rainwater can affect the slope both mechanically and chemically as a result of mechanical and chemical reactions respectively (Ahmed et al., 2016). This shows that rainfalls facilitates both chemical and mechanical weathering and determine the rate and type of weathering. This is frequently happened during rain seasons. Under conditions of low rainfall, there is a dominance of mechanical weathering which reduces the size and increases the surface area with little change in volume (Cabria, 2015; Miščević and Vlastelica, 2014). The increase in moisture content encourages both chemical as well as mechanical changes.

3.4.4 Gravity

Force of gravity is the main driving force acting on the slope. It is directly proportional to the slope inclination (Hamza and Raghuvanshi, 2017; Raghuvanshi et al., 2014). On the flat surface it holds the material to stay in its position. However, on the slope it resolved in to two components as shown in figure 3.7. These are the force that acting perpendicular to the slope and the force that acting tangential (parallel) to the slope. The perpendicular force helps to hold the objects in place on the slope while the tangential component force causes shear stress that pull the object down the slope. The shear stress or tangential component of gravity increases as slope angle (θ) increases, while the perpendicular component of gravity decreases. The steep slope can increase shear stress more than the resisting forces can pull the slope mass down the slope (Fikre Girma et al., 2015).

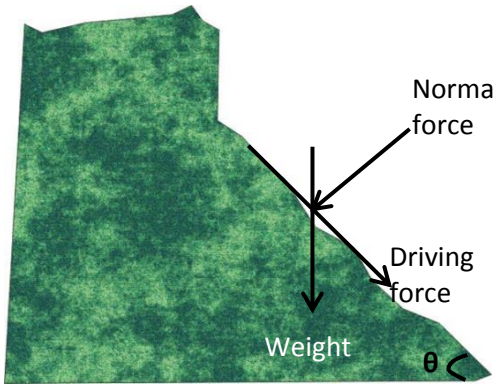

Fig. 3.17 Role of gravity on slope failure

Component of weight "normal" or perpendicular to the slope

Holds the rock in place= Wcosθ

Contributes to a force the resists movement down the slope

Resisting forces = friction+ cohesion

θ= 0, normal force =weight

Component of weight parallel to the slope=driving force=Wsinθ

Small slope angle (θ) = small pulling force

Large slope angle (θ) = large pulling force

3.4.5 Geologic factors

Geology or rock type is one of the most influential parameters concerning slope failure (Zare et al., 2011). Slope geology determines the mechanical behavior of the rock slopes. Rocks slopes composed from different geologic units have different strength as well as different resistance to weathering. Rocks which possess high strength are relatively more resistant to erosion (Hamza and Raghuvanshi, 2017). Soft rocks such as marl, shale or mudstone fails or eroded within short period of time while hard rocks such as basalt, sandstone gypsum, limestone, can stay for long times. Therefore, the slope geology determines the resistance of the rock to the weathering processes.

3.4.6 Geomorphic factors

Geomorphology has an important contribution for susceptibility of slope stabilities. It is directly related to the topography and slopes including slope gradient, aspect and shape of the slope (Biruk Wolde., 2013; Dai and Lee, 2002). According to Dai and Lee (2002) report, the shape of a slope influences the direction and amount of surface runoff or subsurface drainage. The stability of a slope depends upon the inclination of the slope in relation to the strength of slope materials, the strength and orientation of discontinuities (Price, 2009). The steeper slope will be more susceptible to instability as compared to gentle slope (Hamza and Raghuvanshi, 2016). Due to this reason, mountainous and hilly regions are frequently affected by slope stability problems when constructing infrastructure (Mulenga, 2015).

3.4.7 Anthropogenic factors

Human activities play a significant role on slope stability performances. The hilly and mountainous areas are frequently influenced by human activities such as farming, settlement, ditch construction , road cuts, quarrying of building stones or mining activities etc. (Raghuvanshi et al., 2014). Modification of a slope during engineering projects which is changing the slope angle from gentle to steep slope or removing of the slope toe are responsible for a rapid slope failure. Besides, the steeper slope is more prone to instability as compared to gentle slopes (Hamza and Raghuvanshi, 2017). This shows that, as slope angle increase the chance of slope failure also increase. Improper dumping of waste materials from road cut and quarrying operation can cause an overloading of slopes (Biruk Wolde., 2013). This additional weight may increase the chance of slope failure. Generally, human activities such as intensive agriculture, gully erosion, quarrying, road construction, urbanization, land use changes, populations expansion on to new land, removing vegetation, disturbing or changing drainage patterns, destabilizing slopes, over steepening of slopes by undercutting the bottom and loading the top of a slope and improper excavating of slopes are common factors that may trigger landslides are responsible for rock slope instability (Bekele Abebe et al., 2010; Birhanu Ermias et al., 2017).

3.4.8 Effect of vegetation

Plants and their roots are very active in the process of rock disintegration and weathering. The plants roots grow through cracks are made wider and eventually the rock breaks up (Cabria, 2015; Price, 2009). Movement of the trees by the wind produces leverage by the roots on loose blocks. Plants also grow in joints and cracks of the rocks and push them further apart through mechanical weathering. This root wedging is a dominant process in mountains regions which covered by forests and natural vegetation. The general loosening of the rock on the face by tree roots also permits increased infiltration of water that can cause further opening of the cracks.

Plant root affects the rock slope in two distinctive forms, the first effect is the disintegration of rocks in place and the second effect is the splitting off of rocks from steep slopes (https://gammathetaupsilon.org/the-geographical-bulletin/1970s/volume06/article3.pdf).
Disintegration and splitting both proceed much more rapidly in the softer rocks such as sandstones than in igneous material because of the tremendous differences in resistance to stress.

Roots can penetrate through the cracks of rocks to depths of several meters. As the roots grow, they exert a tremendous amount of pressure on the walls of the cracks. This breaks them into pieces(http://epgp.inflibnet.ac.in/epgpdata/uploads/epgp_content/earth_sciences/the_dynamic_earth/17._weathering_processes/et/995_et_et17.pdf).

3.4.9 Dynamic forces

Dynamic forces such as manmade vibrations caused by blasting, machinery, traffic or by earthquakes and dynamic loading are significantly disturb the rock slope (Price, 2009; Hack, 2002). These affect the intergranular bonds of the material and reduce its cohesion.

Uncontrolled blasting results over breaks and extension of tension cracks, opening and loss of cohesion between weak planes, shattering of slope mass and allowing easier infiltration of surface water which produce unfavorable ground water pressures (Karaman et al., 2013; Hoek et al., 2000). Due to effect of blasting and vibration, shear stresses are momentarily increased and it maximizes the dynamic acceleration of material which in turn causes instability in the slope plane (Umrao et al., 2011). It causes the ground motion, fracturing of rock masses or disturbs the intergranular bonds of the material which reduces its cohesion (Youssef et al., 2012).

Earthquake shaking and vibration is a major triggering factor for natural slope to fail (Hack, 2002; Pantelidis, 2009; Birhanu Ermias et al., 2017). Seismic waves passing through rock increase stress which could cause fracturing (Hack and Huisman, 2002). Slopes composed of rock mass having considerable structural discontinuities are significantly affected by ground accelerations. When discontinuous rock slopes subjected to ground acceleration results into widening or opening of structural discontinuities. Tension cracks may develop and normal stress on discontinuities may be reduced during tension phases of an earthquake wave. This allows the movement of blocks in the surrounding ground and then losses the integrity of a rock mass and its consequent collapse (Price, 2009).

3.5 Rock mass slope stability assessment methods

There are a number of rock slope stability assessment approaches or techniques developed by different scholars and organizations.

The assessment of slope stability in rocks is usually determined by kinematic analysis, limit equilibrium analysis, empirical or rock mass classification system.

3.5.1 Kinematic method

Kinematic analyses are carried out using stereographic projection techniques to show the influence of discontinuity sets on the stability conditions and also to indicate the type of potential failure mechanism (Alade and Abdulazeez, 2014; Alzo'ubi, 2016). Kinematic analysis is based on the motion of bodies without consideration of the forces that cause the motion (Karaman et al., 2013; Alzo'ubi, 2016). It also does not consider important geotechnical parameters, such as cohesion and unit weight (Karaman et al., 2013). It is a form of an assessment based on plotting all measured discontinuity planes on a stereographic projection net and evaluating the position (dip and dip orientation) of particular planes (major discontinuity sets) represented as the poles at the centers of the concentration zones (Aksoy and Ercanoglu, 2007). Kinematic analysis, which is purely geometric, examines which modes of slope failure are possible in a jointed rock mass (Yoon et al., 2002). Angular relationships between discontinuities and slope surfaces are applied to determine the potential and modes of failures (Yoon et al., 2002). Based on kinematic considerations and frictional properties of joint planes, stability analyses are performed to see the potentials of toppling, planar sliding and wedge sliding on a stereonet (Alade and Abdulazeez, 2014).

3.5.2 Limit equilibrium method

Limit equilibrium method is based on the concept of the factor of safety (Alzo'ubi, 2016). These system considers shear strength along a failure surface, the effects of pore water pressure and the influence of external forces, such as reinforcing elements or seismic accelerations (Karaman et al., 2013). This system is often inadequate if the slope fails via complex mechanisms (Karaman et al., 2013).

The factor of safety is directly proportional to the shear strength of the potential failure plane which is defined by cohesion (c) and angle of friction (ϕ) (Hoek and Bray, 1981 as cited in Raghuvanshi, 2017). The factor of safety of a slope subject to shear failure can be defined as ratio of shear strength (resisting force) to shear stress (driving force) (Stead and Wolter, 2015; Alzo'ubi, 2016).

If a factor of safty less than 1 indicates that failure is possible, if factor of safty greater than 1 indicates the slope is stable slope and if factor of safty is equal to 1 indicates the slope is in a cretical state of equilibrium (Alzo'ubi, 2016). This method is most commonly used and presents simple solution techniques. However, it is not applied when the slope is failed by complex mechanisms such as internal deformations, progressive creep, etc.

3.5.3 Numerical methods

Numerical techniques are mathematical techniques that use some sort of procedure to obtain the models behavior over time. This technique has been widely used to simulate rock slopes as well soil slopes with complex conditions. Large rock slopes are in general complex due to the heterogeneity of geological formation, stress state, discontinuities, coupled processes (e.g., pore pressures, seismic loading, etc.), geometry, progressive failure and non-linearity of material behavior (Alzo'ubi, 2016; Stead et al., 2006). Because of such complexities, numerical methods are required. The most important numerical methods which are employed for stability analysis of rock slopes are continuum methods, discontinuum methods and hybrid modellings (Stead et al., 2006; Umrao et al., 2011; Alzo'ubi, 2016; Raghuvanshi, 2017).

3.5.4 Empirical method

Empirical methods are based on previous experiences (Alzo'ubi, 2016). According to Alzo'ubi (2016), this method incorporate several factors controlling instability of slopes including slope height, slope angle, geological structure, material type, groundwater conditions other parameters affecting the slope. The empirical method is relatively easy to apply and give the engineer a chance to learn from the past experience. However, it cannot be applied to design large slopes involve very complex geometry, coupled problems and/or complex network of discontinuities, especially if these slopes associated with high risk (Alzo'ubi, 2016).

3.5.5 Rock mass classification system

The rock mass classification systems can serve as an empirical method (Alzo'ubi, 2016). The evaluation of slope stability by rock mass classification system is widely practiced by many researchers, explorers, designers and constructors to facilitate the characterization, classification, interpretation and knowledge of rock mass properties (Tomás et al., 2012). This system provides a quantitative description of the conditions of the rock mass (Salmi and Hosseinzadeh, 2014).

The results from such classification systems are applied to predict both the strength and the deformation characteristics of a rock mass (Salmi and Hosseinzadeh, 2014). There are number of classification systems for assessment of slope stability. Some of geo-mechanical classifications for slope assessments include slope mass rating (SMR), modified slope mass rating (MSMR), geological index strength (GSI) and slope stability probability classification (SSPC).

3.5.5.1 Slope mass rating (SMR) rock mass classification

Slope Mass Rating (SMR) classification system was proposed by Romana in 1985. This geomechanical classification is mostly used for the characterization of rock slopes (Taheri, 2012). The system enables the preliminary assessment of the susceptibility of rock slopes to failure (Irigaray, 2003). It is obtained from Bieniawski's basic RMR (RMRb) by adding a factorial adjustment factor depending on the relative orientation of joints and of the slope as well as an adjustment factor depending on the method of excavation (Romana et al., 2003; Taheri, 2012). The basic RMR is a part of RMR classification system without considering the joint orientation (Trufat Hailemariam, 2009). This is because the joint orientation applied in RMR is without any guideline what unfavorable – favorable means (Trufat Hailemariam., 2009). Romana used the same basic rock mass rating as basic RMR but develop new adjustment factors for joint orientation and excavation to account for the lack of guidelines in the RMR methods.

Therefore, SMR system considers the relationship between parallelism of the rock slope faces and discontinuities, dip amount of the discontinuity and relation between the slope inclination and dip of the discontinuity as well as the excavation method used (Fereidooni et al., 2015; Tomás et al., 2012; Helsdingen, 2017).

3.5.5.2 Modified Slope Mass Rating (MSMR) rock mass classification

Modified Slope Mass Rating (MSMR) classification system was proposed by Anbalagan et al. (1992). It is a modification of rock mass rating (RMR) and slope mass rating (SMR) classification systems in terms of parameters calculation and determination methods (Rahim, 2015). In SMR classification proposed by Romana (1985), wedge failure is not discussed separately. Anbalagan et al. (1992) has modified SMR to make it applicable for wedge failure analysis (Taheri, 2012; Raghuvanshi, 2017). The unstable wedge is a result of combined effect of the intersection of different joints.

In the modified SMR the same method is applicable for plane and toppling failure (Taheri, 2012). However, in case of wedge failure, the plunge and the direction of line of intersection of the unstable wedge are used instead (Taheri, 2012). Thin wedges with low angles are likely to be stable and should not be considered (Taheri, 2012).

MSMR was used to characterize and to propose preliminary rock cut slope design. Design model review and slope remapping was formulated based on the level of recommendation for detailed design model review and slope remapping and the experience level of the engineering geologist/geotechnical engineer (Rahim, 2015). The calculation of MSMR parameters is based on Bieniawski (1989) scheme except uniaxial compressive strength (UCS), discontinuity spacing, and infill material, degree of weathering, roughness and discontinuity orientation (Rahim, 2015). The total value of MSMR is 100 and produced from the sum of basic RMR (RMRb) (Bieniawski, 1989) and discontinuity orientation factor (Rahim, 2015).

3.5.5.3 Geological strength index (GSI) rock mass classification

The geological strength index (GSI) was introduced by Hoek (1994) and Hoek et al. (1995) in order to determine the rock mass strength in different geological conditions (Razmi et al. , 2014). GSI is estimated based on geological descriptions of the rock mass involving two factors, rock structure or block size and joint or block surface conditions (Cai et al., 2004). These produces rock mechanics parameters which give a quantitative output through qualitative input (Xiaohu et al., 2015). However, the rock structures weathering assessment values quantization process is too rough, preventing accurate GSI values to be obtained (Xiaohu et al., 2015).

The GSI system is also related with the concept of block size and condition considering quantitative block volume (Vb) in defined geometric block and the descriptive joint condition factor (Jc) as shown in Fig. 3.8. Vb is determined from the joint spacing, joint orientation, number of joint sets and joint persistence (Palmström, 1995; Trufat Hailemariam, 2009). Vb is significantly important to indicate rock mass quality.

GSI values can be obtained from block volume and joint condition factor Jc which are determined from field descriptions (Cai et al., 2004). The descriptive block size is supplemented with the quantitative block volume (Vb) and the descriptive joint condition is supplemented with the quantitative joint condition factor (Jc) (Cai et al., 2004).

Joint condition factor, on the other hand, is defined by the roughness, weathering, and infill condition. The combination of these factors defines the strength of a joint or block surface.

Cai et al. (2004) proposed a chart for the quantitative classification of the GSI system in which the block volume (Vb) and joint conditions (Jc) are used as quantitative indices. The addition of block volume Vb and joint condition factor JC to the GSI chart represents the quantification of the original qualitative system (Fig. 3.8). The GSI value ranges from 0 to 100.

I. Block volume (Vb)

The block volum (Vb) is strongly related to the degree of jointing, density of joints and intensity of joints. According to Palmstrom (1995) explanation, the block size and its variation depend on the density of the jointing influenced, the number of joint sets and the spacing in these sets. The greater the block size the smaller will be the number of joints penetrating the rock masses. Hence, there is an inverse relationship between the block volume and the number of joints (Palmström, 1995).

The block volume is calculated by using Eq. 3.1, but according to Cai et al. (2004) discussion, compared to the variation in joint spacing, the effect of the intersection angle between joint sets is relatively small. Hence, for practical purpose, the block volume can be approximated using Equ. 3.1. Therefore, the block volume can be measured from the three main joint sets as follow;

$$Vb = \frac{S1*S2*S3}{Siny1*Siny3*Siny3} \quad \text{(eq.3.1)}$$

Where, Vb, s1, s2, s3 and y1, y2, y3 denotes the block volume, joint spacing and the angle between joint sets, respectively.

$$Vb = S1 * S2 * S3 \quad \text{(eq.3.2)}$$

II. Joint condition factor(Jc)

In the GSI system, the joint surface condition is defined by the roughness, weathering and infilling condition (Cai et al., 2004). The joint condition factor is meant to represent the friction properties of the block faces (i.e. joints) and the relative scale effect imposed by the joints (Palmström, 1995).

The combination of these factors defines the strength of a joint or block surface. Joint condition factor (Jc) is defined using the following expressions;

$$Jc = \frac{JwJs}{Ja} \quad \text{(eq.3.3)}$$

Where Jw and Js are the large-scale waviness (1 to 10m) and small-scale smoothness (from 1 to 20 cm) and Ja is the joint alteration factor (Cai et al., 2004). The joint condition factor Jc ranges from 0.1 to 12.

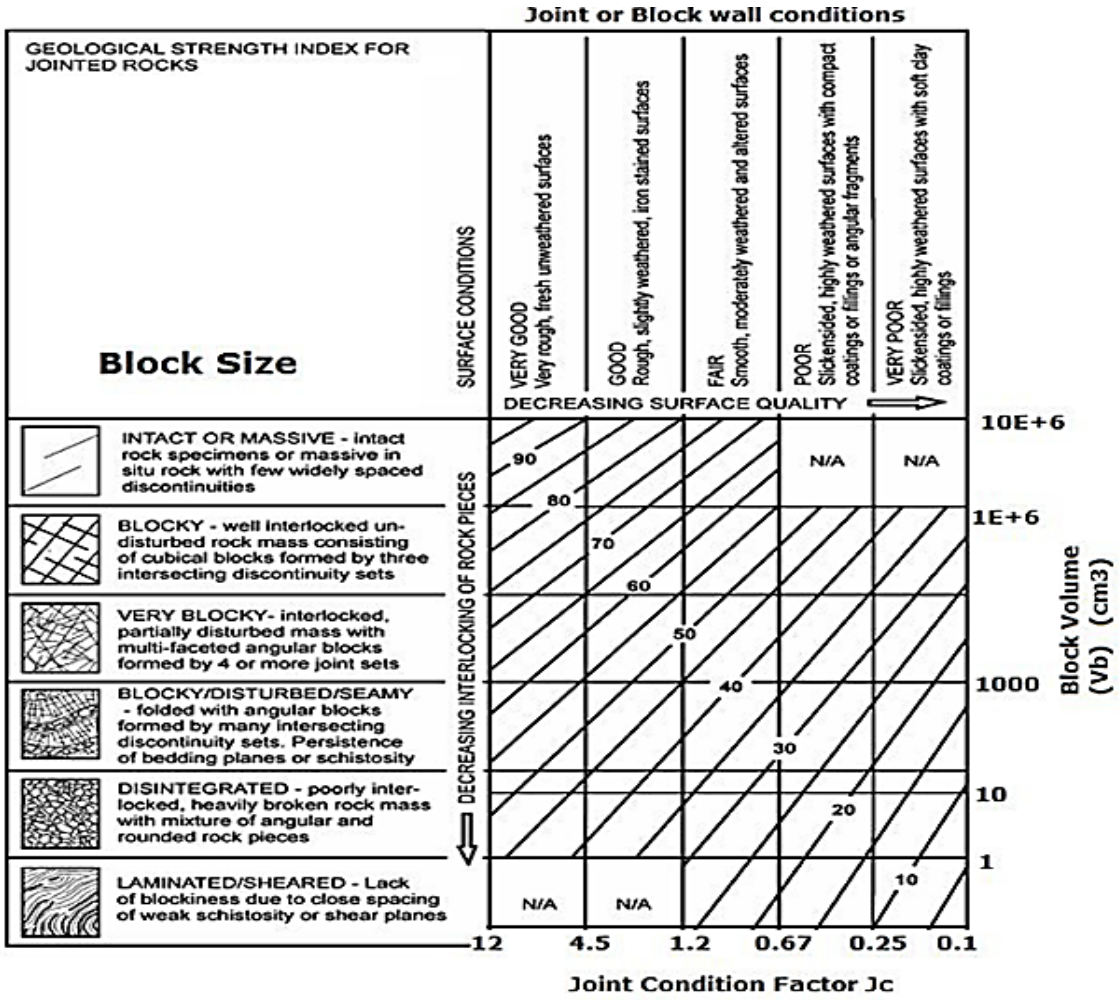

Fig. 3.18 Quantification of GSI chart (after Cai et al., 2004)

Modified GSI system introduces the parameters such as surface condition rating and structure rating (Fig. 3.9). Because, the lack of parameters to describe surface conditions of the discontinuities and the rock mass structure prevents to obtain a more precise value of GSI.

For these reasons, the authors suggest two terms namely, `structure rating, SR' and `surface condition rating, SCR'. Structural rating(SR) is defined based on volumetric count (Jv), whereas surface condition rating (SCR) were estimated from input parameters such as (roughness (Rr), weathering (Rw) and infilling (Rf) as shown in Fig.3.9 (Singh and Tamrakar, 2013; Cai et al., 2004; Sonmez and Ulusay, 1999; Singh et al. , 2015).

Volumetric joint count (Jv), which is defined as the sum of the number of joints within a unit volume of rock mass.

It is suggested to be used for the description of structure of the rock mass (Sonmez and Ulusay, 1999). Volumetric joint count can be calculated using the following equation (Singh and Tamrakar, 2013).

$$Jv = \frac{1}{S1} + \frac{1}{S2} + \frac{1}{S3} \quad \text{(eq.3.4)}$$

Where, Jv volumetric joint count and S1, S2 and S3 are the average discontinuity spacing the joints sets. Therefore, SR and SCR can be calculated using the following equations.

$$SR = -17.5 \ln (Jv) + 79.8 \quad \text{(eq.3.5)}$$

Where, SR and Jv denotes structure rating and volumetric joint count respectively

$$SCR = Rr + Rw + Rf \quad \text{(eq.3.6)}$$

Where, SCR, Rr, Rw and Rf denotes the ratings for surface condition, roughness, weathering and infilling, respectively.

It is now possible to estimate a more precise GSI value from the intersection point of SCR and SR ratings when the modified GSI chart (Fig. 3.9). Descriptive terms corresponding block size and intervals of Jv suggested by ISRM (1981) and by Sonmez and Ulusay (1999, 2002) are given in Table 3.1.

Table 3.1 Descriptive terms corresponding block size and intervals of Jv suggested by ISRM (1981) and by Sonmez and Ulusay (1999, 2002)

Description by ISRM(1981)	Jv(joint/m3)	Descriptions for GSI(Sonmez and Ulusay,1999)	Descriptions for GSI (Sonmez and Ulusay,2002)
Very large blocks	<1	Blocky(B)	Intact or massive(M)
Large blocks	1-3	Blocky(B)	Blocky(B)
Medium size blocks	3-10	Very blocky(VB)	Very Blocky(VB)
Small blocks	10-30	Blocky/disturbed(B/D)	Blocky/disturbed(B/D)
Very small blocks	30-60	Disintegrated(D)	Disintegrated(D)
Crushed	>60	Disentegrated(D)	Disintegrated(D)

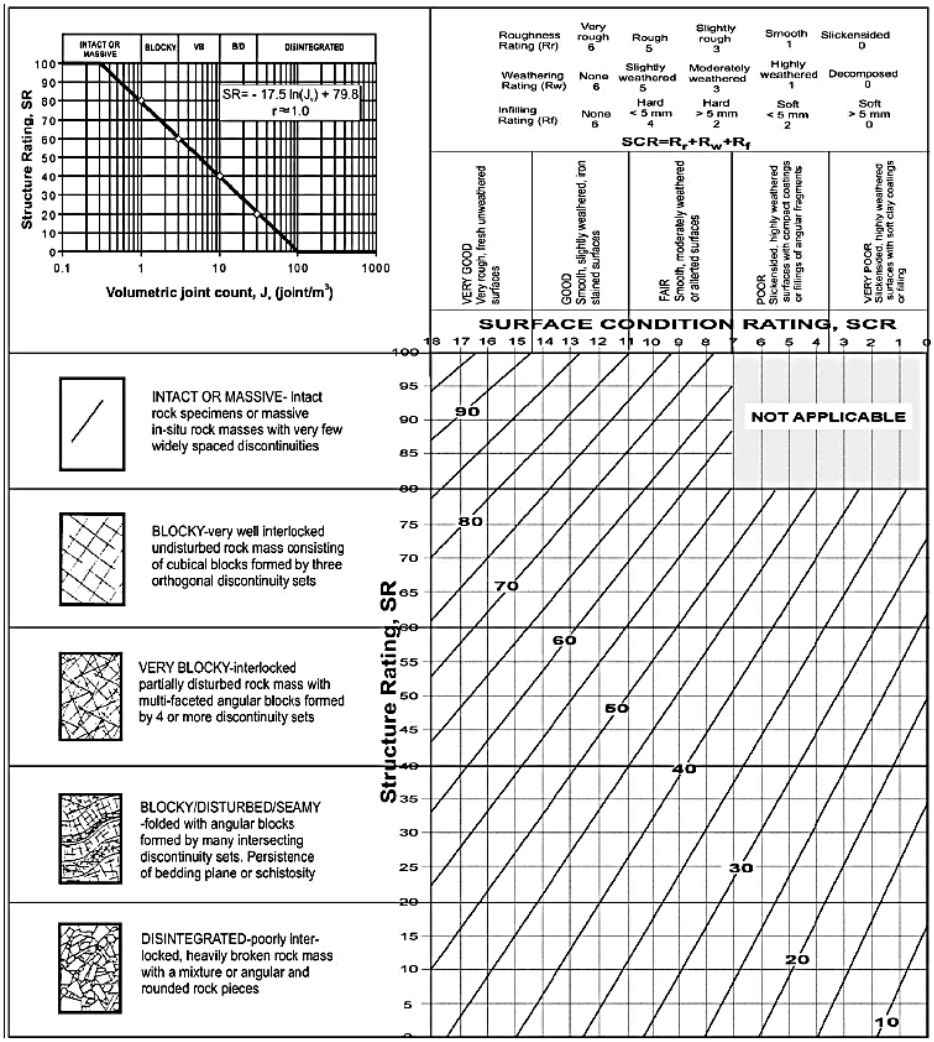

Fig. 3.19 The modified quantitative GSI chart (after Sonmez et al., 2003)

3.5.5.4 Slope Stability Probability Classification (SSPC)

The slope stability probability classification (SSPC) system was introduced by Hack (1996) in order to determine rock mass slope stability probability condition. Further, Hack (1998) modified the initial systems and parameters in the system and provided a better and appropriate indication of maximum influence of each parameter on the final slope stability probability. The SSPC system provides the slope stability probability which is important for assessment the slope failures.

According to Hack et al. (2002) explanation, in existing classification systems, some parameters are difficult or impossible to measure. These parameters include water pressure, deformation of rock mass. Moreover, most systems present the final stability as a single point value with a description. These might give results that are difficult to appreciate. Parameters influence the stability rating for a slope whose instability may be caused by a physical mechanism that is independent of those parameters. For example, intact rock strength is used to calculate the stability rating, while a slope is unstable because of sliding on a discontinuity with a thick clay infill (Hack et al., 2002). This shows that, intact rock strength has no importance for the stability or instability of that slope.

Expressions for uncertainty in establishing rock mass properties and for variation of properties and the applicability of the calculation method are also absent in existing rock mass classification systems, although they have a fundamental importance in establishing the safety of a slope design (Nilsen, 2000 as cited in Hack et al., 2002). Another important problem identified in existing systems is that generally no distinct differentiation is made between the rock mass in the exposures used for the classification and the rock mass in which a slope is to be made (Hack et al., 2002). Local influences such as weathering and method of excavation may be the cause of major differences (Hack et al., 2002).The raveling type of failure of slopes is again generally not considered in classification systems, although rock mass classification is the only feasible option for the predicting this type of failure (Maerz, 2000 as cited in Hack et al., 2002).

For these reasons which are described by (Hack et al., 2002) and the generally unsatisfactory results obtained with existing rock mass classification systems, a new classification system for

slope stability assessment has been developed by Hack (1998). The newly developed classification system (SSPC) is mainly based on the following three concepts (Hack et al., 2002).

1. The introduction of the principle of a three step classification system to describe the 'exposure', 'reference' and 'slope' rock mass in a slope unit.
2. The assessment of stability by determining the probability of the occurrence of different failure mechanisms instead of a single-point rating value.
3. Unambiguous (clear) and simple data collecting procedures in the field.

3.5.5.4.1 Three step classification system

According to the three step analysis method in the SSPC system, failure probability of the rock slopes was assessed based on the possible failure mechanisms and modes of the slopes.
This three-step analysis method classifies rock mass into three categories RRM, RRM, and SRM and obtains the parameters related to the three types of rock mass in the field, then makes a stability analysis of a slope (Hack et al., 2002).

1. Exposure rock mass (ERM) - ERM is rock mass under exposure, and is mainly affected by factors such as weathering and the excavation method.
2. Reference rock mass (RRM) - RRM is an imaginary, un-weathered and undisturbed rock mass.
3. Slope rock mass (SRM) – SRM is the rock mass in which the existing or new slope is to be situated.

Rock mass parameters of importance are described and characterized in an exposure, resulting in the 'exposure rock mass'. Local influences on the parameters measured in the exposure such as weathering and the disturbance due to the excavation method used to create the exposure are then taken into account. This converts the parameters for the ERM to those of the theoretical fresh rock mass that exists below the zone of influence of weathering and other disturbances - the 'reference rock mass' (RRM) (Hack et al., 2002; Hack, 1997).

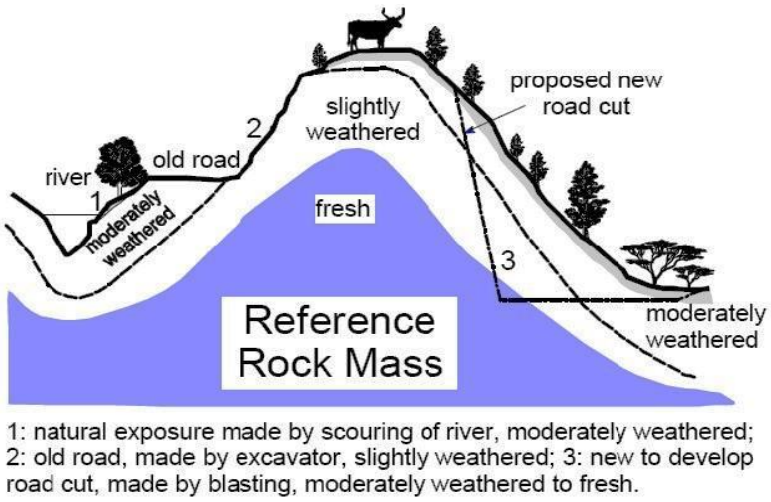

Fig. 3.20 Sketch of exposures in rock masses with various degrees of weathering and different types of excavation, and indicating the concept of the 'reference rock mass (After Hack et al., 2002)

3.5.5.4.2 Failure mechanisms

Slope failure mechanisms (such as shear displacement) and the resulting different failure modes (plane sliding, wedge failure, partial toppling and buckling) are discontinuity related (Hack, 1998; Hack et al., 2002). These failure modes depend on the orientations of the slope and discontinuity. On the hand, there are also failure mechanisms which are not related to the orientations of the slope and the discontinuities can cause failure of a slope. For example, the breaking of intact rock under the influence of the stresses in the slope and the removal of slope surface material due to surface (rain) water and seepage of water out of the rock mass (raveling) (Hack et al., 2002).

3.5.5.4.3 Rock mass parameters

The determination of discontinuous rock mass properties can be done with relatively simple means in the field. The rock mass properties necessary for the SSPC system includes intact rock strength and discontinuity spacing and condition.

I. Intact rock strength

Intact rock strength is mostly defined as the strength of the rock material between the discontinuities and often it is not very important (Hack and Huisman, 2002).

Intact rock strength mainly determines the strength of the intact rock block material however it also governs partially the strength of a rock mass. Intact rock strength is established with relatively simple means in the field through a simple approach involving geological hammer blows and finger pressure or crumbling by hand (Hack and Huisman, 2002).

II. Orientation, spacing and condition of discontinuities

The orientation of discontinuities in combination with the shear strength along discontinuities determines the possibility of movement along discontinuities and thus has a major influence on the mechanical behavior of a rock mass (Hack et al., 2002). It should first be established whether discontinuities belong to a 'set' or should be treated as a 'single' feature. The parameters for a set of discontinuities are determined by averaging of the parameters of individual discontinuities. The characteristic properties of each discontinuity set are the average of the properties of each measured discontinuity belonging to that set (Hack et al., 2002).

III. Shear strength of a discontinuity

The shear strength of a discontinuity is determined by the sliding criterion that converts a visual and tactile (roughness established by touch) characterization of a discontinuity into an apparent friction angle along the discontinuity plane (Hack and Price, 1995).

3.5.5.4.4 Stability assessment

The stability of rock slopes is determined by two different approaches. The first approach is related to the orientation of the discontinuities and the slope ('orientation-dependent stability'). This is the determination of the stability of the slope related to the discontinuities in the rock mass. The second approach is the determination of the stability of the slope in relation to the strength of the rock mass in which the slope is made. This the second assessment is independent of the orientation of the discontinuities and of the slope ('orientation- independent stability') (Hack, 1998; Hack et al., 2002; Li and Xu, 2015; Hack, 2002) .

I. Orientation dependent failure

As the name indicate the orientation dependent failure mechanisms depend on the orientation of the slope and the discontinuities in the rock mass which is mainly governed by shear strength of the discontinuity (Hack et al., 2002).

Slope failure mechanisms such as shear displacement and the resulting different failure modes including plane sliding, wedge failure, partial toppling and buckling are discontinuity-related (Hack et al., 2002). In SSPC system, sliding and toppling criteria were developed to predict the orientation-dependent stability of a slope.

II. Orientation independent failure

As the names indicate the orientation independent is not related to the orientations of the slope and the discontinuities in the rock mass. Intact rock strength, block size and shear strength along discontinuities thus have an influence on the development of this failure (Hack et al., 2002;). Most of the failures in these slopes were approximately linear, although not following one and the same existing discontinuity plane (Hack, 2002). An example of this type of failure is the breaking of intact rock under the influence of the stresses in the slope and the removal of slope surface material due to surface (rain) water and seepage of water out of the rock mass (raveling). In addition the shear strength along a discontinuity 'sliding criterion' and 'rock mass cohesion' and 'rock mass friction' can be determined (Hack et al., 2002).

The orientation independent stability of a slope assessment leads to a rock mass strength criterion. The rock mass strength criterion is based on a Mohr-Coulomb model for shear strength in which the cohesion and friction are those of the rock mass and determined by classification of the rock mass properties, e.g. by determining intact rock strength, discontinuity spacing and discontinuity condition (Hack et al., 2002). The rock mass friction and cohesion are dependent on intact rock strength, block size (e.g. discontinuity spacing) and shear strength (e.g. the condition of discontinuities) along all discontinuities in the rock mass (Hack et al., 2002; Hack, 2002).

3.6 Previous works

In the present study area, there were no researches conducted related to rock slope stability assessments. However, there are two main studies which have been carried out around Alem Ketema. These works were focused on the landslide hazards. The first study was conducted by Birhanu Ermias et al. (2017), which was entitled by landslide hazard zonation following the route from Alem Ketema town to Ambat village and the second study was conducted by Tsion Aragaw (2017), which was also entitled by an integrated expert evaluation and statistical

approach for landslide hazard evaluation and zonation – A case along Alem Ketema – Fetra Route corridor.

Both studies have delineated the locations which have a serious landslide hazard problem in the study area. According to Tsion Aragaw (2017) and Birhanu Ermias et al. (2017) presentation, the study area falls in to two landslide hazard zones. These are moderate hazard zone and high hazard zone. The high hazard zones are characterized by moderate steep to steep slopes, moderately weathered rock mass, soil slope deposits and disintegrated rock mass, significant groundwater surface traces such as flowing and dripping, slope instabilities due to structural discontinuities. The moderate hazard zones are characterized by relatively gentler slopes, dry to low groundwater surface traces, alluvial soil deposit, and blocky disturbed (mainly) and disintegrated but fresh to slightly weathered rock mass and the effect of structural discontinuities is relatively less (Birhanu Ermias et al., 2017).

3.7 Genesis of methodology for the present study

A thorough literature review was carried out to have a detailed knowledge on the subject matter. This helped to understand various aspects related rock to mass classification systems. Literature review also provided clear information on, the influencing factors, failure mechanisms, and triggering factors of rock slope instability. Literatures include journal, unpublished reports, online internet sources and books.

Slope stability probability classification (SSPC) technique was considered and applied in the present research study; as this technique has some degree of subjectivity during field slope rock mass parameters descriptions which are responsible for slope instability or assigning weight and ratings. The main advantage of this technique is that it considers many parameters that are responsible for slope instability as well as the technique is simple and cost effective.

GSI technique was also practiced in the present research for the comparison purpose. This comparison was very helpful to assess stability condition of the slope rock mass in the study area. Such approach of using two different methods has helped to provide more rational results as it was possible to compare the results of each technique.

*****

Chapter IV Methodology And Data Collection

4.1 Preamble

In achieving the objectives of this research, a certain defined set of methodological approaches were followed (Fig 4.1); that incorporates the collection of secondary and primary data; engaging slope stability probability classification (SSPC) and geological strength index (GSI).

The secondary data are those data that aided to delineate preferred slope sections. This data also helped to describe the general conditions of the study area includes geological map (EGS, 1996), topographic map (1:50,000), published and unpublished landslide hazard zonation maps (Birhanu Ermias et al., 2017; Tsion Aragaw., 2017), DEM (STRM, 30m resolution), satellite image from USGS and Google Earth and meteorological data (Annual rain fall and temperature) from Ethiopian Meteorological Agency. The DEM and satellite images were found to be very important to organize all maps in this research.

On the other hand, the primary data were also collected through systematic and careful field measurements and mapping on selected slope rock masses. These data are slope rock mass parameters including geometrical features, discontinuity nature, degree of weathering, lithology and intact rock strength, which are involved in slope rock mass assessments using SSPC and GSI. These classification approaches were selected as they are relevant in characterization of slope rock mass stability by considering easily measureable parameters to define slope instability conditions in the study area.

In this study, the rock mass slopes were selected based on their accessibility, representation, slope geometry, discontinuity pattern, stability conditions and degree of exposure. Accordingly, 92 slope sections have been selected within three lithological units (basalt, mud and chert) and examined thoroughly to define the rock slope stability assessment of the study area. Each slope's discontinuity conditions were measured and described. Determining the parameters for a 'set' of discontinuities requires a form of averaging of the parameters of individual discontinuities.

The characteristic properties of each discontinuity set are the average of the properties of each measured discontinuity belonging to that set. These collected data were utilized for SSPC and GSI systems to assess the stability condition of slope rock masses in the study area. Generally, three discontinuity sets were identified on the slopes in the study area.

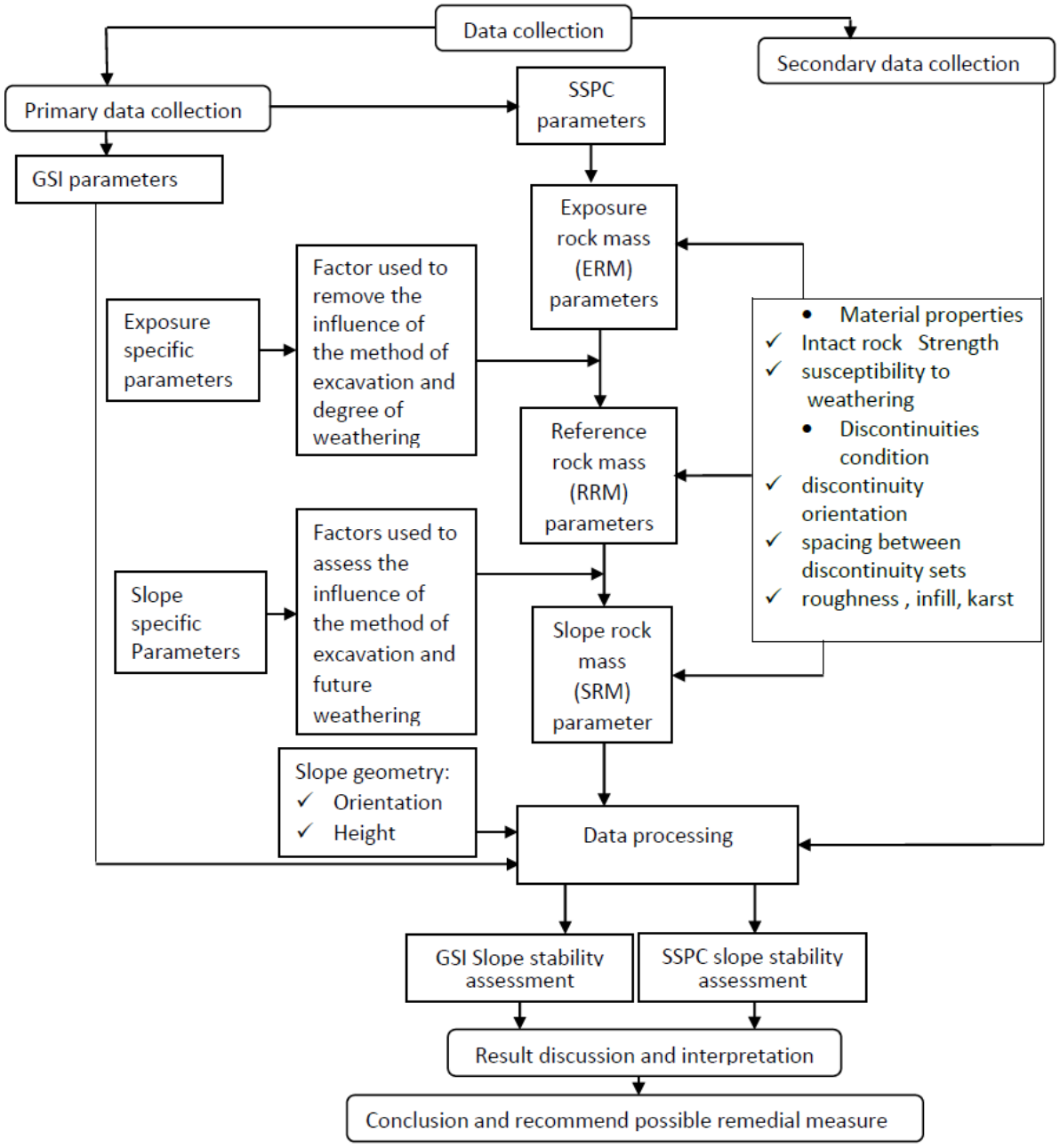

Fig. 4.21 Flow chart of methodology based on the concept of SSPC

4.2 Slope rock mass delineation

Before field work, spatial delineation of rock slopes were performed from DEM using geometrical features such as aspect, steepness and slopes conditions. Initial site reconnaissance survey was conducted on the delineated slopes. Further, detailed slope parameter measurements were made through systematic approach.

Field rock mass slope delineations were performed by considering the accessibility, slope geometry, discontinuity pattern, stability conditions and degree of exposure. Accordingly, 92 rock mass slope sections were delineated (Fig. 4.2) and the geographical coordinates of slope sections are given in Annex 8.9.

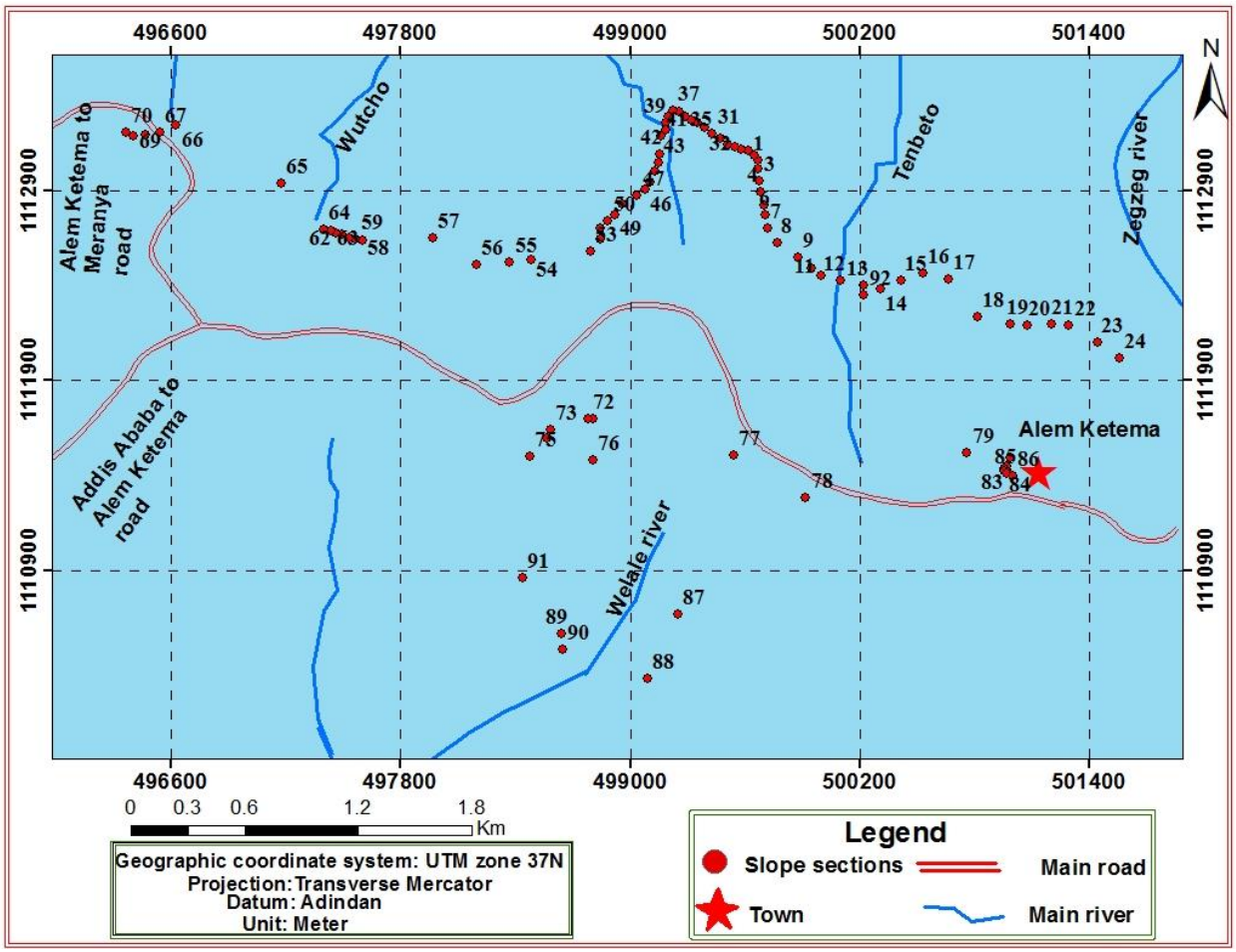

Fig. 4.22 Delineated slope rock mass locations

4.3 Visual estimation of slope stability

In defining the stability status of the slopes, simplified visual estimation of slope stability conditions were primarily estimated based on the practical geotechnical engineering approach (Hack, 1998). Accordingly, slopes stability for 92 sections has been classified in to three classes depending upon the absence, presence or impending presence of stability problems (Table 4.1). The slope stability status then used to verify the results of the slope stability evaluations by SSPC and GSI assessments. The visual slope stability assessment values are given in Annex 8.8.

Table 4.2 Standards for the visual estimation of slope stability (after Hack, 1998) and number of slope sections in each stability class

Class		Description	Number of slope faces
1	Stable	No signs of present or future slope failure	19
2	Problems in near future	Slopes show all signs of impending failures but no failure has taken place	43
3	Problems	Slopes presently shows of active failure and have the potential for future failure	30
Total			92

4.4 Set of discontinuities

A discontinuity set is a differentiating and grouping of discontinuities in a given slope rock masses. Discontinuity differentiating and grouping are very essential, because the descriptions of each single discontinuity in a slope rock mass would lead to an unreasonable quality of work. A major problem with many classification systems (except SSPC) incorporate the properties of only one discontinuity set to express the effects of discontinuities in their system. There may not be problems if all discontinuity sets have the same properties. However, a rock mass with discontinuity sets having different properties is often difficult to decide which discontinuity set should be considered in the determination of the rock mass quality.

Some authors (Bieniawski, 1989; Barton, 1976; Laubscher, 1990 as cited in Hack, 2002) indicated that, the condition of the discontinuity set with the poorest condition should be

included or the condition of the discontinuity set that has the most adverse influence on the rock mass quality or engineering application should be included. According to Romana (1985) recommendation, the rating should be calculated for each discontinuity set and the lowest resulting rating should be used to determine the slope stability.

Some effort initial goes to define the general set of discontinuities in the study area through stereographic analysis and was found that three sets of discontinuity sets rationally define in the slopes (Plate 4.1). Consequently, the descriptions and characterization of discontinuities were given for a set. Representative values for a discontinuity set are then set from the individual measurements using simple mathematical mean.

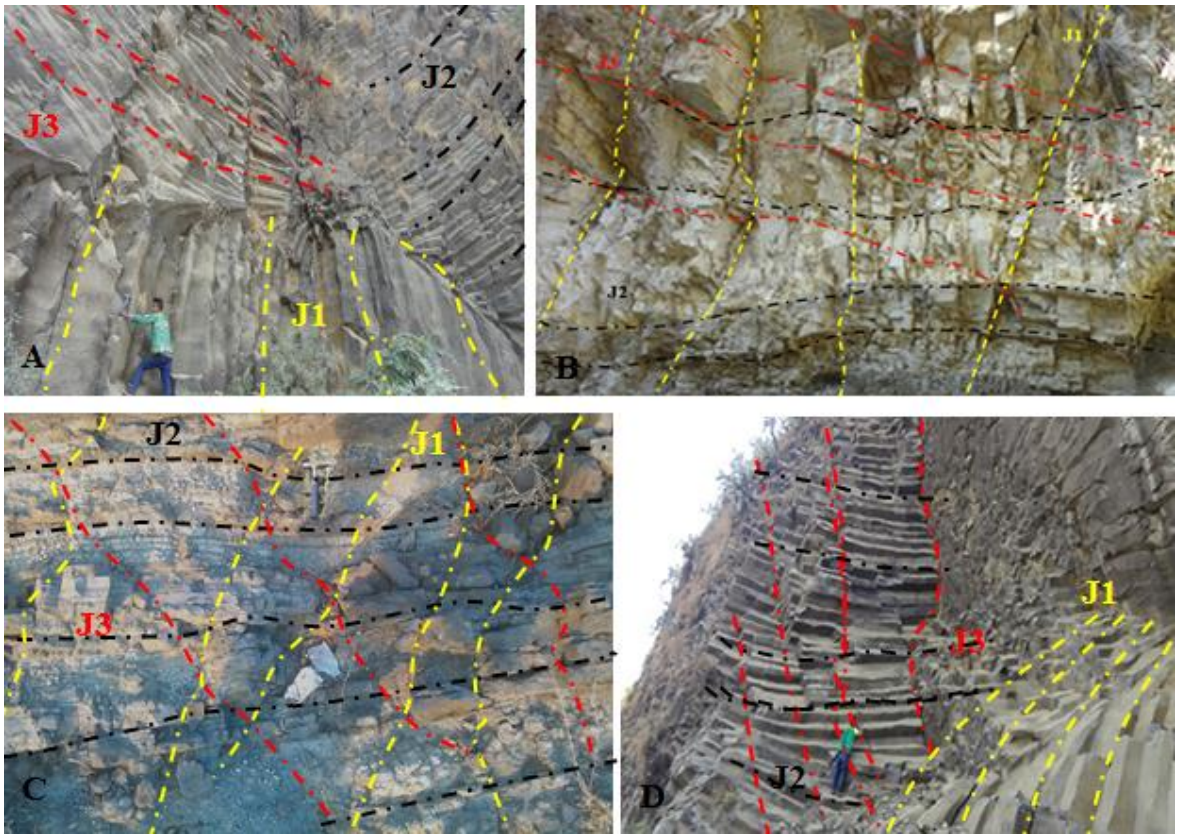

Plate 4.7 Photo showing different discontinuity sets orientations ((A), discontinuities in columnar basalt (B), discontinitite in chert unit (C), discontinuities in mud unit (D), discontinuities in columnar basalt

4.5 SSPC data acquisition

For SSPC system, slope rock mass parameters which were collected during field work include slope lithology, degree of weathering, slope and discontinuity orientation, discontinuity spacing

(block size), infill material, karst condition, intact rock strength, slope height, method of excavation, large scale roughness, small scale roughness, persistency, ground water condition and discontinuity separation (aperture).

4.5.1 Slope lithology

Slope lithology plays a major role on the mechanical behavior of the rock mass. As discussed in the previous sections, lithologic difference causes variabilities in strength and resistance to weathering that further influences slope stability conditions (Hamza and Raghuvanshi, 2017).

In the present research, different lithological units were mapped along the slope sections. The slope lithology mapped in the 92 rock slopes are basalt, mud and chert units (Table 4.5). It is found that about 82.6% slopes were constituted by basalt; while the rest 9.8% and 7.6% of the slopes were constituted by mud and chert, respectively. Basalt is relatively strong as compared to chert and mud units. It is more resistance to weathering. The rock mass slopes constituted by basalts are generally characterized by stable slope conditions. On the other hand, the slopes constituted by chert and mud units are relatively weak and susceptible to weathering; thus are relatively weaker slopes.

4.5.2 Degree of weathering

Weathering has a considerable influence on mechanical and geotechnical properties of rock masses. It is one of the prominent factors that could reduce the stability of a slope by weakening the rock mass via extension, solution and alterations (Mulenga, 2015). It also lowers the values of intact rock strength. When the rock mass are exposed for a long time, the rock breaks into small pieces and the number of joint sets becomes visible. The development of new joints and fractures speeds up physical weathering and enables deeper penetration of chemical weathering effects on a rock mass (Hack and Price, 1995).

In SSPC system, weathering is also considered as one of the significant local influences. The three-step approach allows for correction of weathering. The exposure rock mass parameters are determined and converted into reference rock mass parameters by correction for local weathering and method of excavations. However, the present research was conducted on natural slopes; so that, method of excavation has no influences on parameters. Therefore, the only local influencing

factor is weathering. Resistances to weathering are different in different lithologies. Strong rocks such as basalt has high resistance to weathering than soft rocks such as mud and chert units (Hamza and Raghuvanshi, 2017). . During field work, it was observed that mud and chert units were more weathered as compared to basaltic rock units.

In this study, the degree of weathering was determined through critical observation, hand pressure and geological hammer. It is then estimated in the field based on BS5930 (1981) standard (Annex 8.7.1) and the values are given in Annex 8.1.1. Accordingly, about 18.5% were found to be highly weathered, 32.6% moderately weathered and 48.9% of the slope sections are slightly weathered. Field descriptions of degree of weathering are given in Table 4.3.

4.5.3 Slope and discontinuity orientation

It is an important parameter affecting rock slope stability, because failure type and kinematic instability are influenced mainly by this feature (Jiang et al., 2013). The relationship between discontinuities and slope orientation controls the failure mechanism and modes of rock slopes subjected to structural control failure (Hack, 2002; Li and Xu, 2015). In SSPC method, the effect of discontinuity orientation on slope stability primarily shows the change of the apparent angle of the dip of the discontinuity plane in the direction of the slope dip (AP) (Li and Xu, 2015). In each rock slopes, the discontinuity sets defined specifically within the slope (Table 4.2); though the general discontitnty orientation in the study area discontinities are mainly grouped in to three sets as shown in rose diagrams (Fig.4.3) and contur plots (Fig. 4.4). The rose diagrams and contour plots are given for three lithology units separately.

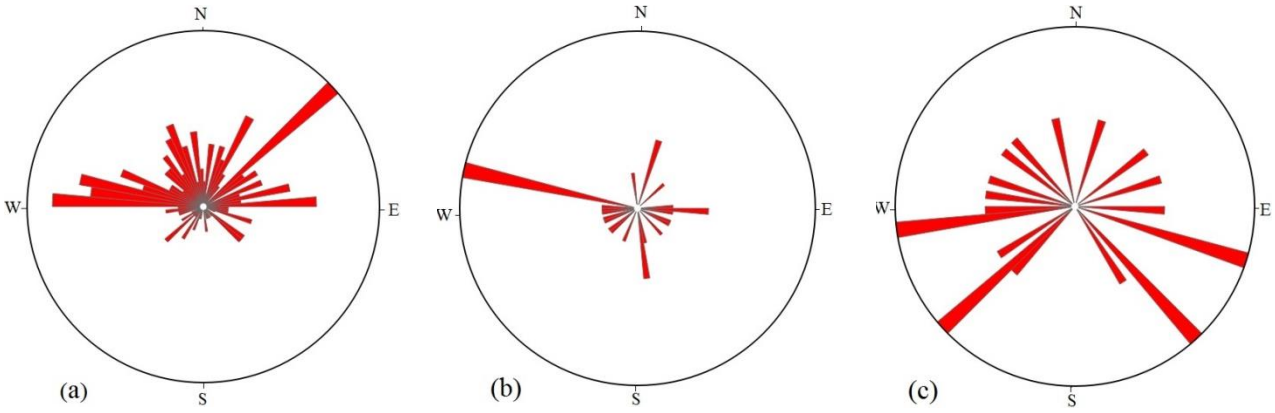

Fig. 4.23 Rose diagram (a) in basalt unit, (b) in mud unit, (c) in chert unit

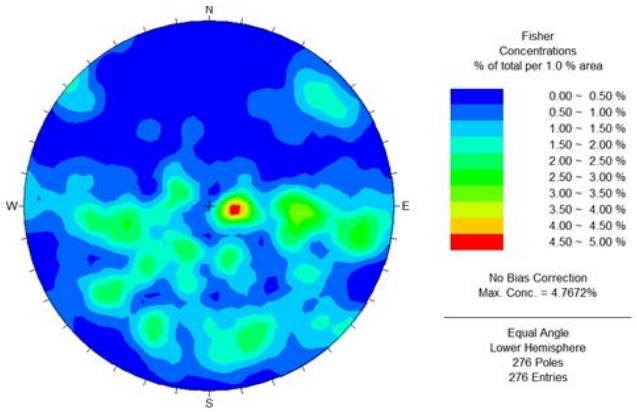

Fig. 4.24 Contour plot of all measured discontinuities

4.5.4 Discontinuity spacing

Discontinuity spacing (block size) is the perpendicular distance between two discontinuities from the same set. This describes the frequency of jointing. A highly jointed rock mass (closely spaced joints) is generally of poor quality than a sparsely jointed rock mass (widely spaced joints) (Hack, 1998). Discontinuity spacing is the main parameter in the SSPC system and used as input to derive other parameters which are important for stability assessments. These derived parameters include discontinuity spacing parameter (SPA) and overall weighted discontinuity condition (CD).

In the present study, systematic measurements of the spacing have been done and the final results are given in Table 4.2. The spacing values, in rock sections, are extremely different and ranges from 10 to 130cm.

During field observations, the slopes that are characterized by the closely spaced joint are highly fractured and weak; and it can be easily detached using single hammer blow. Generally, such type discontinuity frequencies were more frequently observed in highly weathered slope sections.

4.5.5 Infill material condition

Infill material is also important to characterize each discontinuity sets in terms of the values. It separates the adjacent rock walls of a discontinuity and that is usually weaker than the parent rock. The type of infill material and whether the walls of the discontinuity will be in contact or not during shearing, have a very strong influence on the shear strength characteristics (Hack, 1996). Typical filling materials include sand, silt, clay, breccia, infill material in discontinuities were determined.

Non-softening infill materials does not change in shear characteristics under the influence of water nor under the influence of shear displacement, while softening infill material will under the influence of water or displacements, attain in a lower shear strength and will act as a lubricating agent (Hack, 1998). Both classes of softening and non-softening infill material can be further sub-divided in classes according to the size of the grains in the infill material or the size of the grains or minerals in the discontinuity wall. A cemented discontinuity or a discontinuity with cemented infill has higher shear strength than a non-cemented discontinuity if the cement or cemented infill is bonded to both discontinuity walls (Hack, 1998). Infill material field descriptions are given in Table 4.2 and the values and ratings standards are given in Annex 8.1.1 and 8.7.4, respectively.

Accordingly, it is found that those slopes characterized by soft fine material (0.4%), non-softening sheared fine material (40.9%), non-softening sheared medium material (23.9%), and non-softening sheared coarse material (15.9%), cemented infill (1.8%) and no infill - surface staining (17.1%). In the study area, most discontinuities do not contain cement or cemented infill and soft sheared fine material. No infill defines a discontinuity that may have coated walls but no other infill.

4.5.6 Intact rock strength estimation

A rock mass contains rock material and discontinuities. The discontinuities are defined as planes of physical weakness. The blocks of rock material in between the discontinuities are defined as the intact rock. Intact rock strength involved obtaining data on the strength of slope rock masses for the investigated exposures.

The properties of the intact rock material are not influenced by the discontinuities. The rock mass containing discontinuities is weaker than the intact rock and also more deformable than intact rocks (Hack, 1993). In most existing classification systems for slope stability assessment intact rock strength is a parameter, as it is one of the basic parameter to classify the strength of slope rock mass. Rock mass with low intact rock strength has often also small discontinuity spacing or low shear strength along discontinuities or both (Hack, 2002).

In SSPC system, IRS is the most essential parameter of the exposure rock mass for estimate the slope stability. It is an input parameter to determine the rock mass friction and cohesion (ϕ 'mass and Coh' mass) of reference rock mass and slope rock masses.

In the present study, intact rock strength for various rock types was estimated in the field using ('simple means' test) using standard geological hammer according to BS 5930(1981) standards (Annex 8.7.2). The values were attained by averaging the upper and lower values of ranges provided in standards. Intact rock strength field descriptions are given in Table 4.3 and the values are given in Annex 8.1.1 .The intact rock strength of the slope sections are found to be 16.3% very strong, 30.5% strong, 39.9% moderately strong, 3.3% weak, 4.4% moderately weak and 5.5% very weak. Intact rock strength has a direct relation with lithology. Accordingly, slope section found in mude and chert units have low intact rock strength as compared to basaltic units.

4.5.7 Slope height

The height of the slope has a direct influence on the stress levels in the rock mass of the slope (Hack, 1998). High slope should cause challenges related to the discontinuity failure, since the quantity of discontinuities intersected by the slope is larger (Hack, 1998). Slope stability decreases sharply if the height of slope increases.

Rock blocks in higher slopes have more potential energy than rocks in lower slopes; thus they present a greater hazard and are more failure prone (Zare et al., 2011). Moreover, the SSPC method also more effective for slopes with a height of less than or equal to 45 m (Li and Xu, 2015; Hack et al., 2003).

In SSPC system, slope height is very essential to assess orientation independent stability problems. This was done together with slope rock mass friction (SFRI), slope dip and maximum height (H_{max}) using (H_{max} / H_{slope})) versus (SFRI / dip_{Slope}) ratio graph (graph 5.4).

In the present study, due to the ruggedness, accurate measurement of the slope height was not possible in the field. Slope heights were then determined from DEM. Accordingly, the height of the delineated slopes section ranges from 5m to 110m.The higher slope sections were present in basaltic units, while the small slopes sections were occurred in mud and chert units. These soft units were found following stream cuts and also at the center of the Alem ketema. The heights of the slope section are given in Table 4.3.

4.5.8 Method of excavation

The way the exposure has been made has a significant influence on the parameters measured or observed in the rock slopes. The structure and coherence of the rock mass and in particular of the thinly bedded units have been disturbed by the method of excavation.

In SSPC system, damage due to the method of excavation used to create the exposure was considered. However, the present study mainly conducted on natural slopes sections and the ratings for all slope section were taken as one (i.e. 1.00). The ratings of method of excavation used are given in Annex 8.7.3.

4.5.9 Discontinuity roughness condition

Rock joint roughness is one of the most important parameters in SSPC to characterize the slope nature. Shear strength of rock mass depends upon the rock joint roughness conditions (large scale roughness and small scale roughness).

In SSPC system, the large-scale roughness is determined following the large-scale roughness profiles on an area of greater than 0.2m x 0.2m, while the small-scale roughness factors are a combination of visible roughness on an area of less than 0.2m x 0.2m and tactile roughness. Visible small-scale roughness (e.g. stepped, undulating and planar) is determined following the

small-scale roughness profiles and tactile roughness is determined by touch (e.g. rough, smooth and polished).

The rock joint roughness has been estimated in the field by close observation judgment and using hand pressures together with the large scale and small scale roughness profiles (Annex 8.7.4). These were estimated according to Hack, 1998 standards (Annex 8.7.4) and accordingly, the large scale and small scale roughness conditions of the present slope sections were determined (Table 4.3) and the rating values are given in Annex 8.1.1. In the study area, degrees of roughness are different according to lithology type and degree of inclinations. In cliff slopes and hard rocks (basalt) are rougher as compared to gentler slopes and soft rocks (mud and chert).

4.5.10 Persistence of discontinuity

Persistence is the measure of the continuous length or lateral extent of a discontinuity plane. It can be crudely quantified by the observed trace length on exposed slope faces. Persistent discontinuities are continuous plane in the slope face and non-persistent end in intact rock.
Non persistence discontinuity sets do not have the same influence on the stability of a rock mass as persistence discontinuities have. Discontinuity persistence determines the possibilities of relative movement along a discontinuity. Persistence discontinuities have the significance influence on the stability of a rock slope mass as compared to non-persistence discontinuities.

In SSPC system, according to Hack et al. (2003) and Hack (1998), in this research, non-persistent discontinuity (e.g. a discontinuity ending in intact rock) is treated as a discontinuity with a small-scale roughness of 'rough stepped'(Table 4.3). All discontinuities in unstable slopes that are prone to sliding according to the sliding criterion are persistent.

In the study area, persistent discontinuity that range long distances along the rock slope mass are observed in form of bedding planes and columnar joints. The persistence discntinities were recorded and considered in this research when it traveled for a considerable distance (at least 1.5 m) in the exposure.

4.5.11 Ground water condition

Water can pass in the form of inflow (rainfall precipitation) or out flow (springs). Water adds to the weight of the rock mass, acts as a lubricant in discontinuities, causes softening of some infill materials(e.g. clay),and water pressure in discontinuities reduces the shear strength of the infill material and of the discontinuity wall (Hack, 1998). Passage of water in discontinuities increases the weight of the rock mass and facilitates discontinuity weathering rates.

SSPC system does not explicitly incorporate a factor for the presence of water pressures. However, the presence of water is incorporated in the parameters describing the infill material in discontinuities; because, the presence of water in a discontinuity can cause for lubricating and softening of infill materials and losing of material strength (Hack, 1998; Hack et al.,2003).

In the study area, groundwater conditions were investigated. Accordingly, only nine slope sections were defined by springs that flow out at different slope heights. However, there are numbers of spring traces that flow during rainy season and dry out when the rain season passes. These spring traces were considered as dry condition in this research (Table 4.5).

4.5.12 Discontinuity separation (aperture)

Discontinuity separation is the perpendicular distance between the adjacent rock surfaces of the discontinuity. This will be a constant value for parallel and planar adjacent surfaces, a linearly varying value for non-parallel but planar adjacent surfaces, and completely variable for rough adjacent surfaces (Hudson and Harrison, 2000).

In this research, the apertures values were determined by averaging the measurements obtained along a discontinuity. Most discontinuities along the slope sections are commonly open or moderately wide in aperture to some extent, whereas tight apertures were observed at certain slope sections. These tight discontinuities were commonly observed along columnar basalts.
From the non-tight discontinues 83% were filled with material over a certain distance with different infill material while the remaining 17% were completely open without any contact between the walls of the discontinuity and some of them are tight without any infill materials.

In some slope sections, the aperture values are different in different points along a discontinuity. It can be tight at the beginning and open at the end or vise verse or it may show other irregular aperture features. However, in the study area, the apertures values of columnar joints are somewhat constant along the discontinuity. Generaly, the aperture was found from ranging 5 to 200mm and most of the aperture measurements fall below 100mm. The field measurements are given in Table 4.5.

4.6 GSI data acquisition

In GSI system, rock mass slope parameters that were collected during field investigation include joint wall alterations, small-scale smoothness, large-scale waviness, infilling, roughness and weathering. In Table 4.4 and 4.5, the field description of slope rock mass parameters are presented. Accordingly, the values are given in Annex 8.5.1 and 8.5.2.

Joint alteration defines the character of the joint wall. It represents both the strength of the joint wall and the effect of filling and coating materials. The strength of the surface of a joint is a very important component of shear strength and deformability. Roughness and waviness parameters are also have a great importance for the stability of discontinuity controlled failures (Palmström, 1995). An increasing roughness profile of a discontinuity results in a substantial rise in discontinuity shear strength.

The strength of the joint surface is determined by the condition of the surface in clean joints, the type of coating on the surface in closed joints, the type, form and thickness of filling in joints with separation (Palmström, 1995). Often the quality (strength) of the discontinuity wall is lower than the intact rock strength. The decrease in strength may have been caused by weathering feature, brought about by chemically charged water percolating through discontinuities that reacted with the wall, etc. (Hack, 1996).

In the present study, it is found that most of slope sections are characterized by very blocky structure conditions and the GSI values ranges from 25-63 and these all values are given in annex 8.5.1 based on the standards given in Annex 8.7.5, 8.7.6, 8.7.7 and 8.7.8 . Low GSI values are frequently observed in mud and chert units, while high GSI values are common in basaltic units.

Table 4.3 infill material, discontinuity orientation and average discontinuity spacing: Infill material (nsf: non-softening, sheared fine material; nsm: non-softening, sheared medium material; nsc: non-softening, sheared coarse material; ssf: soft sheared fine material; cem: cemented; nfi: no fill)

Slope sec.	Infill Material			Discontinuity orientation (dip/dip orientation)			Average spacing (Block size)(cm)		
	J1	J2	J3	J1	J2	J3	J1	J2	J3
1	nfi	nfi	nsf	52/332	20/332	75/025	50	35	26
2	nsm	nsf	nfi	80/325	30/020	50/295	95	67	30
3	nsf	nfi	nsf	63/005	35/320	15/105	85	40	25
4	nsm	nsf	nsf	60/083	25/280	42/079	60	52	35
5	nsc	nsm	nsf	72/085	30/025	56/145	100	66	38
6	nsm	nfi	nsf	68/050	24/125	52/075	90	50	26
7	nsc	nsc	nfi	62/085	85/320	20/130	85	34	22
8	nsf	nsc	nfi	74/073	85/280	26/103	105	70	40
9	nfi	nsf	nsf	75/350	80/008	40/030	60	37	20
10	nsc	nsm	nsm	75/030	62/075	45/310	70	45	25
11	nfi	nsm	cem	32/340	50/335	66/280	88	50	36
12	cem	nsc	nsf	45/045	45/007	85/170	100	66	30
13	nsf	nsc	nfi	65/300	75/305	35/350	65	44	40
14	nsm	nsm	nsm	15/270	76/355	85/130	80	45	36
15	nsm	nsf	nsf	65/315	70/325	10/275	95	55	20
16	nsf	nfi	nsf	70/340	53/290	15/270	110	38	24
17	nsf	nsf	nfi	30/320	46/320	69/025	65	30	25
18	nfi	nsf	nsm	42/260	80/220	60/200	90	75	48
19	nsc	nsf	nsm	15/275	78/360	85/190	95	70	40
20	nsm	nfi	cem	25/293	72/360	64/305	85	47	36
21	nsc	nsc	nsf	65/005	18/270	80/255	100	63	30
22	nsc	nsc	nsm	70/054	45/293	85/210	80	60	40
23	nsm	nsf	nsf	54/108	80/285	70/045	82	55	25
24	nsc	nfi	nsm	85/315	22/109	64/210	111	60	50
25	nfi	nsf	nsm	67/330	20/275	75/045	85	74	45
26	nsf	nsm	nfi	58/046	10/316	86/265	95	36	20
27	nsf	nfi	nsf	45/055	15/330	80/355	80	40	30
28	nfi	nsf	nsf	50/048	10/320	75/344	100	50	35
29	nfi	nsm	nsm	38/065	20/085	70/050	75	46	27
30	nfi	nfi	nfi	56/345	30/015	75/025	56	34	45
31	nsf	nsf	nsf	66/270	42/045	80/016	90	80	60
32	nfi	nsf	nsf	50/290	34/045	80/017	78	40	10
33	nsf	nsf	nsf	55/070	30/017	70/055	52	38	25

34	nfi	nsm	nsc	50/085	26/045	72/030	70	44	30
35	nsf	nsf	nsf	73/020	85/235	25/075	66	54	28
36	nsm	nsm	nfi	50/045	25/045	55/310	98	76	42
37	nfi	nsf	nfi	46/110	32/290	65/295	86	53	30
38	nsf	nsf	nsf	75/280	50/070	85/090	72	68	47
39	nfi	nsf	nfi	61/275	52/065	75/300	86	60	35
40	nsc	nsm	nsf	78/282	44/270	80/054	105	78	26
41	nsm	nsf	nsm	80/058	65/275	45/058	94	50	40
42	nsc	nsf	nsf	80/067	55/006	50/270	60	46	20
43	nsc	nsf	nsm	80/350	30/085	60/303	75	61	33
44	nsc	nsm	nsm	75/289	62/355	25/056	80	70	60
45	nsm	nsm	nsc	74/352	30/036	65/352	85	40	32
46	nsm	nsc	nsc	76/335	45/335	20/279	50	30	12
47	nsf	nsm	nsm	60/077	36/336	18/288	66	52	45
48	nsm	nsf	nsf	65/236	36/337	30/160	87	58	42
49	nsm	nfi	nsm	62/225	76/338	36/280	120	85	50
50	cem	nsf	nfi	75/339	70/255	25/296	95	75	36
51	nsc	nsc	nsf	80/340	66/210	52/270	85	33	24
52	nsm	nsm	nsm	70/341	80/100	56/280	112	60	30
53	nsc	nfi	nsm	62/025	45/275	85/195	125	80	76
54	nfi	nsf	nsm	85/230	30/130	50/035	130	54	35
55	nsc	nfi	nsf	76/225	56/280	20/225	65	45	22
56	nsc	nsm	nsf	16/250	20/170	10/275	20	10	15
57	nsf	nsf	nsf	45/265	57/015	30/350	25	14	11
58	nsf	nsf	nfi	25/015	20/260	30/345	18	10	12
59	nsc	nsc	nsc	85/240	35/045	65/045	85	50	45
60	nsf	cem	nsf	60/065	50/290	68/080	70	58	20
61	nsf	nsm	nsm	66/310	45/350	80/280	100	40	35
62	nsf	nsm	nfi	70/90	50/270	85/125	30	25	27
63	nsf	nsm	nsf	85/218	65/020	48/088	110	80	46
64	nsf	nfi	nfi	80/085	60/267	50/010	87	64	29
65	nsm	nsc	nsc	74/270	62/005	30/330	77	65	35
66	nsm	nsm	nsf	65/335	50/290	45/020	38	34	23
67	nsc	nsm	nsf	85/130	55/277	58/085	40	32	30
68	nsf	nsm	nsf	85/280	75/285	40/350	35	24	18
69	nsf	nfi	nsm	70/325	45/082	70/260	30	26	22
70	nfi	nsf	nfi	65/345	35/066	47/015	40	30	20
71	nsm	nsf	nsf	20/195	85/310	30/200	60	45	32
72	nsc	nsf	nsm	30/225	48/075	69/095	55	36	25
73	nsf	nsf	nsf	25/260	20/115	06/090	30	17	15
74	ssf	nsf	nfi	45/200	20/110	30/245	50	35	24
75	nsc	nsm	nfi	25/250	45/170	30/135	30	25	22

76	nsc	nsc	nsm	39/285	58/260	35/270	60	38	32
77	nsf	nsf	nsf	75/220	15/050	60/105	45	34	27
78	nsf	nsf	nsf	10/305	80/278	69/105	35	30	18
79	nsf	nsf	nsf	26/280	53/280	35/085	35	28	16
80	nsc	nsc	nsf	56/045	80/230	62/170	50	45	30
81	nsc	nsm	nsf	44//090	50/269	60/225	65	30	20
82	nsf	nsf	nsf	20/280	66/280	10/280	25	18	15
83	nfi	nsm	nsm	80/270	45/015	30/090	37	24	15
84	nsm	nsm	nsf	12/285	76/135	80/225	68	40	35
85	nsc	nsm	nsf	85/315	45/070	10/145	40	30	20
86	nsc	nsm	nsf	78/238	40/260	15/135	45	32	18
87	nsc	nsc	nsm	85/270	30/079	35/150	80	65	50
88	nfi	nsf	nsf	66/086	85/330	52/250	90	65	30
89	nsf	nsf	nsf	32/025	54/139	10/025	70	60	40
90	nsf	nsf	nfi	54/270	35/125	72/105	100	85	66
91	nsc	nsf	nsf	49/095	25/170	32/225	30	25	20
92	nsf	nsf	nsf	75/315	85/025	45/025	60	52	45

Table 4.4 slope height (m), orientation, weathering, Large Scale Roughness (RL) and Small Scale Roughness (RS): Degree of weathering (swe, slightly weathered; mwe, moderately weathered; hwe, highly weathered; cwe, completely weathered); Intact rock strength (IRS) (vst, very strong; str, strong; mst, moderately strong; mwk, moderately weak; wek, weak; vwk, very weak); Large scale roughness (RL) (str, straight; cur, curved; scu, slightly curved; wav, wavy; swa, slightly wavy); Small scale roughness (RS) (spl, smooth planar; ppl, polished planar; rpl, rough planar; run, rough undulating; sun, smooth undulating; rst, rough stepped; sst, smooth stepped).

Slope sec.	Slope condition				Large scale roughness (rl)			Small scale roughness (rs)		
	Height (m)	Orientation	Weathering	Irs	J1	J2	J3	J1	J2	J3
1	45	72/060	mwe	mst	str	str	scu	spl	spl	run
2	65	67/063	swe	str	str	swa	str	run	spl	rpl
3	90	73/010	swe	str	scu	str	swa	run	rpl	run
4	75	77/005	swe	str	scu	str	str	run	run	run
5	75	64/025	mwe	mst	str	str	scu	rpl	rpl	spl
6	85	61/060	swe	str	scu	str	str	run	spl	run
7	50	80/077	mwe	mst	swa	scu	str	run	run	spl
8	60	82/073	swe	str	scu	str	str	sun	run	spl
9	45	85/030	swe	vst	str	str	scu	sun	spl	run

10	100	80/040	swe	str	scu	scu	str	run	run	run
11	85	75/025	mwe	mst	str	scu	scu	spl	run	sun
12	80	75/030	mwe	mst	str	str	swa	spl	rpl	run
13	93	82/310	swe	str	cur	str	str	spl	rpl	run
14	45	80/010	swe	vst	str	swa	scu	run	run	run
15	65	75/345	mwe	mst	scu	scu	str	run	run	sun
16	70	78/350	mwe	mst	str	str	swa	run	sun	run
17	35	69/025	swe	str	str	swa	str	run	sun	run
18	35	80/045	swe	vst	scu	scu	swa	sun	run	sun
19	80	78/360	mwe	mst	swa	str	scu	rpl	run	run
20	77	72/360	mwe	mst	str	swa	str	run	rpl	ppl
21	69	65/005	mwe	mst	cur	str	scu	run	run	rpl
22	72	75/015	mwe	mst	scu	scu	scu	rst	run	rst
23	68	70/045	mwe	mst	str	swa	swa	spl	spl	rst
24	40	60/039	swe	str	str	str	str	run	spl	run
25	25	75/045	swe	vst	swa	swa	str	rpl	run	rpl
26	25	80/050	swe	vst	swa	str	scu	run	spl	run
27	27	85/047	swe	str	scu	str	cur	run	run	run
28	21	85/044	mwe	mst	str	scu	str	run	run	spl
29	30	78/058	mwe	mst	scu	str	str	spl	run	run
30	19	76/015	mwe	vst	str	str	cur	spl	spl	spl
31	22	80/016	swe	str	str	swa	scu	rpl	sun	sun
32	24	85/017	swe	vst	str	scu	scu	run	run	run
33	24	69/028	mwe	mst	scu	str	str	sun	run	run
34	24	73/030	swe	str	scu	scu	str	run	sun	sun
35	25	73/015	swe	vst	swa	str	scu	sun	run	run
36	23	70/020	swe	str	str	scu	swa	spl	sun	rpl
37	15	85/290	swe	vst	scu	str	swa	run	run	run
38	20	85/291	swe	vst	str	str	scu	run	run	run
39	20	79/292	swe	str	str	str	str	run	run	run
40	21	80/293	swe	vst	str	str	str	rpl	rpl	run
41	28	75/275	swe	vst	str	str	str	run	spl	run
42	28	70/276	mwe	mst	str	scu	scu	run	run	run
43	26	80/350	mwe	mst	scu	str	str	run	sun	run
44	20	67/355	swe	str	str	scu	swa	run	run	rst
45	38	74/352	mwe	mst	scu	swa	str	run	run	sun
46	30	76/335	swe	str	scu	str	str	spl	sun	run
47	25	80/336	swe	vst	str	str	scu	spl	spl	rpl
48	29	83/337	swe	str	scu	str	scu	run	rpl	run
49	25	76/338	mwe	mst	str	scu	str	sun	run	run
50	34	84/339	mwe	mst	scu	str	scu	run	sun	spl
51	34	85/340	swe	str	str	str	str	run	run	run

52	34	78/341	mwe	mst	str	str	scu	rpl	sun	run
53	20	81/275	swe	str	cur	str	swa	run	run	run
54	25	75/035	swe	str	str	swa	scu	run	run	run
55	20	70/282	swe	str	scu	str	str	run	run	run
56	30	35/195	cwe	mwk	scu	scu	scu	run	run	run
57	20	30/345	cwe	mwk	scu	str	str	spl	rpl	spl
58	21	40/340	hwe	mst	scu	wav	scu	rpl	run	sun
59	15	65/045	hwe	mst	cur	cur	scu	run	run	run
60	60	68/080	hwe	mst	str	scu	str	run	run	run
61	30	78/350	mwe	mst	scu	str	str	sst	run	sst
62	55	80/330	swe	str	str	scu	str	sun	sst	run
63	40	65/020	swe	str	str	scu	str	run	rpl	run
64	45	80/010	swe	vst	str	swa	str	sun	sun	sun
65	35	76/005	swe	str	cur	str	cur	run	run	run
66	20	70/350	mwe	mst	str	scu	cur	rst	rpl	spl
67	50	73/340	swe	vst	str	str	scu	run	rst	run
68	65	75/068	swe	str	str	str	str	spl	spl	sst
69	60	70/075	swe	str	str	str	str	spl	spl	spl
70	60	55/065	swe	str	str	str	str	spl	spl	spl
71	95	30/135	hwe	mst	scu	scu	scu	rst	rst	run
72	26	40/160	hwe	mwk	cur	scu	str	run	sun	run
73	35	20/165	cwe	vwk	wav	swa	wav	sun	sun	sun
74	40	30/245	cwe	vwk	str	swa	str	sun	spl	spl
75	15	45/170	cwe	wek	scu	str	scu	sun	sun	sun
76	15	62/250	hwe	mst	scu	str	scu	run	rst	run
77	5	75/135	hwe	mwk	str	str	scu	spl	spl	spl
78	6	85/157	swe	str	str	swa	str	spl	spl	spl
79	12	45/015	cwe	vwk	wav	swa	wav	sun	sun	sun
80	25	39/085	cwe	wek	scu	swa	scu	run	run	run
81	8	73/150	cwe	wek	str	str	scu	sun	run	run
82	12	25/035	cwe	vwk	swa	wav	swa	sun	sun	sun
83	15	40/075	mwe	mst	str	scu	scu	run	run	run
84	14	63/050	mwe	mst	str	str	scu	run	run	run
85	10	75/286	mwe	mst	str	scu	scu	run	spl	run
86	11	78/066	mwe	mst	str	str	scu	run	run	run
87	60	35/150	mwe	mst	cur	scu	scu	run	run	run
88	30	80/330	swe	vst	str	scu	str	run	run	run
89	25	65/102	swe	str	str	str	scu	run	rpl	run
90	28	60/135	swe	str	str	str	cur	spl	spl	run
91	30	25/170	cwe	vwk	swa	str	swa	sun	sun	sun
92	20	85/025	mwe	mst	str	str	str	spl	spl	spl

Table 4. 5 Joint alteration (Ja), Small-scale smoothness (Js) and Large-scale waviness (Jw): Joint alteration (Ja) field description (frw, Fresh rock walls; stm, slightly to moderately weathered; tf, thin filling; hw, highly weathered; scm, Swelling clay materials); Small-scale smoothness (Js) field description (rou, rough; vro, very rough; sro, slightly rough; sli, slickenside; smo, smooth); Large-scale waviness (Jw) (pla, planar; lun, large undulation; int, interlocking; smu, small to moderate undulation; stp, stepped)

Slope sec.	Joint alteration (ja)			Small-scale smoothness (js)			Large-scale waviness(jw)		
	J1	J2	J3	J1	J2	J3	J1	J2	J3
1	tf	frw	stm	sro	sro	rou	pla	pla	int
2	stm	stm	stm	rou	smo	sro	pla	smu	pla
3	stm	stm	frw	rou	sro	rou	int	pla	smu
4	tf	stm	stm	rou	rou	rou	int	pla	pla
5	stm	stm	stm	sro	smo	rou	pla	pla	smu
6	frw	stm	stm	rou	smo	rou	int	pla	pla
7	stm	stm	stm	vro	rou	smo	smu	int	pla
8	stm	frw	stm	smo	rou	smo	smu	smu	pla
9	frw	stm	stm	sro	sro	rou	pla	pla	int
10	stm	stm	stm	rou	rou	sro	int	int	pla
11	tf	tf	stm	sro	rou	smo	pla	int	smu
12	stm	stm	stm	sro	sro	rou	smu	pla	smu
13	frw	stm	stm	smo	sro	rou	smu	pla	pla
14	stm	stm	stm	rou	vro	rou	pla	smu	int
15	stm	stm	tf	vro	rou	smo	int	int	pla
16	stm	stm	stm	rou	smo	rou	pla	pla	smu
17	stm	frw	frw	vro	rou	rou	pla	smu	pla
18	stm	stm	stm	smo	rou	smo	smu	int	smu
19	stm	tf	stm	sro	rou	rou	smu	pla	int
20	tf	tf	stm	vro	sro	sli	smu	smu	pla
21	stm	stm	stm	vro	rou	sro	int	pla	smu
22	stm	stm	stm	vro	rou	vro	stp	int	stp
23	stm	stm	stm	vro	smo	vro	pla	smu	smu
24	frw	stm	stm	vro	smo	rou	smu	smu	smu
25	stm	stm	stm	vro	rou	sro	smu	smu	pla
26	stm	stm	stm	vro	smo	rou	smu	pla	int
27	stm	stm	stm	vro	rou	rou	int	pla	int
28	stm	stm	stm	vro	rou	smo	smu	int	pla
29	hw	hw	stm	vro	rou	rou	smu	pla	smu
30	stm	stm	stm	vro	smo	rou	smu	pla	smu

31	stm	stm	stm	vro	smo	rou	smu	smu	smu
32	stm	stm	stm	vro	rou	rou	smu	int	int
33	tf	stm	stm	vro	rou	rou	smu	pla	smu
34	stm	stm	stm	vro	smo	smo	int	smu	pla
35	stm	stm	stm	vro	rou	rou	smu	pla	int
36	stm	stm	stm	vro	smo	sro	pla	smu	smu
37	stm	stm	stm	vro	rou	rou	int	pla	smu
38	hw	stm	stm	vro	rou	rou	smu	smu	int
39	stm	stm	stm	vro	rou	rou	smu	smu	pla
40	hw	stm	stm	vro	sro	rou	smu	smu	smu
41	stm	stm	stm	vro	smo	rou	smu	smu	smu
42	tf	hw	stm	vro	rou	rou	smu	int	int
43	stm	tf	stm	vro	smo	rou	int	smu	pla
44	stm	stm	stm	vro	rou	vro	smu	int	smu
45	hw	hw	stm	vro	rou	smo	int	smu	pla
46	stm	stm	stm	vro	smo	rou	smu	pla	pla
47	hw	stm	stm	vro	smo	sro	smu	smu	smu
48	stm	stm	stm	vro	sro	rou	int	pla	int
49	tf	stm	stm	vro	rou	rou	pla	int	pla
50	tf	hw	stm	vro	smo	smo	int	pla	smu
51	stm	stm	stm	vro	rou	vro	smu	smu	pla
52	hw	stm	hw	vro	smo	rou	smu	pla	int
53	stm	hw	stm	vro	rou	vro	int	pla	smu
54	hw	hw	stm	vro	rou	rou	smu	smu	int
55	stm	stm	stm	vro	rou	rou	int	pla	pla
56	tf	tf	tf	vro	rou	rou	int	int	int
57	tf	tf	tf	vro	smo	sro	smu	smu	smu
58	tf	tf	tf	vro	smo	smo	smu	int	smu
59	tf	tf	tf	vro	rou	rou	int	int	int
60	tf	tf	tf	vro	rou	rou	pla	int	pla
61	stm	stm	stm	vro	rou	vro	smu	pla	pla
62	stm	stm	stm	vro	vro	rou	smu	smu	pla
63	frw	stm	stm	vro	sro	rou	smu	smu	pla
64	stm	stm	stm	vro	smo	vro	pla	smu	pla
65	stm	stm	stm	vro	rou	vro	smu	smu	int
66	hw	stm	stm	vro	sro	rou	pla	smu	smu
67	stm	stm	stm	vro	vro	rou	smu	pla	int
68	stm	stm	stm	vro	smo	vro	smu	smu	smu
69	stm	stm	stm	vro	smo	rou	pla	smu	pla
70	stm	stm	stm	vro	smo	rou	smu	pla	pla
71	tf	hw	tf	vro	vro	rou	stp	stp	int
72	tf	tf	hw	vro	rou	rou	int	smu	pla

73	scm	stm	scm	vro	smo	smo	lun	smu	lun
74	scm	scm	scm	vro	smo	smo	pla	smu	pla
75	scm	scm	scm	vro	smo	smo	smu	smu	smu
76	tf	tf	hw	vro	vro	rou	int	pla	int
77	tf	hw	tf	vro	smo	smo	smu	pla	smu
78	hw	stm	hw	vro	smo	smo	smu	smu	pla
79	scm	scm	scm	vro	smo	sro	lun	smu	lun
80	scm	scm	scm	vro	rou	rou	int	smu	int
81	hw	tf	hw	vro	rou	rou	pla	pla	int
82	scm	scm	scm	vro	smo	smo	smu	lun	smu
83	scm	scm	scm	vro	rou	rou	smu	int	int
84	hw	hw	hw	vro	rou	sro	pla	pla	int
85	hw	hw	frw	vro	smo	rou	smu	smu	int
86	hw	hw	hw	vro	rou	rou	pla	pla	int
87	stm	stm	stm	vro	rou	rou	int	int	int
88	stm	stm	frw	vro	vro	vro	pla	int	pla
89	frw	stm	stm	vro	sro	rou	pla	pla	int
90	stm	stm	stm	vro	rou	rou	pla	pla	int
91	scm	scm	scm	vro	sro	smo	smu	pla	smu
92	frw	stm	stm	vro	rou	sro	pla	pla	pla

Table 4.6 Infill material (Rf), Rough rating (Rr), Aperture (mm), Weathering rating (Rw), Lithology type and Groud water: Rough rating (Rr) and (Rw) (smo, smooth; slightly rough; rou, rough; sro, vro, very rough); Weathering rating (sw, slightly weathered; mw, moderately weathered; hw, highly weathered)

Slope sec.	Infill material rating(rf)			Rough rating (rr)			Aperture/width (mm)			Rw	Lithology type	Ground water
	J1	J2	J3	J1	J2	J3	J1	J2	J3			
1	soft	hard	soft	sro	sro	rou	14	19	10	mw	basalt	dry
2	hard	hard	none	rou	sro	sro	105	56	70	sw	basalt	dry
3	hard	none	hard	rou	sro	rou	90	62	45	sw	basalt	dry
4	hard	hard	hard	rou	rou	rou	125	21	9	sw	basalt	dry
5	soft	hard	hard	sro	sro	sro	200	30	60	mw	basalt	dry
6	soft	none	hard	rou	sro	rou	35	5	20	sw	basalt	dry
7	hard	hard	none	vro	rou	sro	110	90	15	mw	basalt	dry
8	hard	hard	none	sro	rou	sro	45	57	8	sw	basalt	dry
9	none	hard	hard	sro	sro	rou	60	30	26	sw	basalt	dry
10	hard	soft	hard	rou	rou	rou	52	15	20	sw	basalt	dry
11	none	hard	hard	sro	rou	sro	31	48	38	mw	basalt	dry
12	hard	soft	hard	sro	sro	rou	25	37	27	mw	basalt	dry

13	hard	soft	none	sro	rou	rou	20	30	33	sw	basalt	dry
14	hard	hard	hard	rou	vro	rou	65	51	46	sw	basalt	moist
15	hard	soft	hard	vro	rou	sro	23	42	28	mw	basalt	dry
16	hard	none	hard	rou	sro	rou	107	78	69	mw	basalt	dry
17	hard	hard	none	vro	rou	rou	27	20	60	sw	basalt	dry
18	none	hard	hard	sro	rou	rou	30	25	75	sw	basalt	moist
19	hard	hard	soft	sro	rou	rou	20	10	14	mw	basalt	dry
20	hard	none	hard	vro	sro	sro	45	14	29	mw	basalt	dry
21	soft	soft	hard	vro	rou	sro	74	51	37	mw	basalt	dry
22	hard	hard	hard	vro	rou	vro	106	118	130	mw	basalt	dry
23	hard	hard	hard	sro	sro	vro	80	44	122	mw	basalt	dry
24	hard	none	hard	rou	sro	rou	160	112	59	sw	basalt	moist
25	none	hard	soft	vro	rou	rou	180	15	138	sw	basalt	dry
26	hard	hard	none	rou	sro	rou	45	74	11	sw	basalt	dry
27	hard	none	hard	vro	rou	rou	16	50	19	sw	basalt	dry
28	none	hard	hard	rou	rou	sro	40	15	10	mw	basalt	dry
29	none	hard	soft	sro	rou	rou	150	22	16	mw	basalt	dry
30	none	none	none	rou	sro	rou	53	13	32	mw	basalt	dry
31	hard	hard	hard	rou	sro	rou	138	18	17	sw	basalt	dry
32	none	hard	hard	rou	rou	sro	27	49	62	sw	basalt	dry
33	hard	hard	hard	sro	rou	rou	140	95	129	mw	basalt	dry
34	none	hard	soft	rou	sro	sro	165	105	119	sw	basalt	dry
35	soft	hard	soft	sro	rou	rou	16	23	26	sw	basalt	dry
36	hard	hard	none	sro	sro	sro	124	99	40	sw	basalt	dry
37	none	hard	none	vro	rou	rou	78	16	47	sw	basalt	dry
38	hard	hard	hard	vro	rou	rou	91	32	10	sw	basalt	dry
39	none	hard	none	rou	rou	rou	180	17	64	sw	basalt	dry
40	hard	hard	hard	sro	sro	rou	110	29	88	sw	basalt	dry
41	soft	hard	hard	rou	sro	rou	71	9	63	sw	basalt	moist
42	hard	hard	hard	vro	rou	rou	127	139	19	mw	basalt	moist
43	soft	hard	hard	rou	sro	rou	40	51	68	mw	basalt	dry
44	hard	soft	soft	rou	rou	vro	200	67	95	sw	basalt	dry
45	hard	hard	hard	rou	rou	sro	118	33	25	mw	basalt	dry
46	hard	hard	hard	sro	sro	rou	55	82	17	sw	basalt	dry
47	hard	hard	hard	sro	sro	sro	49	15	38	sw	basalt	dry
48	hard	hard	hard	rou	sro	rou	100	52	44	sw	basalt	dry
49	soft	none	hard	sro	rou	rou	154	12	67	mw	basalt	dry
50	hard	hard	none	rou	sro	rou	69	35	55	mw	basalt	dry
51	soft	hard	hard	vro	rou	vro	44	41	22	sw	basalt	dry
52	soft	soft	soft	sro	sro	rou	185	147	60	mw	basalt	dry
53	hard	hard	hard	rou	rou	vro	200	138	115	sw	basalt	dry
54	none	hard	hard	rou	rou	rou	100	30	75	sw	basalt	dry

55	hard	none	hard	rou	rou	rou	129	96	43	sw	basalt	dry
56	soft	hard	hard	sro	sro	sro	20	12	16	hw	basalt	dry
57	soft	soft	soft	smo	smo	sro	19	16	15	hw	mud	dry
58	soft	soft	soft	sro	smo	smo	85	43	72	hw	chert	dry
59	hard	hard	hard	rou	sro	rou	168	113	137	hw	basalt	dry
60	hard	hard	hard	rou	rou	rou	37	80	17	hw	basalt	dry
61	hard	hard	hard	vro	rou	vro	156	82	97	mw	basalt	dry
62	hard	hard	none	sro	vro	rou	45	36	42	sw	basalt	dry
63	hard	hard	hard	rou	sro	rou	87	169	135	sw	basalt	dry
64	hard	none	none	rou	rou	vro	81	20	102	sw	basalt	moist
65	soft	soft	hard	vro	rou	rou	108	95	131	sw	basalt	dry
66	hard	hard	hard	vro	rou	rou	25	19	32	mw	basalt	dry
67	hard	hard	hard	rou	vro	rou	37	50	28	sw	basalt	dry
68	hard	hard	hard	rou	rou	vro	110	39	66	sw	basalt	dry
69	hard	none	hard	vro	rou	rou	80	67	75	sw	basalt	dry
70	none	hard	none	rou	sro	rou	45	24	29	sw	basalt	dry
71	hard	hard	hard	vro	vro	rou	36	45	33	hw	basalt	dry
72	hard	hard	hard	rou	rou	rou	16	11	12	hw	basalt	dry
73	soft	soft	soft	smo	sro	smo	18	10	13	hw	mud	dry
74	soft	soft	soft	sro	smo	smo	22	11	16	hw	mud	dry
75	soft	soft	soft	sro	sro	sro	20	14	27	hw	mud	dry
76	none	hard	hard	rou	vro	rou	24	39	15	hw	basalt	dry
77	soft	soft	soft	sro	sro	sro	10	13	14	hw	chert	moist
78	soft	soft	soft	sro	smo	sro	10	12	14	sw	chert	dry
79	soft	soft	soft	sro	sro	rou	16	18	10	hw	mud	dry
80	soft	soft	soft	rou	sro	sro	145	29	86	hw	mud	dry
81	soft	soft	soft	sro	sro	rou	17	12	15	hw	chert	moist
82	soft	soft	soft	sro	sro	sro	15	17	20	hw	mud	dry
83	soft	soft	soft	rou	rou	sro	18	20	16	mw	mud	moist
84	soft	soft	soft	vro	rou	sro	31	18	12	mw	chert	dry
85	soft	soft	soft	rou	sro	rou	85	56	42	mw	chert	dry
86	soft	soft	soft	sro	rou	rou	27	138	36	mw	chert	dry
87	hard	hard	hard	vro	rou	rou	26	18	39	mw	basalt	dry
88	none	hard	hard	rou	vro	vro	58	95	81	sw	basalt	dry
89	hard	hard	hard	rou	sro	rou	75	144	97	sw	basalt	dry
90	hard	hard	none	rou	rou	rou	14	94	23	sw	basalt	dry
91	hard	hard	hard	sro	sro	sro	13	19	14	hw	mud	dry
92	hard	hard	hard	sro	rou	sro	10	16	20	mw	basalt	moist

*****

Chapter V Data Analysis Techniques

5.1 Preamble

Rock slope failures are frequently controlled by a complex combination of discontinuities that facilitate kinematic release (Brideau et al., 2009). The discontinuities such as joints, bedding planes are fundamental for slope stability, especially their geometrical and geotechnical characteristics. The shear strength as a major parameter for stability is directly related to the geotechnical properties such as cohesion, friction angle, aperture, infilling, and weathering (Fischer and Huggel, 2008).

In the present research, two sets of parameters were employed in rock slope stability assessments. The first set parameters are those data which were collected from the field measurement. While the second set of parameters are those derived data from the field measured data using empirical correlations stated in the SSPC slope stability assessment scheme. Thus, slope rock mass parameters as well as the derived parameters are described in selected rock slopes according to the detail step-wise assessment stated in the SSPC. The calculation of SSPC and GSI has been performed for all nighty two slope sections and the detail ratings are given based on standards.

5.2 Determining of SSPC parameters

The SSPC system considers three rock masses. First, the rock mass in the exposure defined as exposure rock mass (ERM). Rock mass parameters of importance are described and characterized in an exposure resulting in the exposure rock mass. This is directly observed on the outcrop of a slope rock masses. The second rock mass is an imaginary un-weathered and undisturbed (fresh) rock mass which is defined as reference rock mass (RRM) and the third rock mass in which the existing or new slope is to be made (excavated) and defined as slope rock mass (SRM).

Local influences such as degree of weathering and method of excavation has considerable influences on the rock mass parameters.

However, in this study method of excavation has no more influences in the slope stability assessments techniques, because the study was carried out on the natural rock slope sections. Therefore, the rating for method of excavation for natural slopes was given as one (1.00) for all slope sections.

In the present research, ERM, RRM and SRM parameter were calculated using different empirical relations and the full list of results are given in Annex 8.1, 8.3 and 8.4 respectively. The flow chart of three step concept of the SSPC system for three sets of parameters or rock masses is given in Fig 5.1.

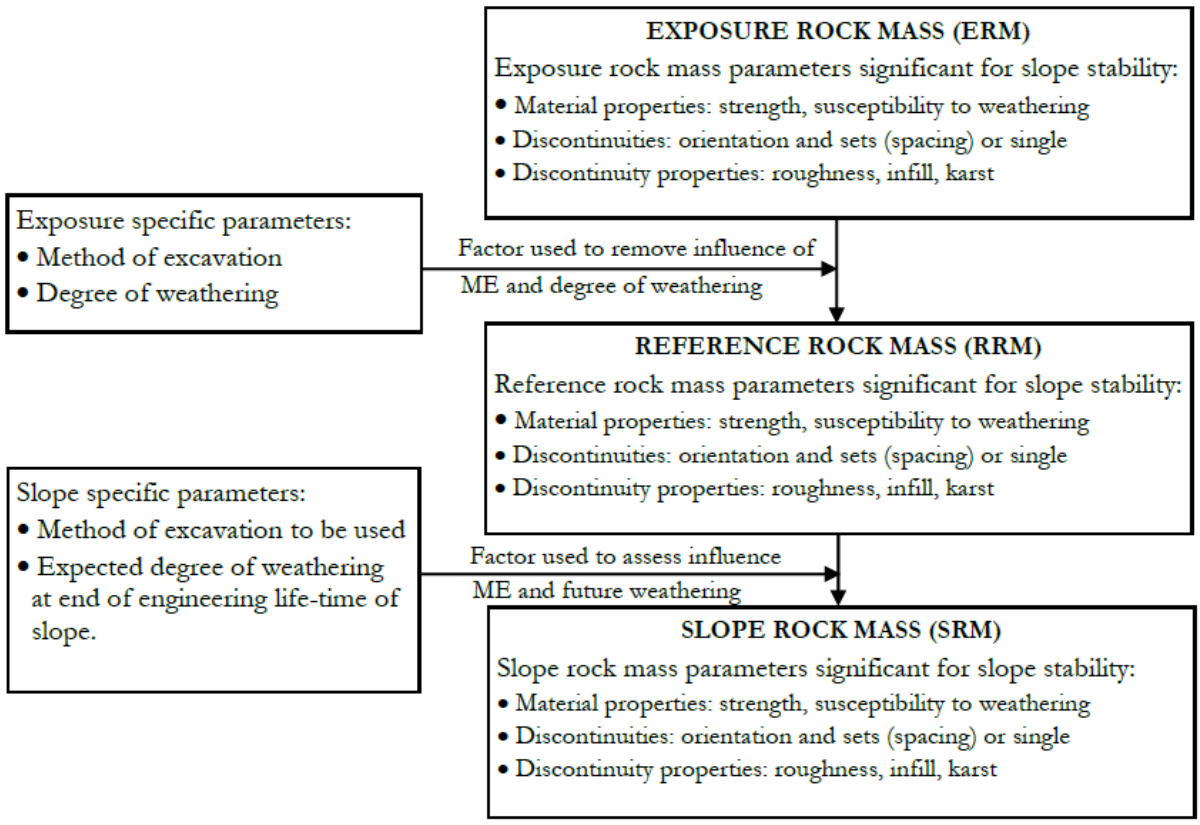

Fig. 5.25 Flow chart of three step concept of the SSPC system (after Hack, 1996)

5.2.1 Determining the exposure rock mass (ERM) parameters

Stated parameters significant for slope stability were determined for the exposure rock masses. Rock mass parameters which are described and characterized in an exposure resulting in the exposure rock mass (ERM).

These parameters including intact rock strength (IRS), degree of weathering (WE), discontinuity spacing (DS) and condition properties (i.e., persistence, roughness, infill, and presence of karst) of discontinuities are determined in the field. These are input parameters for the SSPC, the intact rock strength (IRS), internal friction angle of the rock mass (FRI), cohesion of rock mass (COH), spacing parameter (SPA), condition of discontinuities (TC), weighted discontinuities condition (CD). The values of parameters (except IRS) for exposure rock mass were determined using equations. In the following sections, detailed description and expression were provided.

5.2.1.1 Exposure intact rock strength (IRS)

The intact rock strengths of the exposure rock masses were estimated in the field using simple means testes that are related to the strength classes of the British Standard (BS 5930, 1981) (Annex 8.7.2). The exposure intact rock strength values are given in Annex 8.1.1. The estimated values of IRS are found ranging from 1.25MPa to 150MPa. However, if intact rock strength is higher than 132MPa, then RIRS is accepted as 132MPa, then RIRS is 132MPa since a RIRS value of about 132MPa, the stability of slopes do not further increase with an increment in RIRS (Hack et al., 2003).

5.2.1.2 Exposure internal friction and cohesion (ϕ 'mass and Coh' mass)

The exposure internal friction angle and cohesion were calculated by the optimizing the Mohr-Coulomb failure criterion utlizing the intact rock strength (IRS), spacing parameter (SPA) and weighted discontinuities condition (CD) using Eq.5.1 and 5.2.

ϕ 'mass = IRS * 0.2417 + SPA * 52.12 + CD * 5.779……(eq.5.1)

Coh' mass= IRS * 94.27 + SPA + 28629 + CD *3593……..……(eq.5.2)

Accordingly, the calcuacted internal friction values are ranging from 13.5° to 57.1°. While, the cohesion values are ranging from 0.27MPa to 0.72MPa respectively.

5.2.1.3 Exposure discontinuity spacing parameter (SPA)

SPA is parameters for overall spacing of a number of discontinuity sets in an exposure rock mass unit.

The determination of the spacing parameter (SPA) is done by using the values for the spacing factors for discontinuity sets which are calculated from a series of formulas determined by Taylor (1980). The SPA is calculated based on the three discontinuity sets with the smallest spacing in following expressions. If three or more discontinuity sets exist, all the three factors (i.e. maximum, intermediate, and minimum) were determined for sets with minimum spacing. If only two discontinuity sets exist, two factors (minimum and maximum) were determined and if only one set is present, a single factor was determined. SPA values were calculated using Equ. 5.3.

SPA= factor $_{maximum}$ * factor $_{intermediate}$ * factor $_{minimum}$ (for three discontinuity sets)…..… (eq.5.3)

SPA= factor $_{maximum}$ * factor $_{minimum}$ (for two discontinuity sets)

SPA= factor (for one discontinuity set)

In this research, the spacing factors were determined in two ways, using equation Eq.5.4 or spacing factor versus discontinuity spacing graph (Fig.5.2). In both cases the result was the same.

Table 5.7 Spacing factor equations

For a rock mass with one discontinuty set	For a rock mass with two discontinuty set	For a rock mass with three discontinuty set
$Factor_1=0.45+0.264* \log_{10}^{(DS)}$ $Factor_2=Factor_3=1$	$Factor_1=0.38 + 0.259* \log_{10}^{(DS\text{-}minimum)}$ $Factor_2=0.28 + 0.30* \log_{10}^{(DS\text{-}maximum)}$ $Factor_3=1$	$Factor_1=0.30 + 0.259* \log_{10}^{(DS\text{-}minimum)}$ $Factor_2=0.20 + 0.296* \log_{10}^{(DS\text{-}intermediat)}$ $Factor_3=0.1 + 0.333* \log_{10}^{(DS\text{-}maximum)}$ …….(eq.5.4)

However, in this study, all slope faces consists of three discontinuty sets, therefore, spacing factors were determined using Eq.5.4.

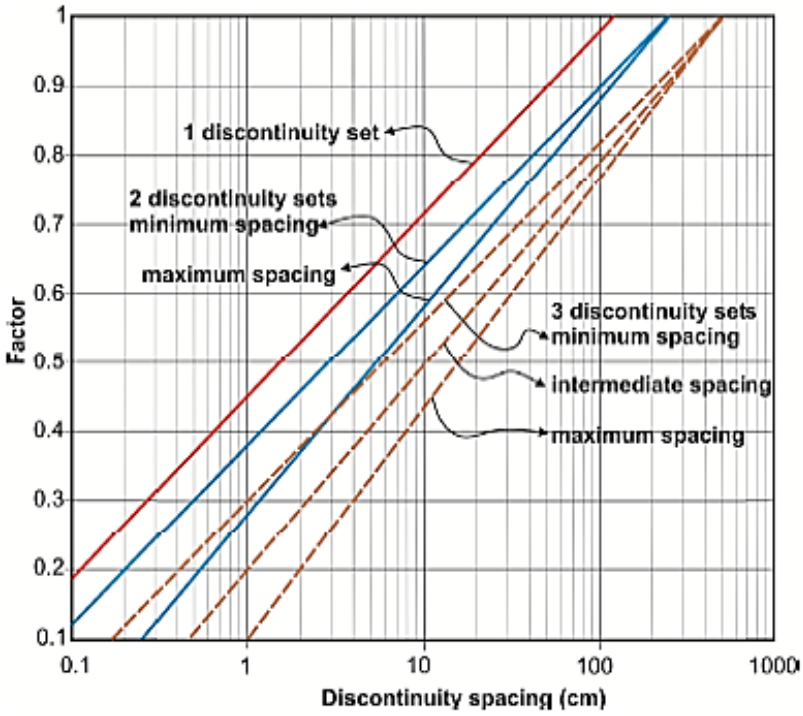

Fig. 5. 26 Spacing factor vs. discontinuity spacing graph (after Hack, 1996)

5.2.1.4 Exposure condition of discontinuities (TC)

TC is a parameter for the condition of a discontinuity set in an exposure rock unit (discontinuity condition factor). The condition factors (TC) of a discontinuity were calculated by a simple multiplication of large-scale roughness (Rl), small scale roughness (Rs), infill (lm) and karst (Ka) fators. The total conditions of discontinuities (TC) were calculated using the following expression;

TC = Rl x Rs x Im x Ka ……...…… (eq.5.5)

5.2.1.5 Exposure overall weighted discontinuity condition (CD)

CD is a parameter for the weighted overall condition of a number of discontinuity sets in an exposure rock mass unit. Weighted discontinuity conditions were calculated by using condition of discontinuities (TC) and spacing (DS) based on the following formula with the mean of condition factors of three discontinuity sets weighted against the spacing of discontinuity (DS). The weighted overall discontinuity condition were calculated using the following expression;

$$CD = \frac{\frac{TC_1}{DS_1} + \frac{TC_2}{DS_2} + \frac{TC_3}{DS_3}}{\frac{1}{DS_1} + \frac{1}{DS_2} + \frac{1}{DS_3}} \quad \text{.....(eq.5.6)}$$

5.2.2 Determining reference rock mass (RRM) parameters

The reference rock mass is an imaginary un-weathered and undisturbed rock mass (Hack, 1998). The reference rock mass parameters were determined from the exposure rock mass parameters by using correction factors for the influence of local weathering (WE) and method of excavation (ME).

Local influences on the parameters measured in the exposure are compensated to convert the parameters for the exposure rock mass to that of the theoretical rock mass that exists below the influence zones of weathering (fresh rock mass) and other disturbances called the reference rock mass (RRM) (Hack et al., 2003). This compensation is done with the help of correction parameters (i.e. exposure specific parameters). The resulting rock mass parameters are those of the reference rock mass. The influence of weathering has been investigated for intact rock strength (IRS), overall discontinuity spacing in a rock mass (SPA), condition of discontinuity set (TC), the overall weighted condition of discontinuities in a rock mass (CD), the rock mass friction φ_{mass} and cohesion coh_{mass}.

5.2.2.1 Reference Intact Rock Strength (RIRS)

In reference rock mass, the parameters for intact rock strength (RIRS) can be measured in the exposure (IRS) corrected with local influencing factor of weathering in the exposure rock mass (WE). Reference intact rock strengths were calculated using Eq.5.7. Accordingly, the maximum and the minimum values of reference intact rock strength are 132 MPa and 3.6MPa respectively.

RIRS = IRS / WE……..……. (eq.5.7)

5.2.2.2 Reference internal friction (RFRI) and cohesion (RCOH)

Reference internal friction (RFRI) and cohesion (RCOH) are the major reference rock mass parameters.

These can be calculated using a linear combination of reference intact rock strength (RIRS), reference discontinuity spacing (RSPA) and a parameter describing the weighted condition of the discontinuity (RCD) (Hack et al., 2003). Reference internal friction and cohesion were calculated using Eq.5.8 and 5.9. Accordingly, the maximum and the minimum values of reference internal friction are 59° and 25.4° respectively. Likewise, the maximum and the minimum values for reference cohesion are 32,760Pa and 12,874.2Pa respectively.

RFRI = RIRS * 0.2417 + RSPA * 52.12 + RCD * 5.779……..……(eq.5.8)

RCOH = RIRS * 94.27 + RSPA * 28629 + RCD *3593…….…..……..…...(eq.5.9)

5.2.2.3 Reference discontinuity spacing parameter (RSPA)

The reference discontinuity spacing (RSPA) is calculated by considering factors of weathering (WE) and method of excavation (ME) in the following expresson.

RSPA = SPA / (WE x ME)……...…….. (eq.5.10)

5.2.2.4 Reference condition of discontinuities (RTC)

In reference rock mass, the parameters for each conditions of discontinuity set (RTC) can be measured in the exposure (TC) corrected with local influencing factor of weathering in the exposure rock mass (WE). Discontinuity condition of reference rock mass (RTC) were calculated for each discontinuity sets after weathering correction using the following equations;

RTC = TC / Sqrt (1.452-1.220*e $^{(-WE)}$) ……..…… (eq.5.11)

5.2.2.5 Reference overall weighted discontinuity condition (RCD)

The reference weighted discontinuity condition (RCD) is determined by considering the factor of weathering degree in the following expression.

RCD=CD/WE……..……..……..…… (eq.5.12)

5.2.3 Determining slope rock mass (SRM) parameters

The actual stability assessment was made in the slope rock mass (SRM). This is derived from the reference rock mass (RRM) by modifying the reference rock mass (RRM) parameters using the slope specific parameters. Slope specific parameters are correction parameters for the influence of future weathering condition of the slope and for the influence of the method of excavation to be used. However, this study was carried out on natural rock slopes. Therefore, excavation method used has no significant influences on assessment systems. The 'exposure rock mass' and 'slope rock mass' are the same if an existing slope is examined and future weathering is not considered (Hack et al., 2003). Then, it also not necessary to use the exposure and slope specific parameter (method of excavation and weathering) as these are the same. Slope rock mass intact rock strength (SIRS), slope rock mass spacing parameter (SSPA) and slope rock mass of weighted discontinuities condition (SCD) parameters are important to determine the slope rock mass angle of internal friction (SFRI) and slope rock mass cohesion (SCOH) parameters. The SIRS, SFRI, and SCOH are considered important for use in assessing deterioration in strength and shear strength parameters as well as in stability assessments.

5.2.3.1 Slope rock mass intact rock strength (SIRS)

Deriving the slope rock mass intact rock strength (SIRS) were calculated by assessing the influence of slope rock mass degree of weathering (SWE) on the reference rock mass intact rock strength (RIRS) using Eq.5.13. The intact rock strength is ranging from 1.25MPa to 150MPa.

SIRS=RIRS*SWE……...……...…….. (eq.5.13)

5.2.3.2 Slope rock mass internal friction (SFRI) and cohesion (SCOH)

Deriving the slope rock mass friction (SFRI) and cohesion (SCOH) were calculated by replacing the reference rock mass parameters RIRS, RSPA, and RCD. Slope rock mass internal friction and cohesion were calculated using Eq.5.14 and 5.15. Accordingly, the calcuacted internal friction values are ranging from 13.5° to 57.1°. While, the cohesion values are ranging from 0.27MPa to 0.72MPa respectively.

SFRI = SIRS * 0.2417 + SSPA * 52.12 + SCD * 5.779…...……...……(eq.5.14)

SCOH = SIRS * 94.27 + SSPA * 28629 + SCD *3593…….…….……..(eq.5.15)

5.2.3.3 Slope rock mass discontinuity spacing (SSPA)

The slope rock mass overall spacing of discontinuities (SSPA) were calculated by assessing the influence of SWE and slope method of excavation (SME), on the reference rock mass spacing parameter (RSPA) using Eq.5.15.

SSPA=RSPA*SWE*SME…….……...…… (eq.5.16)

5.2.3.4 Slope rock mass condition of discontinuities (STC)

The STC were calculated as follows with respect to RTC and the weathering factor of slope in the engineering life time (SWE).

STC = RTC / Sqrt (1.452-1.220*e $^{(-SWE)}$)…….…… (eq.5.17)

5.2.3.5 Slope rock mass weighted discontinuity condition (SCD)

The slope rock mass weighted discontinuity conditions were calculated by assessing the influence SWE on the reference rock mass condition of discontinuities (RCD) using Eq. 5.18.

SCD=RCD*SWE…….…… (eq.5.18)

5.3 SSPC slope stability assessment

In the SSPC system, there are two types of slope stability methods based on failure mechanism and controlling factors of rock slopes (Li and Xu, 2015); orientation-dependent stability and orientation- independent stability. The former type is used for the stability analysis of slopes with structural control failure, and the latter type is used for the stability analysis of slopes with non-structural control failure.

5.3.1 Determination of orientation dependent SSPC assessment

The final step of the SSPC system is the determination of slope stability probability. These are defined by orientation dependent and orientation independent conditions in the system. Orientation dependent SSPC assessment related to the orientation of the discontinuities and the slope unit.

The orientation dependent stability assessment identifies the sliding and the toppling mode of failure within a rock mass and assesses the probability of failure based on the condition of the discontinuity. Two criteria were developed in the SSPC system to predict the orientation-dependent stability of a slope. These are sliding and toppling criteria (Hack et al., 2003). Accordingly, the present orientation dependent assessments were determined.

5.3.1.1 Sliding criterion

Discontinuity condition (TC) and the apparent angle of the dip of discontinuity plane in the direction of slope dip (AP) are taken into consideration during the orientation dependent stability probability evaluation in the SSPC system (Hack et al., 2003).

In the orientation–dependent analysis, additional conditions (Table 5.13), which consider the relationship between AP and slope dip, were also considered for the evaluation of toppling and sliding failure. The values of AP were determined using Eq.5. 20. The following equation (Eq.5.19) was used as the boundary condition for sliding in slopes.

Sliding occurs if;

$TC < 0.0113\ AP$…… (eq.5.19)

The AP is expressed as follows:

$$AP=\arctan(\cos\delta * \tan dip_{discontinuity})$$…… (eq.5.20)

$$\delta = \text{dip direction}_{slope} - \text{dip direction}_{discontinuity}$$

If $AP > 0° \rightarrow$ AP = Apparent discontinuity dip in the direction of the slope dip

If $AP < 0° \rightarrow |AP|$ = Apparent discontinuity dip in the direction opposite the slope dip

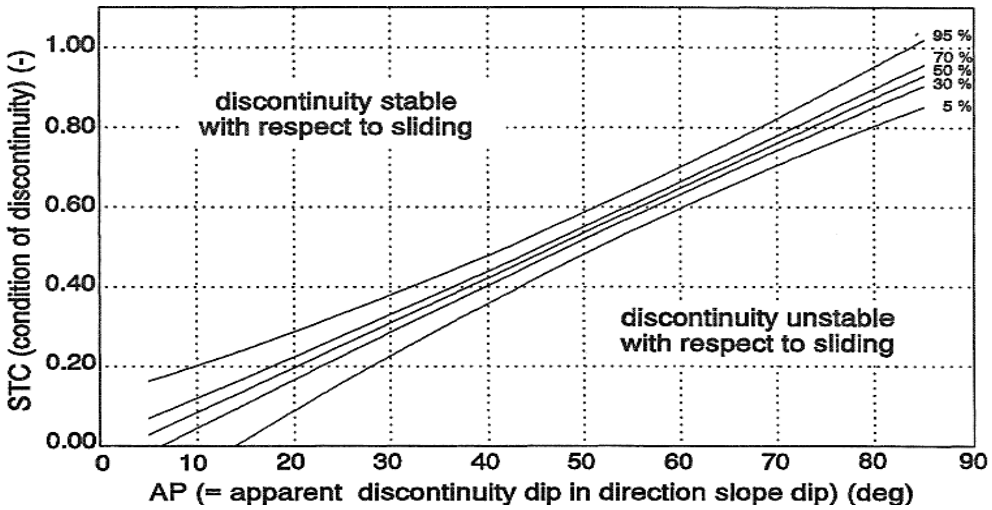

Fig. 5.27 Sliding probability for orientation dependent slope stability (after Hack, 1996)

5.3.1.2 Toppling criterion

The following equation (Eq.5.21) was considered as the boundary condition for toppling in slopes. That is, toppling occurs if;

$$TC < 0.0087\ (-90° - AP + dip_{discontinuity}) \quad \text{(eq.5.21)}$$

Where TC is the condition factor and AP is the apparent angle of the dip of the discontinuity plane in the direction of the slope dip.

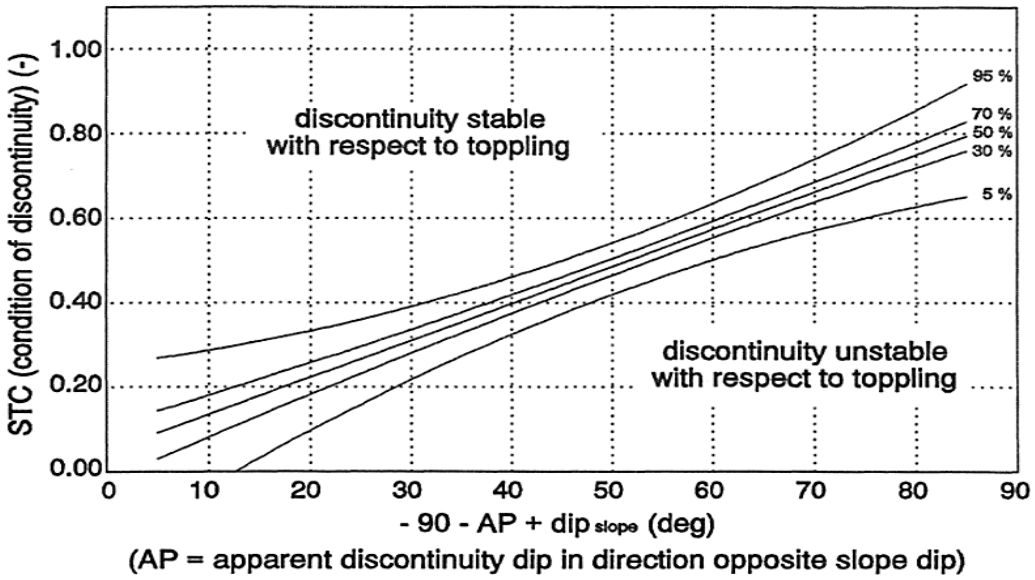

Fig. 5.28 Toppling probability for orientation dependent slope stability (after Hack, 1996)

Table 5.8 Additional conditions considered for sliding and toppling modes in the orientation–dependent analysis (after Hack et al., 2003)

Conditions	Sliding	Toppling
AP>84° or AP<-84	%100	%100
Slope dip+5<AP<84	%100	%100
Slope dip-5<AP<slope dip+5	%100	%100
0°<AP< (slope dip–5)	use sliding graph	%100
AP<0 and -90-AP+slope dip<0	%100	%100
AP<0 and -90-AP+slope dip>0	%100	use toppling graph

5.3.2 Determination of Orientation–independent SSPC assessment

Orientation–independent SSPC assessment is related to the strength of the rock mass in which the slope occurs. It is independent to the orientation of both the discontinuities and the slope unit. The stability of highly jointed rock slopes mainly depends upon the shear strength of rock mass and slope height. The failure surface also passes partially through intact rock and partially along existing discontinuities. For such slope masses, the SSPC system considers a linear shear plane model following the Mohr-Coulomb failure criterion to assess stability (Hack et al., 2003).

In this case, the internal friction angle and cohesion in Mohr-Coulomb failure criterion are represented by rock mass shear parameters which directly depend on intact rock strength, block volume and shear strength of all discontinuities in the rock mass (Hack et al., 2003).

In this research, to assess the orientation independent stability conditions, intact rock strength of slope mass (SIRS), discontinuity spacing (SSPA) and discontinuity condition (SCD) were determined as a function of reference rock mass values corrected by the factors of weathering degree (SWE) and method of excavation (SME) for existing/excavated slope. It is important to note that the weathering grade and method of excavation factors are similar to those determined for the exposure rock mass in case the stability of an existing slope is assessed and future weathering is neglected.

Orientation independent stability problem is not occurred if slope dip is less than or equal to SFRI for the investigated slope (Hack, 1998). Therefore, the maximum slope height (H_{max}) were calculated when slope rock mass friction (SFRI) is smaller than the dip of the slope. Later, the

ratio of (slope rock mass friction and slope dip (SFRI / dip_{slope})) and (maximum height (H_{max}) and natural height of the slope (H_{slope}) (H_{max} / H_{slope})) were determined. The maximum possible height of a rock slope (H_{max}) is infinite if the slope dip angle is less than the rock mass friction (φ_{mass}) (Hack et al,. 2003). Finally, the results of these ratios were plotted in Fig.5.5 to define the orientation independent probability stability of a slope sections.

In SSPC system, the maximum slope height (H_{max}) also calculated using cohesion, friction angle and slope dip. The maximum slope heights (H_{max}) were computed using Eq.5.22.

$H_{max} = [1.6*10^{-4} * SCOH * \sin(\text{slope dip}) * \cos(SFRI)]/ [1-\cos(dip_{slope} - SFRI)]$……. (equ.5.22)

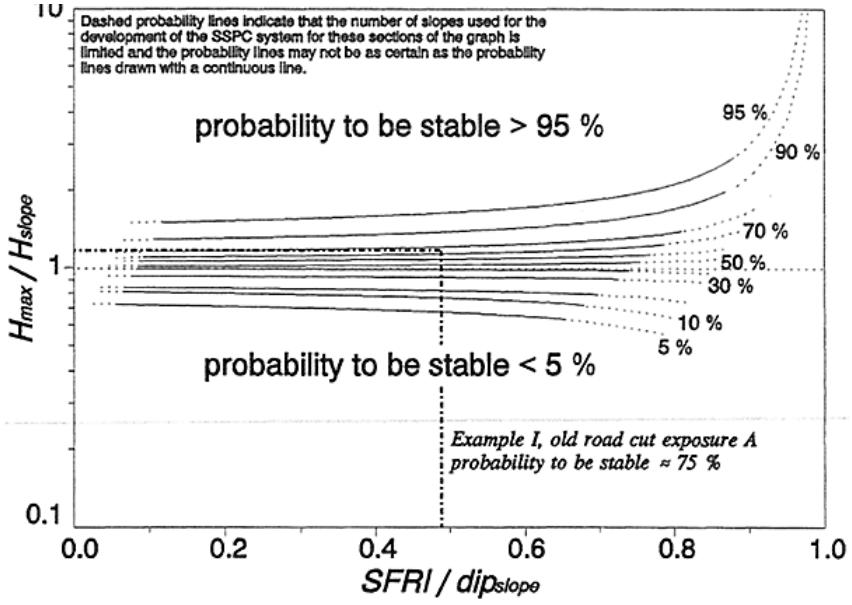

Fig. 5.29 Orientation independent slope stability Probability, Values indicate the probability of a slope to be stable (after Hack, 1996)

5.4 Determining of GSI parameters

To determine the geological strength index (GSI) values of slope rock mass, the old and modified GSI system were applied to compare the results. In old GSI system, GSI values were estimated based on block volume (Vb) and joint condition factors (Jc).

The block volume were determined based on joint spacing while, joint condition factors were determined based on large-scale waviness (Jw), small-scale smoothness (Js) and joint alteration factor (Ja) by using equ.3.2 and 3.3 respectively.

In modified GSI system, GSI values were estimated based volumetric joint count (Jv), slope rock mass structures (SR) and surface condition (SCR) (Fig. 3.9). The SR values were determined based on the volumetric joint count (Jv), whereas the SCR of discontinuities were determined by considering roughness, weathering and infilling parameters of discontinuities.

5.4.1 GSI assessments

Finally, based on results obtained from calculation, the slope rock mass conditions were characterized using graphs (Fig.3.8 and 3.9). The values obtained in both cases, the old and modified GSI systems are more or less the same. The GSI value provides a numerical representation of the overall geotechnical quality of the rock mass. In the present study, GSI estimated values ranges from 25 – 63 (Annex 8.5.1). Accordingly, the percentages of blocky slope sections are defined as 78.2% very blocky and 21.8% blocky/disturbed.

*****

Chapter VI Results, Interpretation And Discussion

6.1 Preamble

Slope stability assessments are essential for understanding slope rock mass performance and in particular with their stability, reliability and deformations. The study is based on the primary and secondary data analysis. The required data was obtained through extensive field investigation on the selected critical slope sections of the study area.

As described in the previous sections, the assessments were carried out using SSPC and GSI field based approaches. SSPC system calculates the slope stability probability using two different approaches. The first one is 'orientation dependent stability' which is related to instabilities that controlled by the nature of discontinues. It is assessed using the discontinuity data related to the rock slope mass that determines the failure mechanism and modes of rock slopes subjected to structural control failure (Li and Xu, 2015). The second one is 'orientation independent stability', where the instability is rather controlled by the strength of the slope rock mass. It is independent to the orientation of both the discontinuities and the slope unit.

In the chapter 5, the collected primary and derived data were processed to define the controlling parameters for SSPC and GSI were presented. This chapter deals further with a detailed assessment and discussion on results and systematic interpretations.

6.2 Field visual estimation of slope stability conditions

During field work, for all 92 slope rock mass sections stability condition was visually estimated based on standards produced by Hack (1998).This was done for the purpose of cross checking of results obtained by SSPC and GSI assessments and also know the general physical condition of slope rock mass. Accordingly, most of the slope sections are characterized as class 2 (Table 6.5) that is; 43 slope sections are characterized as class 2, 30 slope sections as class 3 and the rest 19 slope sections are characterized as class1. Based on field visual estimation the following map was produced by using buffer zoning technique (Fig.6.1).

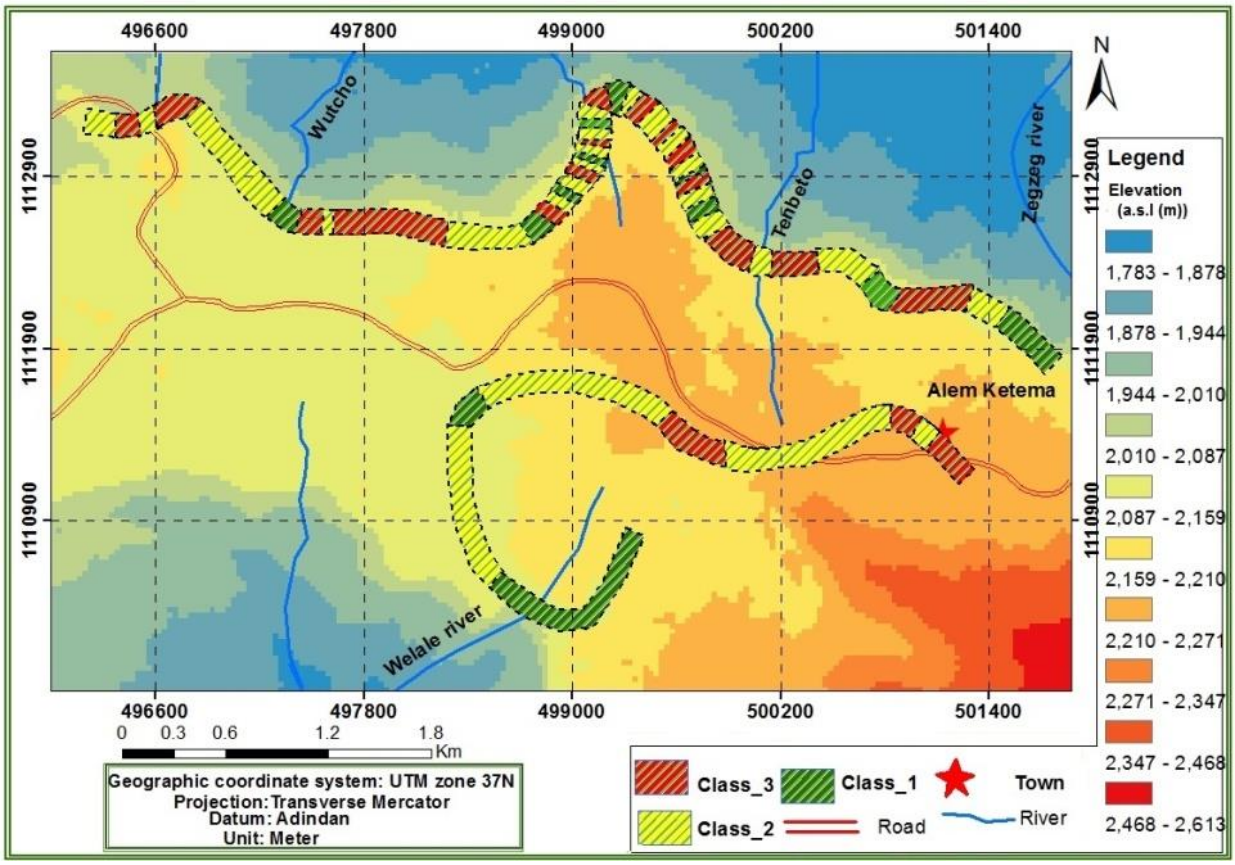

Fig. 6.30 Map showing visually estimated slope rock mass conditions

6.3 SSPC assessments and results

In this study, SSPC is involved to calculate the slope stability probability of each investigated slope rock masses. Before calculating the slope stability assessment, it is essential to calculate the rock mass parameters, as it is done in chapter 5. The SSPC calculates slope stability probabilities as a function of slope geometry and rock mass characteristics that include degree of weathering (Hack et al., 2003).

SSPC system considers the orientation of discontinuities in combination with the shear strength to determine the possibility of movement along the discontinuities (Hack et al., 2003). The failure probabilities of the slopes were then calculated according to two different analyses, orientation-dependent and orientation independent stability assessments, after obtaining the related parameters. A final assessment of the slopes was done by choosing the smallest stability probability determined via the two analyses of the SSPC method.

6.3.1 Orientation dependent stability probability

The main parameter controlling orientation dependent stability probability type of failure is the shear strength of the discontinuity.

Slope failure mechanisms such as shear displacement and the resulting different failure mechanisms are discontinuity related and are dependent on the orientations of slope and discontinuity. Therefore, it is necessary to know which discontinuity set plays an important role for the slope failure. Based on the calculated data, the apparent discontinuity dip (AP) is derived to all slope sections (Annex 8.1.3). Using the provided criteria, sliding and toppling, SSPC orientation-dependent stability assessments were determined.

6.3.1.1 Sliding and toppling failure assessment

The description of slope rock masses was done in 92 slope section within three geological units around the town Alem Ketema. Accordingly, several parameters were calculated to all discontinuities in each slope sections (Annex 8.1.2 and 8.1.3). The calculated values for both sliding and toppling criterion are given in Annex 8.6.

I. Sliding criterion

Based on the established relation between the condition values of discontinuity (TC) and the apparent angle of the dip of the discontinuity plane in the direction of the slope dip (AP) (Equ. 5.19 and 5.20); the sliding criterion is calculated as stated in Hack (1998). That is;

$$TC < 0.0113*AP \text{ and}$$

$$AP=\arctan(\cos(\sigma s-\sigma j)*\tan\beta j).$$

Where, σs refers slope dip direction, σj refers discontinuity dip direction, βj refers discontinuity dip.

1) If $AP > 0°$, AP = apparent discontinuity dip in the direction of the slope dip

2) If $AP < 0°$, $|AP|$ = apparent discontinuity dip in the direction of opposite the slope dip

Those result fall below probability line (TC=0.0113*AP) are referring to unstable condition for the sliding criteria.

Accordingly, the sliding criterion was verified in the slope rock masses and showed that 67 slope rock masses have one or more discontinuities which dip towards the slope. Moreover, these all have one or more day-lighting discontinuities (Table 6.1). Plotting the day-lighting discontinuities on TC versus AP graph showed that 51 below line TC=0.0113*AP and the rest 16 slopes are above the line (Fig. 6.2).

According to sliding graph (Fig. 5.3), these slope sections showed that most of them have less than 5% (44 slope sections) stability probability, while the rest showed that 8 slope sections from 5-49%, 13 slope sections from 50-95% and 2 slope sections greater than 95% stability probability (Table 6.1). This shows that, most of the day-lighted slope section showed less than 5% stability probability. These indicate that, the study area is highly prone for slope failures with respect to sliding.

Moreover, the results obtained through sliding criterion are verified by using visually estimated results. Therefore, during field investigation, several sliding traces were observed. Specially, on wet slope section it is dominantly affected by sliding failures. Accordingly, 30 slope sections were visual estimated as class 2, 24 slopes as class 3 and the rest 13 slopes were estimated as class1(Table 6.1). Comparing the discontinuities with the probability lines showed that those above the sliding criterion are stable with respect to sliding; whiles the rest slope sections below the sliding criterion showed low stability probability.

Table 6.9 Probability of stability of 67 slopes with day-lighting discontinuities in the study area

Class of Visual stability assessment	No. of slopes	No. of set of day-lighting discontinuities	Sliding stability probability		
			<5%	5%-95%	>95%
Class 1 [13]	10	1	6	3	1
	3	2	-	3	-
Class 2 [30]	24	1	14	9	1
	6	2	5	1	
Class 3 [24]	16	1	13	3	-
	8	2	6	2	-

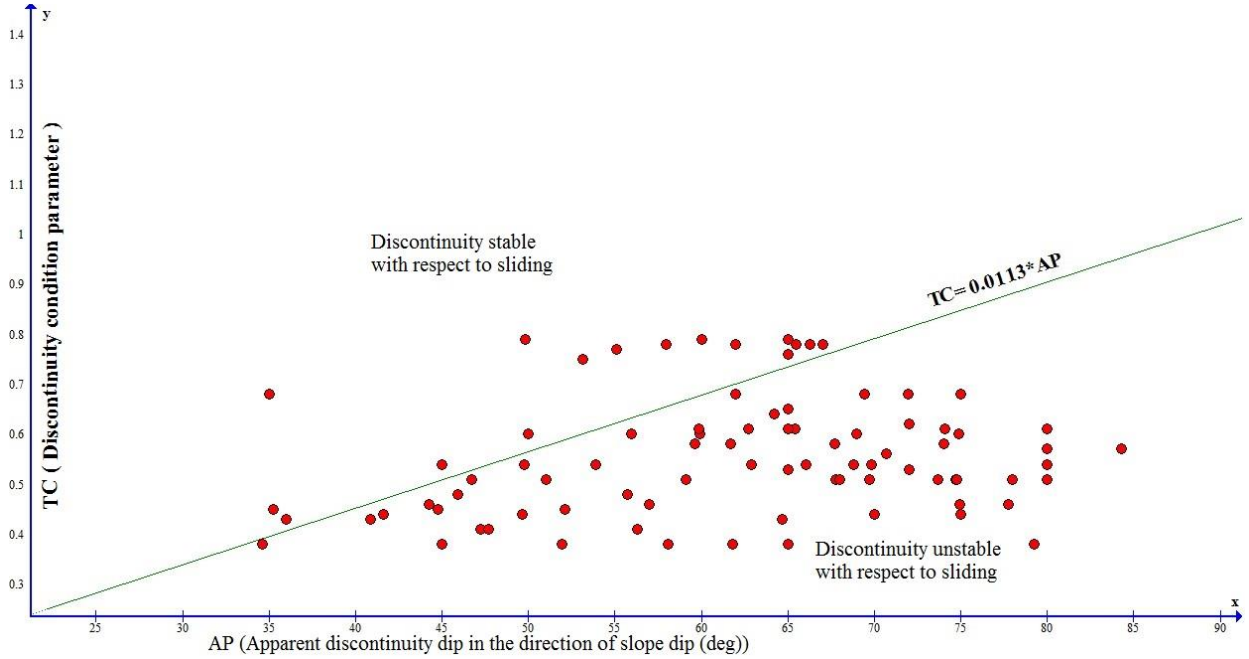

Fig. 6.31 Discontinuity condition TC vs. AP for day-lighting discontinuities in stable and unstable slopes

II. Toppling criterion

Using the toppling criterion (eq.5.21), the SSPC toppling stability status is calculated.

That is; $TC < 0.0087(-90\text{-}AP+dip_{discontinuity})$

It is defined that the toppling condition (-90-AP+slope dip) is less than zero, the stability of discontinuity with respect to toppling is 100 %. These means there are no slope stability problem related to toppling in these slopes.

Therefore, toppling analysis showed that 51 slope sections have one or more discontinuities which dip against the slope and which have positive toppling conditions ($-90\text{-}AP+dip_{discontinuity}$); and all these slope sections were found to topple as they satisfy $TC<0.0087(-90\text{-}AP+dip_{discontinuity})$ (Table 6.2). According to toppling graph (Fig.5.4), these slope sections showed that most of them have greater than 95% (22 slope sections) stability probability, while the rest showed that 11 slope sections less than 5%, 11 slope sections from 5-49% and 7 slope section from 50-95% stability probability (Table 6.2).

Moreover, visually estimated condition showed that from 51 slope sections, 22 slopes are visually estimated as class 2 (problem in near future), while the reset 15 slope sections are estimated as class 3 (problems) and 14 slope sections are estimated as class 1(stable). Accordingly, small numbers problem slope sections were identified and in contrary the numbers of stable slopes sections are increase as compared to sliding. The number of slope sections showed less than 5% stability probability also decreased as compared to sliding criterion. These all implies that, in the study area sliding is more prominent than toppling. However, following basaltic escarpments a number of toppling failures were observed during field investigations. Besides, in some slope section, it was observed that they were affected by both sliding and toppling failures.

Table 6.10 The 51 slopes that showed positive toppling conditions (-90-AP+dipdiscontinuity)

Class of Visual stability assessment	No. of slopes	No. of set of day-lighting discontinuities	Toppling stability probability		
			<5%	5%-95%	>95%
Class 1 [14]	12	1	1	5	6
	2	2	-	1	1
Class 2 [22]	18	1	5	8	5
	4	2	1	1	2
Class 3 [15]	11	1	2	2	7
	4	2	2	1	1

6.3.1.2 Slope stability probability in both sliding and toppling criterions

As discussed earlier, some slope sections were characterized by both sliding and toppling failure. Accordingly, from 92 slope sections, only 7 slope sections showed less than 5% salability probability in both sliding and toppling criteria. Moreover, 4 slope sections showed greater than 95% and one slope sections showed 100% in both criteria (Table 6.3). This also verified during field works and the related results were obtained.

In the study area, the steep cliffs, wet slopes and close jointing are commonly characterized those slopes affected by both sliding and toppling failure. These were frequently observed specially on slope sections which have streams thrown from the top towards the toe of escarpments.

However, those slopes which are affected by the columnar basalt are hardly associated with this type failure. In fact, sliding and toppling failure has a prominent effect on the stability of slope rock masses in the study area.

Table 6.11 slopes having the same stability probability in toppling and sliding criteria

No.	Slope section	Sliding stability probability	Toppling stability probability
1	8	<5%	<5%
2	14	<5%	<5%
3	19	<5%	<5%
4	37	<95%	>95%
5	38	<5%	<5%
6	50	<5%	<5%
7	51	<5%	<5%
8	71	>95%	>95%
9	78	<5%	<5%
10	81	>95%	>95%
11	82	100%	100%
12	83	>95%	>95%

The general result of the orientation dependent assessment showed that only 9 slope sections are stable (>95% stability probability). The rest showed different rate of stability probability: 51 slope sections showed less than 5% stability probability, 14 slope sections showed between 5 and 49% stability probability and the rest 18 slope section showed between 50 and 95% stability

probability. This indicates that most slope sections showed low stability probability values with respect to sliding criterion as compared to toppling.

They are also visually estimated as 19 slope sections as class 1, 43 slope sections as class 2 and the rest 30 slope sections were estimated as class 3. The general stability probabilities of slope section as well as the individual joint set condition in relation with orientation dependent failure are given in Annex 8.8. Accordingly, the orientation dependent map was produced using buffer zoning techniques (Fig.6.3). This map shows the area or slope section where orientation dependent failures are more dominant and the general failure distributions in the study area.

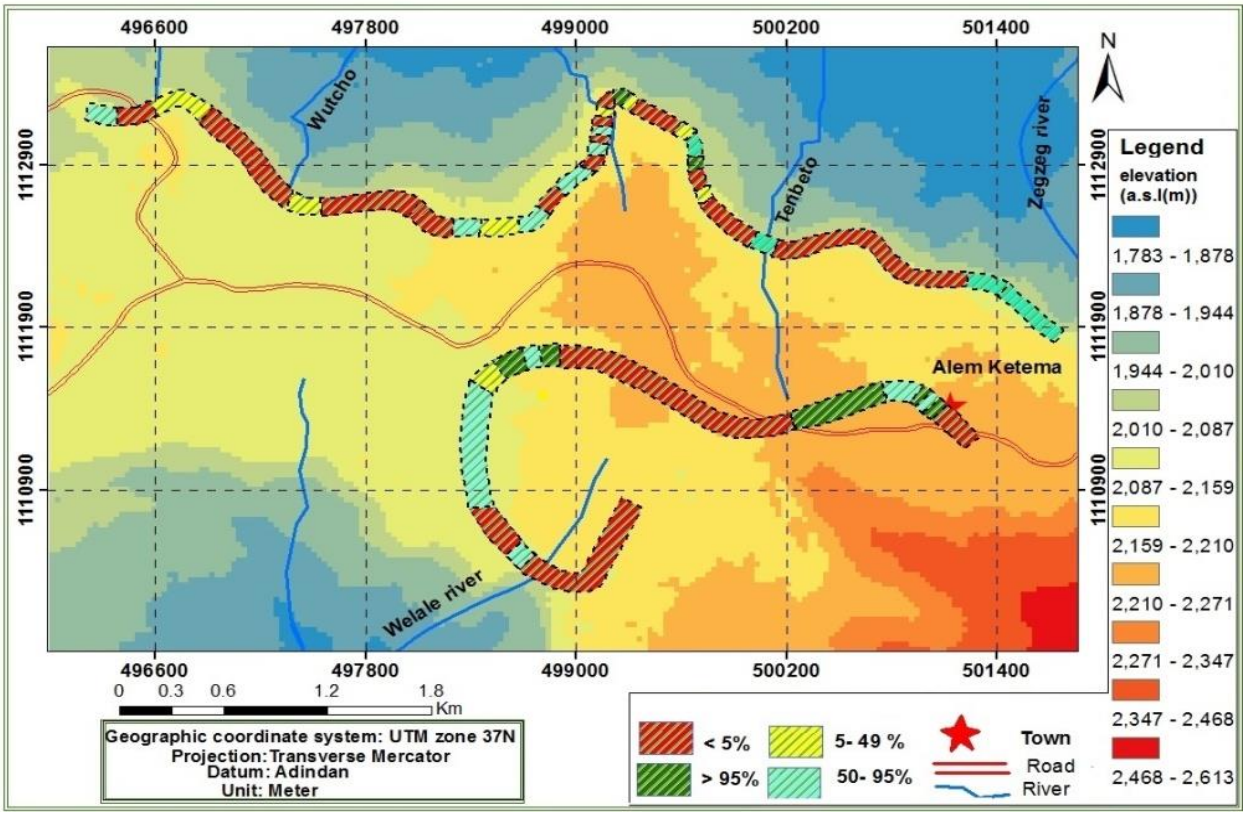

Fig. 6.32 Map showing Orientation dependent slope stability probability of the study area

6.3.2 Orientation independent stability probability

Slope failure is not only related to the discontinuity, but also to the slope mass weakness. The orientation independent stability is related to the strength of the rock mass, which is always independent to the orientation of both the discontinuities and slope (Hack, 1998). It was observed

that a small fracture in the intact rock may results in linear failure planes developing partly through intact rock and partly through the existing discontinuity plane (Hack et al., 2003). This effect can be prominently observed in rock masses when the block size is smaller. Therefore, intact rock strength, block size and the shear strength along the discontinuities have an influence on the development of failure planes, which is not related to the single discontinuity plane (Hack et al., 2003). The deformation of the strength parameters are difficult to evaluate for a large scale deformed rock mass in such assessments, as there are many associated uncertainties (geological and geo-mechanical properties) in the rock mass (Trufat Hailemariam, 2009).

It is also noted that strength prediction in deformed a rock mass at regional scale remains as one of the main challenges of rock mechanics. Besides, as there are not any previous relevant studies in the present study area, it was difficult to check the validity of the results of these assessments.

The orientation independent stability of a slope was modeled by a linear shear plane model following the Mohr - Coulomb failure criterion, related to friction and cohesion of the rock mass (Hack et al., 2003). This implies that the stability of a slope is independent of the height of the slope if the slope has a dip angle less than the friction angle of the rock mass (Hack et al., 2003). If the dip angle is higher than the friction angle, however, the maximum slope height is determined by the stresses in the slope.

The calculated and measured parameters of rock mass friction and cohesion, slope dip, height of the slope and maximum slope height were used to determine the orientation independent stability probability (Hack, 1998; Hack et al., 2003; Lindsay et al., 2001; Canal and Akin, 2016). Rock mass cohesion, friction angle and rock mass strength are derived empirically based upon the intact rock strength, degree of weathering, discontinuity spacing, roughness and condition as well as excavation damage.

The main output of the orientation-independent stability assessment is value of rock mass strength parameters which are cohesion and internal friction angle (Hack, 1998; Hack et al., 2003). These values are based on Mohr-Coulomb failure criterion (Hack et al., 2003). For orientation dependent stability the rock mass parameters are influenced by weathering is the condition of a discontinuity sets. However, in the case of orientation independent stability the rock mass parameters influenced by weathering are φ_{mass} and coh_{mass} (Hack, 1998; Hack et al.,

2003). The height of the slope has a direct influence on the stress levels in the rock mass of the slope (Hack, 1998; Li and Xu, 2015; Canal and Akin, 2016). High slope may also present more opportunities for discontinuity related failure because the quantity of discontinuities intersected by the slope is larger.

The maximum possible height of the slope is the theoretical maximum height of a slope which have same dip as that of the existing slope (dip_{slope}) (Hack et al., 2003). The H_{max} should then be compared to the real or natural slope height of the existing slope rock mass.

Therefore, if maximum possible height of the slope is more than the height of the real slope then slope should be stable ($H_{max} > H_{slope}$), while if natural slope height is more than the height of the maximum possible height of the slope then slope should be unstable (Hack et al.,2003) . The H_{max} in relation to the dip of the slope is governed by the rock mass cohesion and friction if the slope dip is larger than the rock mass friction (Hack, 1998). Therefore, the following are conditions were adopted to characterize slopes whether the slope is stable or unstable;

Stable if;

1. $\varphi_{mass} / dip_{slope} \geq 1$ (stable) and
2. $\varphi_{mass} / dip_{slope} < 1$, $H_{max} / H_{slope} \geq 1$ (stable)
   $H_{max} / H_{slope} < 1$(unstable)

Unstable if;

1. $\varphi_{mass} / dip_{slope} \leq 1$ (unstable) and
2. $\varphi_{mass} / dip_{slope} > 1$, $H_{max} / H_{slope} \geq 1$ (unstable)
   $H_{max} / H_{slope} < 1$(stable)

Accordingly, the maximum possible height of a rock slope (H_{max}) is infinite if the slope dip angle is less than the rock mass friction (φ_{mass}) (Hack et al., 2003). If $\varphi_{mass} > dip_{slope}$, stability probability of slope sections are 100%, else graphs are used for orientation-independent stability. This can be conculed that there will be no orientation independent stability problem if slope dip is less than or equal to rock mass friction ($dip_{slope} \leq \varphi_{mass}$) for investigated slope (Hack, 1996; 1998; 2002; Hack et al., 2003; Li and Xu, 2015).

In the present study, using the stated criterion, $\varphi_{mass} > dip_{slope}$, all 92 slope sections were checked for orientation-independent stability probabilities. Accordingly, it is found that none of the slope sections fulfill criteria and all slope sections were assessed using graph (Fig. 5.5). Due to this, the maximum possible heights (H_{max}) were calculated by using eq.5.22. After this, the ratio of (φ_{mass} and dip_{slope}) and (H_{max} and H_{slope}) were determined. Finally, the stability probabilities of the slope section were determined using a graph (Fig. 5.5). The maximum slope height, H_{max} / H_{slope} and φ_{mass}/ dip_{slope} results are given in Annex 8.2.

Therefore, in this study, slope sections are analyzed for $H_{max} < H_{slope}$ criteria and it is found that 68 slope sections satisfied and considered as unstable. Besides, comparison with probability lines on (φ_{mass}/ dip_{slope}) versus to (H_{max} / H_{slope}) plot showed that 53 of the unstable slope have <5% stability probability. According to the ratio graph (Fig. 5.5), the stability of slope is less than 5% means it is highly unstable.

In fact, having 53 unstable slopes is rather contradicting with the generally expectation of stability conditions in the area where strong volcanic rock mass is dominating. It may be related to the SSPC limitation in the areas where slope height is more than 45m and/or the impact of weathering in the study area. The surface weathering conditions of these slopes show that most of them are associated with moderate to high degree of weathering. However, there are also slopes characterized by slight weathering with high intact rock strengths. Based on field observation, it can be conclude that weathering and human innervations play major role in defining the stability conditions. On the other hand, the remaining 39 slope sections are generally showed stable conditions with variable stability probability values, that is; 11 slope sections showed between 5-49%, 16 slope sections showed between 50-95% and the rest 12 slopes showed greater than 95% stability probability.

The overall results of the orientation independent slope stability probability results are given in Table 6.5 and also compared with visual estimation results to show that from unstable slopes that gave less than 5% stability probability; 56.6% of slope sections are within class 2, 41.5% in class 3 and only 1.9% are visually estimated as Class 1.

On the other hand, from slopes showing stability probabilities between 5-49%; 36.4% of slope sections are visually estimated as class 1, 18.2% of slope sections are visually estimated as class 2 and 45.5% slope sections are visually estimated as class 3.

From slopes showing stability probabilities between 50-95%; 43.8% of slope sections are visually estimated as class 1, 43.8% slope sections are visually estimated as class 2 and the rest 12.5% are estimated as class 3.

From slopes showing stability probabilities of greater than 95%; 58.3% of slope sections are visually estimated as class 1, 33.3% of slope sections are visually estimated as class 2 and 8.3% of slope sections are visually estimated as class 3.

Finally, based on these results, orientation independent map was produced using buffer zoning techniques (Fig.6.4). This map generally showed the location where low strength rock masses were found as well as stability probability condition in relation with rock mass strength that is orientation independent failures. Accordingly, the map was produced by classifying the values in to four classes for the purpose discussions. As shown in the Fig. 6.4, several slope sections are fall under classes having values stability probability less than 5% and the second class having a number of slope sections are values ranging from 50-95% stability probabilities. This shows that, in the study area slope rock mass failure with respect to orientation independent i.e. related to rock mass strength are prominent effect.

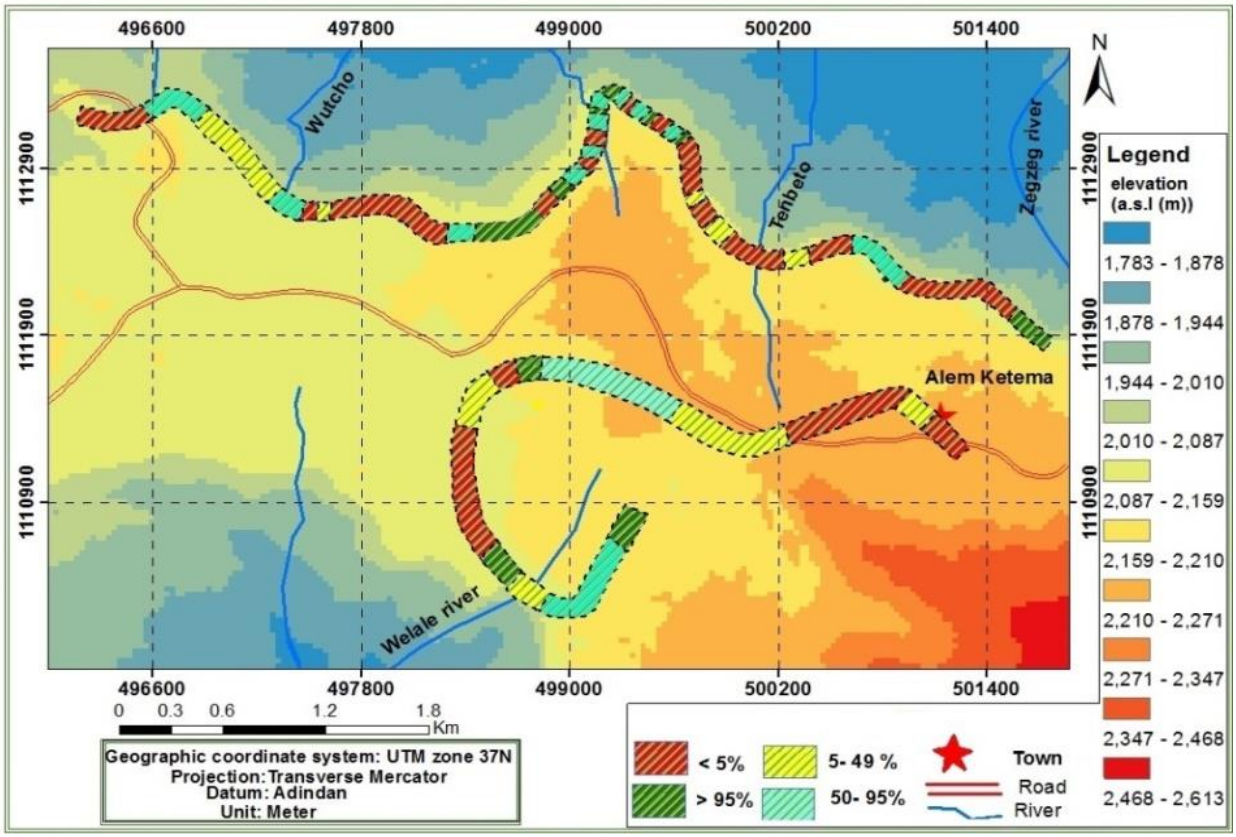

Fig. 6.33 Map showing Orientation independent slope stability probability of the study area

6.3.3 Discussion on SSPC Results

The discussion on SSPC result are given based on the results obtained through orientation dependent and orientation independent assessment techniques. Accordingly, the overall assessment of the slopes was done by choosing the smallest stability probability determined via the two assessments.

Primarily, the orientation dependent assessments were done by considering the result obtained through sliding and toppling criterions. Accordingly, it is found that 55.4% slope section showed less than 5% stability probability, while the rest 34.8% and 9.8% slope section showed from 5-95% and greater than 95% stability probability, respectively. Similarly, in orientation independent assessment it is found that 57.6% slope section showed less than 5% stability probability, while the rest 29.4% and 13 % of slope section showed from 5-95% and greater than 95% stability probability respectively (Table 6.4).

Therefore, through combination of orientation dependent and orientation independent results, the SSPC stability probability conditions were determined. The results obtained in both orientation dependent and orientation independent showed that most of slopes sections are showed <5% stability probability values; indicating their unstable conditions which may fail with in near future. Moreover, the results obtained in both assessment systems are verified by visually estimated condition and showed related results. The assessment result showed more failures are observed in orientation independent techniques; which is not generally expected in areas where strong volcanic rock mass are dominating. However, this contradiction may relate to the SSPC limitation in the areas where slope height is more than 45 m and with variable weathering conditions.

SSPC assessments general showed that 80.4% of slope sections are defined by less than 5%, while the rest 17.4% and 2.2% of slope section defined from 5-95% and greater than 95% respectively. These results indicate that, the study area is general susceptible for slope instabilities and the area is well known with a history of landslides.

Table 6.12 stability probability summery table

6.4 GSI assessment and results

Visual status	No.	SSPC Probability of Failure											
		Sliding Criteria			Toppling Criteria			Orientation dependent			Orientation independent		
		<5 %	5-95 %	>95 %	<5 %	5-95 %	>95 %	<5 %	5-95 %	>95 %	<5 %	5-95 %	>95 %
Class 1	19	6	7	6	1	6	12	6	11	2	1	11	7
Class 2	43	20	12	11	6	9	28	23	14	6	30	9	4
Class 3	30	21	5	4	4	3	23	22	7	1	22	7	1
Total	92	47	24	21	11	18	63	51	32	9	53	27	12
%		51 %	26.1 %	22.9 %	12 %	19.5 %	68.5 %	55.4 %	34.8 %	9.8 %	57.6 %	29.4 %	13 %

Estimation of Vb for blocks was difficult at realistic level to determine in all slope faces as blocks are steep and exhibit erratic geometries, so the Sonmez et al. (2003) chart was used mostly, however, Cai et al. (2004) chart also used in place. The GSI charts can be used to estimate the characteristics of rock masses with discontinuities and filling materials using the descriptions in the columns of poor or very poor condition of discontinuities. If the filling material is systematic and thick (e.g. more than few cm) or shear zones are present with clayey material then the use of the GSI chart for heterogeneous rock masses is recommended (Marinos et al., 2005).

6.4.1 Slope rock mass characterization using GSI

In both cases, SCR, SR, Vb and Jc were calculated to all slope faces to estimate their respective GSI range values as suggested by Marinos et al.(2005). The GSI values of the rock masses at the study area range from 25 and 63 (Table 6.5). The structure rating, surface condition ratings were determined. Structure is related to the block size and the interlocking of rock blocks and surface condition is related to weathering, persistence and condition of discontinuities.

Most of slope sections structurally defined by very block conditions and most of slope sections showed that good surface conditions.

However, slopes sections showing fair surface conditions are also significant in number. Accordingly, GSI map was produced by using buffer zoning techniques (Fig.6.5).

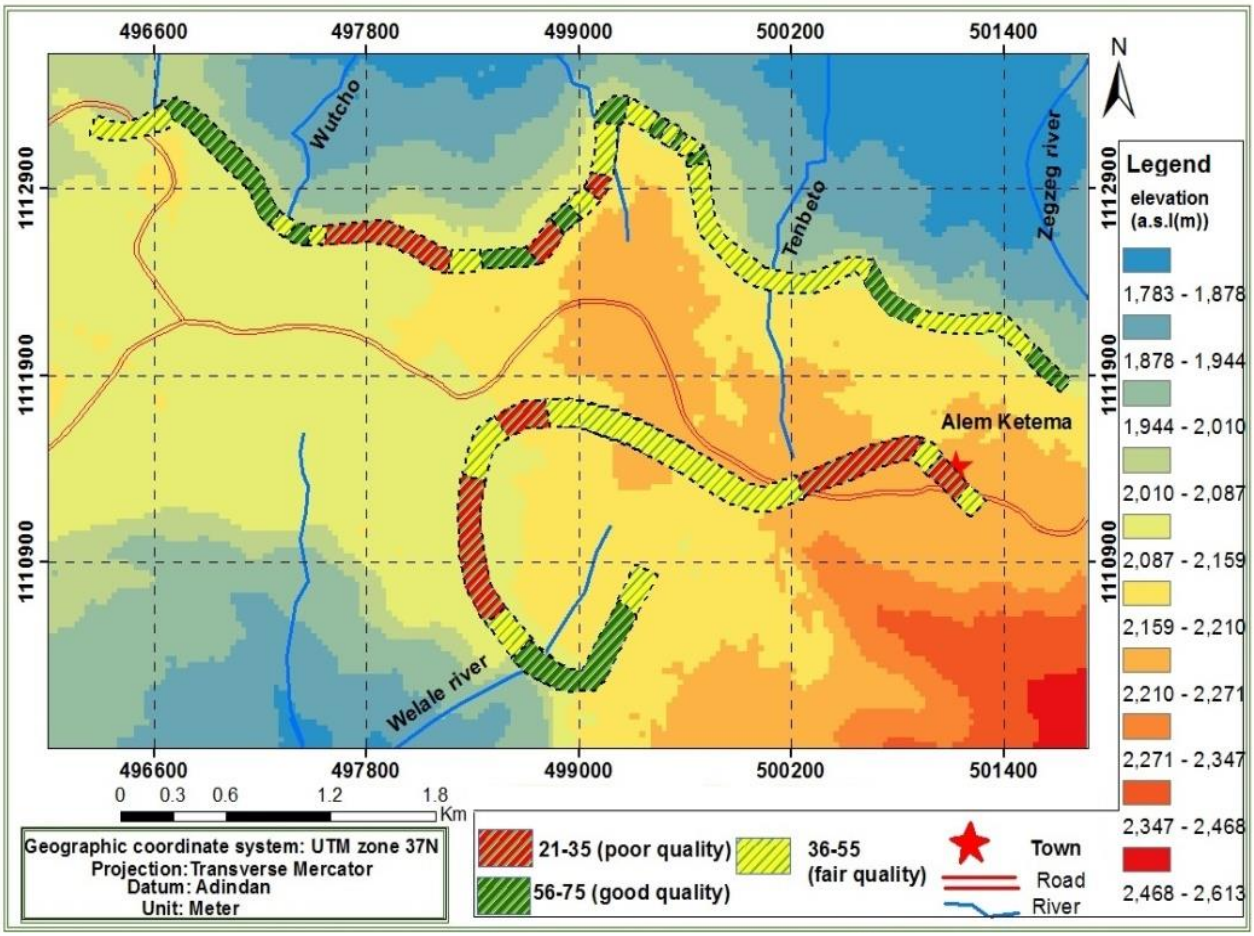

Fig. 6.34 Map showing GSI values of the study area

6.4.2 Discussion on GSI Results

The GSI results showed that most of slope rock masses are characterized by very blocky structures and good/fair surface conditions as well as have 48.9 average GSI values. This implies that most slopes have relatively low GSI values and accordingly showed low rock mass strengths. Based on Bieniawski (1989, as cited in Azzuhry, 2016), the rock mass quality descriptions of GSI result falls in to three classes i.e 20 slope sections from 56-75 (good), 60

slope section from 36-55 (fair) and 12 slope sections from 21-35 (poor). The rating are given in Annex 8.7.9. Accordingly, 65.2% of slope sections are characterized by fair rock mass quality and verified during field visual descriptions . This indicates that the weakness of the rock mass exposed in the study area is prone to orientation independent failure. The comparison between GSI values and field estimated values showed that in most slope sections more or less obtained related results (Table 6.5).

6.5 SSPC and GSI result comparison

The comparison the stability assessment results obtained by SSPC and GSI assessment techniques showed that both assessments techniques provides more or less related results (Table 6.5). In SSPC system, 74 slope sections showed less than 5% stability probabilities. Likewise, in GSI assessment, 60 slope sections have fair rock mass qualities. From these slope sections 50 slope sections are characterized by less than 5% stability probability, very block structures and have fair rock mass quality ranges. In field observation such type of slope section are described by closely spaced discontinuities. From the rest slope sections, 9 slope sections which have fair rock mass quality are defined by the stability probability from 5-95% and one slope section showed greater than 95% stability probability.

Generally, both result showed that most slopes are characterized by weak slope strength conditions as well as low stability probabilities. This implies that slope sections in the study area are highly influenced by both orientation dependent and orientation independent failure. Because, orientation independent slope failures are related to rock mass strengths. These results also verified using visual field estimation and most of slope sections fall under class 2 (Table 6.5). This implies that the area is highly exposed for near future slope failure problems.

6.6 Slope stability probability classification (SSPC) map

The slope stability probability map was prepared based on SSPC results (Table 6.5). SSPC results are obtained from orientation dependent and orientation independent assessments. This was done by choosing the smallest stability probability results determined through these two assessments systems. This general map showed that the different stability probabilities of the delineated slope sections (Fig.6.6). Accordingly, most of slope section fall under stability

probability of less than 5%. Similar to other maps this map also produced by using buffer zoning technique.

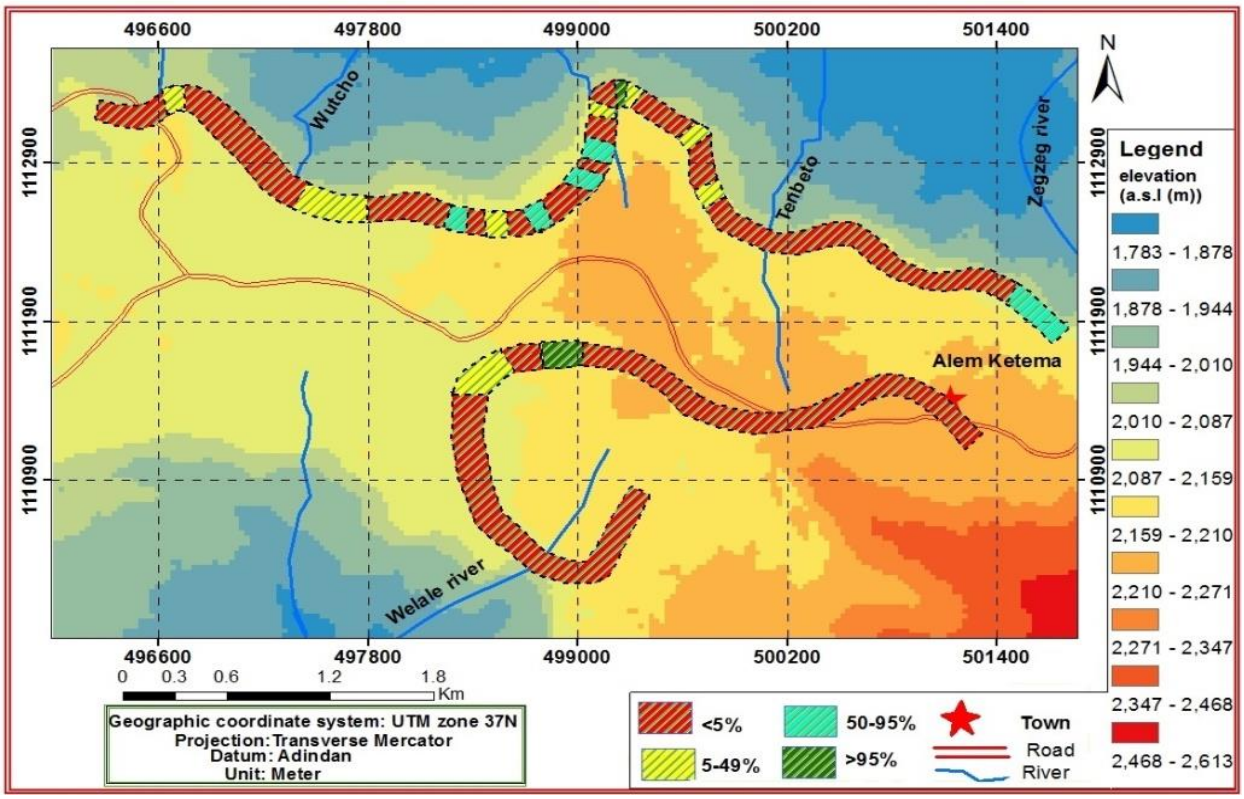

Fig. 6.35 Map showing the general slope stability of the study area

Table 6.13 SSPC, GSI and visual estimation results summery

Slope section no.	SSPC system			GSI system		Visual estimation
	Orientation dependent stability probability	Orientation independent stability probability	SSPC stability probability	GSI	Rock Mass Quality	
1	<5%	<5%	<5%	48	fair	class 3
2	80%	<5%	<5%	54	fair	class 2
3	<5%	<5%	<5%	55	fair	class 2
4	>95%	<5%	<5%	54	fair	class 1
5	<5%	<5%	<5%	45	fair	class 3
6	<5%	<5%	<5%	55	fair	class 2
7	25%	10%	10%	46	fair	class 1
8	<5%	<5%	<5%	55	fair	class 2
9	<5%	10%	<5%	52	fair	class 3
10	<5%	<5%	<5%	50	fair	class 3

11	<5%	<5%	<5%	48	fair	class 2
12	75%	<5%	<5%	48	fair	class 2
13	<5%	<5%	<5%	55	fair	class 3
14	<5%	25%	<5%	52	fair	class 3
15	<5%	<5%	<5%	47	fair	class 2
16	<5%	<5%	<5%	50	fair	class 2
17	<5%	50%	<5%	58	good	class 2
18	<5%	55%	<5%	62	good	class 1
19	<5%	<5%	<5%	48	fair	class 3
20	<5%	<5%	<5%	48	fair	class 3
21	50%	<5%	<5%	47	fair	class 3
22	8%	<5%	<5%	50	fair	class 2
23	15 %	<5%	<5%	46	fair	class 2
24	75%	85%	75%	57	good	class 1
25	<5%	>95%	<5%	60	good	class 2
26	40%	60%	40%	52	fair	class 2
27	<5%	<5%	<5%	58	good	class 2
28	<5%	<5%	<5%	54	fair	class 2
29	<5%	<5%	<5%	47	fair	class 3
30	<5%	50%	<5%	53	fair	class 2
31	<5%	70%	<5%	58	good	class 3
32	<5%	<5%	<5%	52	fair	class 3
33	<5%	<5%	<5%	47	fair	class 3
34	<5%	<5%	<5%	50	fair	class 2
35	<5%	80%	<5%	48	fair	class 1
36	10%	50%	10%	52	fair	class 1
37	>95%	80%	>95%	62	good	class 1
38	<5%	70%	<5%	60	good	class 2
39	<5%	60%	<5%	60	good	class 2
40	<5%	50%	10%	48	fair	class 1
41	<5%	65%	<5%	54	fair	class 2
42	65%	<5%	<5%	48	fair	class 3
43	<5%	<5%	<5%	47	fair	class 2
44	80%	>95%	80%	55	fair	class 1
45	<5%	<5%	<5%	35	poor	class 2
46	20%	<5%	<5%	40	fair	class 3
47	75%	60%	60%	48	fair	class 2
48	75%	>95%	75%	60	good	class 1
49	<5%	65%	<5%	62	good	class 1
50	<5%	<5%	<5%	58	good	class 2
51	<5%	<5%	<5%	54	fair	class 2
52	<5%	<5%	<5%	42	fair	class 3

53	55%	65%	55%	60	good	class 1
54	15%	65%	15%	58	good	class 2
55	50%	80%	50%	55	fair	class 2
56	<5%	<5%	<5%	30	poor	class 3
57	<5%	<5%	<5%	25	poor	class 3
58	<5%	<5%	<5%	28	poor	class 2
59	<5%	10%	<5%	35	poor	class 3
60	<5%	<5%	<5%	38	fair	class 3
61	10%	25%	10%	58	good	class 1
62	8%	<5%	<5%	50	fair	class 3
63	10%	65%	10%	56	good	class 1
64	10%	25%	10%	62	good	class 1
65	<5%	20%	<5%	56	good	class 2
66	25%	50%	25%	45	fair	class 3
67	<5%	<5%	<5%	52	fair	class 2
68	<5%	<5%	<5%	48	fair	class 3
69	70%	<5%	<5%	54	fair	class 2
70	70%	<5%	<5%	53	fair	class 2
71	>95%	>95%	>95%	36	fair	class 2
72	85%	<5%	<5%	33	poor	class 2
73	>95%	<5%	<5%	27	poor	class 2
74	45%	10%	10%	42	fair	class 1
75	80%	<5%	<5%	38	fair	class 2
76	>95%	<5%	<5%	33	poor	class 2
77	<5%	50%	<5%	38	fair	class 3
78	<5%	35%	<5%	40	fair	class 3
79	>95%	<5%	<5%	34	poor	class 2
80	80%	10%	<5%	39	fair	class 3
81	>95%	<5%	<5%	35	poor	class 2
82	100%	<5%	<5%	32	poor	class 3
83	>95%	<5%	<5%	43	fair	class 2
84	75%	<5%	<5%	45	fair	class 2
85	<5%	<5%	<5%	43	fair	class 3
86	10%	<5%	<5%	43	fair	class 3
87	<5%	>95%	<5%	49	fair	class 1
88	<5%	50%	<5%	58	good	class 1
89	<5%	15%	<5%	55	fair	class 2
90	60%	>95%	<5%	63	good	class 1
91	50%	<5%	<5%	33	poor	class 2
92	<5%	<5%	<5%	47	fair	class 3

*****

Chapter VII Conclusion and Recommendations

7.1 Conclusion

Alem Ketema is located in mountainous and rugged terrain. As a result, it is frequently affected by rock mass failure problems. Constructions at the toe or on the top of escarpments are triggering some failures in the area; and raise the need of slope rock mass stability assessment in the area for urban planning and infrastructure development. Thus, in this study, different approaches were applied to estimate the rock mass strength and define the rock slope stability conditions.

In this study, 92 rock slope sections are selected to investigate the slope stability conditions using Slope Stability Probability Classification (SSPC) system that assesses the failure probability of slopes and GSI that help to define the rock mass quality. In SSPC, the sliding and toppling criterion under orientation dependent and orientation–independent analysis were applied.

Detail set of parameters were measured in the field in each slope sections. These are slope lithology, degree of weathering, slope and discontinuity orientation, discontinuity spacing (block size), infill material, karst condition, intact rock strength, slope height, method of excavation, large scale roughness, small scale roughness, persistency, ground water condition and discontinuity separation (aperture). Furthermore, different derived parameters were calculated from the data using empirical relations.

The slope stability probability results of 92 slope sections were classified in to 4 classes. These are, slope sections which showed less than or equal to 5% (unstable), 5- 49%, 50-95% and greater than or equal to 95% (stable) stability probability values. According to SSPC results, it can be conclude that 80.4% of slopes have been found less than 5% stability probabilities. While, the rest slope sections have been found different stability probability values. These are 10.9% of slope sections showed between 5-49%, 6.5% slope sections between 50-95% and 2.2% slope sections showed greater than 95% stability probability values.

The results obtained through GSI assessment showed that most the delineated slope sections are defined by fair rock mass quality condition; i.e., 65.2% of slope sections showed fair rock mass quality, 21.7% of slope sections showed good rock mass quality and the rest 13.1 % of slope sections showed poor rock mass quality status. This reflects that the weakness of rock mass existed in the study area that has a potential to cause instability of orientation independent failures.

The overall assessments indicates that most of the slope exposures have high probability of slope failure, indicating that most rock slopes in the study area are prone to both orientation dependent and orientation independent stability problems.

7.2 Recommendation

From the results and findings of the present study, the following recommendations are forwarded.

- In affirming the results of this study, further deterministic investigation should be required in selected sections. It will be also good to use different approaches to measure the valid of the SSPC and GSI systems in the slope stability assessment in the area.
- Any infrastructure development in the base or in slope sections should consider detail stability assessment.
- Houses constructed near to the sloppy area needs to get attention considering the instability conditions; besides further settlement should be associated with appropriate design and mitigation measures.
- In managing the possible erosion and weathering effects in the area, stream banks that are flowing towards the cliff slopes must be diverted away from these slopes.
- All ditches which constructed standing from Alem ketema flows towards cliff slopes must be diverted or must be planned proper design.
- As mentioned in the previous section, the area is characterized by rugged and mountainous terrain with steep cliff and gentle slopes. Due to this, it is frequently affected by rock slope failures problems throughout the cliff terrains specifically during rain seasons. However, the present research covers only a small area out of the enormous area around Alem ketema.

This is because of time and finance constrains. Therefore further effort has to be made to assess the rest slope rock masses of the study area.

- In future, all possible efforts must be made to make such type of assessment for those mountainous areas of the country where significantly affected by slope rock failure problems. Further studies by multiple researchers with different methods also increase the reliability of the present research result.

*****

VIII. Reference

Acocella, V. and Korme, T. (2002). Holocene extension direction along the Main Ethiopian Rift, East Africa. *Terra Nova* **14**(3):191–197.

Anbalagan, R. (1992). Landslide hazard evaluation and zonation mapping in mountainous Terrain. *Eng. Geol.* **32**: 269–277.

Agliardi, F., Crosta, G. and Zanchi, A. (2001). Structural Constraints on deep-seated slope deformation kinematics. *Eng. Geo.* **59**(1–2):83–102.

Ahmadi, M. and Eslami, M. (2011). A new approach to plane failure of rock slope stability based on water flow velocity in discontinuities for the latian dam reservoir landslide. *J. Mt. Sci.* **8**:124–130.

Ahmed, M. F., Kang, X. and Khan, M. S. (2016). Impact of rain water infiltration on the stability of Earth slopes. *Int. J. Econ. Environ. Geol.* **7**(2):20–25.

Akin, M. (2013). Slope stability problems and back analysis in heavily jointed rock mass: a case study from Manisa, Turkey. *Rock Mech. Rock Eng.* **46:**359–371

Aksoy, H. and Ercanoglu, M. (2007). Fuzzified kinematic analysis of discontinuity-controlled rock slope instabilities. *Eng. Geo.* **89**:206–219.

Alade, S. M. and Abdulazeez, S. S. (2014). Kinematic assessment of rock slope stability at Obajana and Ewekoro quarries. *Earth Sci.* **3**(2):34–41.

Ali, D., Majeed, Y., Shahzad, M., Iqbal, M. M., Liaqat, S., Gill, M. A. and Ali, M. A. (2015). Detailed slope stability analysis of selected slope sites situated along Katas-Choa Saiden Shah road. *Int. J. Eng. Inv.* **5**(1):32–43.

Alzo'ubi, A. K. (2016). Rock slopes processes and recommended methods for analysis. *Int. J. Geomate* **11**(25): 2520–2527.

Azzuhry, Y. (2016). Stability analysis and failure mechanisms of open pit rock slope. *J. Civil Eng.* **2**(3): 171-180.

Barsisa Bekele. (2011). Geochemistry of lower sandstone in Blue Nile Gorge mesozoic sedimentary sequences: Implication for provenance composition and paleoclimate. Unpublished MSc Thesis, Addis Ababa University, Addis Ababa, Ethiopia, 92 pp.

Barton, N.R. (1976a). The shear strength of rock and rock joints. *Int. J. Rock Mech. Min. Sci. and Geomech.* **13**(9):255–279.

Barton N.R. (1976b). Recent experiences with the qsystem of tunnel support design. Pro. Symp. on exploration for rock engineering. *Johannesburg. Ed. Bieniawski. Publ. Balkema,*

Rotterdam. 107-117.

Bekele Abebe, Dramis, F., Fubelli, G., Umer, M. and Asrat, A. (2010). Landslides in the Ethiopian highlands and the Rift margins. *J. Afr. Earth Sci.* **56**(4–5): 131–138.

Bieniawski Zt.(1989). Engineering rock mass classification. Wiley, New York, 251 PP.

Birhanu Ermias, Raghuvanshi, T. K. and Bekele Abebe. (2017). Landslide hazard zonation (LHZ) around Alemketema Town , North Showa Zone , Central Ethiopia - A GIS based expert evaluation approach. *Int. J. Earth Sci. and Eng.* **10**(1):33–44.

Biruk Wolde. (2013). Assessment and mitigation of slope stability hazards along Kombolcha-Desse road, Northern Ethiopia. Unpublished MSc Thesis, Addis Ababa University, Addis Ababa, Ethiopia, 94 pp.

Bois, T., Bouissou, S. and Guglielmi, Y. (2008). Influence of major inherited faults zones on gravitational slope deformation: A two-dimensional physical modelling of the La Clapière area (Southern French Alps). *Earth and Pla. Sci. Let*. **272**(3–4): 709–719.

Bonini, M., Corti, G., Innocenti, F., Manetti, P., Mazzarini, F., Abebe, T. and Pecskay, Z. (2005). evolution of the Main Ethiopian Rift in the frame of Afar and Kenya Rifts propagation. *Tectonics* **24**(1): 1–21.

Brideau, M. A., Yan, M. and Stead, D. (2009). The role of tectonic damage and brittle rock fracture in the development of large rock slope failures. *Geomorphology* **103**(1):30–49.

Cabria, X. S. A. A. (2015). Effects of weathering in the rock and rock mass properties and the influence of salts in the costal road cuts in Saint Vincent and Domin. Unpublished MSc Thesis, Twente University, Enschede, The Netherlands, 91 pp.

Cai, M., Kaiser, P. K., Uno, H., Tasaka, Y. and Minami, M. (2004a). Estimation of rock mass deformation modulus and strength of jointed hard rock masses using the GSI system. *Int. J. Rock Mech. and Min. Sci.* **41**(1):3–19.

Cai, M., Kaiser, P. K., Uno, H., Tasaka, Y. and Minami, M. (2004b). Estimation of rock mass deformation modulus and strength of jointed hard rock masses using the GSI system. *Eng. Geo.* **41**: 3–19.

Canal, A. and Akin, M. (2016). Assessment of rock slope stability by probablistic-based slope probability stability classification method along highway cut slopes in adilcevaz-bitlis(Turkey). *J. Mt. Sci.* **13**(11):1893–1909.

Chen, H., Lee, C. F. and Law, K. T. (2004). Causative mechanisms of rainfall-induced fill slope failures. *J. Geotech. Geoenviron. Eng.* **130**:593–602.

Chen, X., Guo, H. and Song, E. (2008). Analysis method for slope stability under rainfall action. *Landslides and Eng. Slopes* 1507–1515.

Corti, G. (2009). continental rift evolution : from rift initiation to incipient break-up in the Main Ethiopian Rift , East Africa. *Earth Sci. Reviews* **96**:1–53.

Dai, F. C. and Lee, C. F. (2002). Landslide characteristics and slope instability modeling using GIS , Lantau Island , Hong Kong. *Geomorphology* **42**: 213–228.

Daniel, G., 1977. Aspect of Climate and Water Balance in Ethiopia. Addis Ababa University Press, Addis Ababa, Ethiopia, p. 79.

Dawit Lebenie and Bussert, R. (2009). Stratigraphy and facies architecture of adigrat sandstone, Blue Nile Basin, Central Ethiopia. *Zentral Blatt Geol. Paläont* **1**(3/4): 217–232.

Dawit Lebenie (2010). Adigrat sandstone in northern and central ethiopia : adigrat sandstone in northern and central ethiopia : stratigraphy , facies , depositional environments and palynology. Unpublished Ph.D. Thesis, Technische Universität Berlin, Germen,166 pp.

Deep, A., Yoshida, K., Nagata, H. and Pradhan, B. (2014). Rock toppling assessment at mugling – narayanghat road section : "a case study from Mauri Khola landslide", Nepal. *Catena* **114**: 67–77.

Eberhardt, E., Stead, D. and Coggan, J. S. (2004). Numerical analysis of initiation and progressive failure in natural rock slopes the 1991 Randa rockslide. *Int. J. Rock Mech. and Min. Sci.* **41**(1):69–87.

Einstein, H. H., Veneziano, D., Baecher, G. B. and O'reilly, K. J. (1983). The effects of discontinuity persistence on rock slope stability. *Int. J. Rock Mech., Mineral Sci. and Geomech.* **20**(5) :227–236.

El-Aal, A. K. A. and M. K. Ansari. (2016). Slope stability analysis of cut slopes using rock and slope mass rating along Najran – Abha road , Kingdom of Saudi Arabia. **In**: *INDOROCK 2016: 6th Indian Rock Conference*, pp.948. Najran, Saudi Arabia.

Fereidooni, D., Khanlari, G. R. and Heidari, M. (2015). Assessment of a modified rock mass classification system for rock slope stability analysis in the Q-system. *Earth Sci. Res. J.* **19**(2):147–152.

Fikre Girma, Raghuvanshi, T. K., Tenalem Ayenew and Trufat Hailemariam (2015). Landslide hazard zonation in Ada Berga District,Central Ethiopia-a GIS based statistical approach. *J. geomat.* **9**(1): 25-38.

Fischer, L. and Huggel, C. (2008). Methodical design for stability assessments of permafrost-affected high-mountain rock walls Luzia. **In**: *9th international conference on permafrost*, pp. 439–444. Fairbanks, Alaska.

Gani, N. D. and Abdelsalam, M. G. (2006). Remote sensing analysis of the gorge of the Nile , Ethiopia with emphasis on Dejen – Gohatsion region. *J. Afr. Earth Sci.* **44**:135–150.

Gani, N. D., M. G. Abdelsalam, S. G. and M. R. Gani. (2008). Stratigraphic and structural evolution of the Blue Nile Basin, Northwestern Ethiopian Plateau. *Geo. J.* **44**:30–56.

Getaneh Assefa (1980). Stratigraphy and sedimentation of the type Gohatsion Formation (Lias-Malm) Abay River Basin, Ethiopia. *Ethiopian. J. Sci.* **3**: 87–110.

Getaneh Assefa (1981). Gohatsion Formation: A new liasmal lithostragraphic unit from the Abby River Basin. *Ethiopia. Geosci. J.* **2**: 63–88.

Getaneh Assefa (1991). Lithostratigraphy and environment of deposition of the late jurassic - early cretaceous sequence of the central part of Northwestern Plateau , Ethiopia. *N.Jb. Geol. Palaont. Abh*. **182**(3): 255–284.

Gruber, S., Hoelzle, M. and Haeberli, W. (2004). Rock-wall temperatures in the Alps : modelling their topographic distribution and regional differences. *Permafrost and Periglac. Process* **15**: 299–307.

Hack, H. R. G. (1996). *Slope stability probability classification (SSPC)*. ICT, Delft pub., the Netherland, 258pp.

Hack, H. R. G. K. (1993). Slopes in rock. An overview of engineering geology in the Netherlands. **In:** *proceedings of the symposium of the engineering geology student chapter (DIG) on engineering geology*, pp. 111-119. Delft University of Technology, Delft, The Netherlands.

Hack, H. R. G. K. and Price, D. G. (1995). Determination of discontinuity friction by rock mass classification. **In**: *8th international society for rock mechanics (ISRM) Cong*, pp. 23-27. Tokyo, Japan.

Hack, R. (1998). *Slope stability probability classification*, *SSPC*. 2nd edn. Vol.43, ITC Delt Pub., Enschede, The Netherlands, 273 pp.

Hack, R. (2002). An evaluation of slope stability classification. **In**: *ISRM EUROCK'2002, Portugal Madeira Funchal*, pp. 3 – 32. Lisboa, Portugal.

Hack, R. and Huisman, M. (2002). Estimating the intact rock strength of a rock mass by simple means: **In**: *Proceedings of 9th congress of the international association for engineering geology and the environment*, pp.1971–1977. Durban, South Africa.

Hack, R., Price, D. and N.Rengers. (2003). a new approach to rock slope stability – a probability classification (SSPC). *Bull Eng. Geol. Env.* **62**: 167–184.

Hagos Gebreslassie. (2014). Land use-land cover dynamics of Huluka watershed, Central Rift Valley, Ethiopia. *Int. Soil and Water Con. Research* **2**(4):25–33.

Hamza, T. and Raghuvanshi, T. K. (2017). GIS based landslide hazard evaluation and zonation – a case from Jeldu district , Central Ethiopia. *J. K. Saud Uni. Sci.* **29**: 151–165.

Hays, W.W. (1980). Procedures for estimating earthquake ground motion. *U.S. Geol.Surv. Prof. Paper.* 1114, 77pp.

Hautot, S., Whaler, K., Gebru, W.and Desissa, M. (2006). The structure of a mesozoic basin beneath the lake Tana area, Ethiopia, revealed by magnetotelluric imaging. *J. Afr. Earth Sci.* **44**(3):331–338.

Helsdingen, P. Van. (2017). Assessing the stability of road cuttings on the zuurberg pass using romana ' s slope mass rating. **In**:*Proceedings Of The 9th South African Young Geotechnical Engineers Conference*, PP. 665–718. Dolphin Coast, Durban, Kwazulu-Nat.

Hoek, E., Kaiser, P. K. and Bawden, W. F. (1995). *Support of underground excavations in hard rock.* A.A Balkema, Rotterdam, 215pp.

Hoek, E., Read, J., Karzulovic, A. and Chen, Z. Y. (2000). Rock slopes in civil and mining engineering. **In**: *International Conference On Geotechnical And Geological Engineering*, 1–17. Melbourne.

Hudson, J. A. and Harrison, J. P. (2000). *Engineering rock mechanics:an introduction to the principles*, 2nd Ed., Pergamon Press, Amsterdam, 444 PP.

Huisman, M. (2006). Assessment of rock mass decay in artificial slopes.Unpublished Phd thesis,Technische Universiteit Delft,The Netherlands, 283PP.

Http://Epgp.inflibnet.ac.in/epgpdata/uploads/epgp_content/earth_sciences/the_dynamic_earth/17._weathering_processes/et/995_et_et17.pdf accessed on 4.13.2018

Https://Gammathetaupsilon.org/the-geographical-bulletin/1970s/volume06/article3.pdf accessed on 4.13.2018

Irigaray, C. (2003). Preliminary rock-slope-susceptibility assessment using GIS and the SMR classification. Kluwer Academic Pub. **30**:09–324.

Ismail, E. H. and Abdelsalam, M. G. (2012). Morpho-tectonic analysis of the Tekeze River and the Blue Nile drainage systems on the Northwestern Plateau , Ethiopia. *J. Afr. Earth Sci*. **69**:34–47.

Jaboyedoff, M., Baillifard, F., Bardou, E. and Girod, F. (2004). The effect of weathering on Alpine rock instability. *Quarterly J. Eng. Geo. and Hydrogeo.* **37**:95–103.

Jiang, Q., Liu, X., Wei, W. and Zhou, C. (2013). A new method for analyzing the stability of rock wedges. *Int. J. Rock Mech. and Min. Sci.* **60**:413–422.

Jiewen Tu, Aiping Tang, Y. L. and K. L. (2013). Effect of surcharge on the stability of rock slope under complex conditions. *J. Eng. Sci. and Tech. Review* **6** (2):173–178.

Karaman, K., Ercikdi, B. and Kesimal, A. (2013). The assessment of slope stability and rock

excavatability in a limestone quarry. *Earth Sci. Res. Sj*. **17**(2):169–181.

Keir, D., Bastow, I. D., Corti, G., Mazzarini, F. and Rooney, T. O. (2015). The origin of along-rift variations in faulting and magmatism in the Ethiopian Rift. *Agu Tectonics* 464–477.

Kifle Woldearegay. (2013). Review of the occurrences and influencing factors of landslides in the highlands of Ethiopia : With implications for infrastructural development. *Mom. Ethiopian J. Sci.* **5**:3–31.

Kim, Y. S., Peacock, D. C. P. and Sanderson, D. J. (2004). Fault damage zones. *J. Str. Geo.* **26**(3):503–517.

Kun, L. I., Yanjun, S., Wantong, H. E. and Yi, J. (2015). Characteristics and mechanism of bedding rock slope failure : A case study on no . 5 slope at Wutai-Yuxian Expressway. **In**: *Int. Conf. On Advances In Energy, Env. And Chem. Eng.*, PP.460–466. Beijing, China.

Laike Mariam Asfaw, (1986). Environmental hazard from fissures in the Main Ethiopian Rift. *J. Affr. Earth. Sci.* **27** (3/4): 481 - 490.

Laubscher D.H. (1990). A geomechanics classification system for rating of rock mass in mine design. *J. S. Afr. Inst. Min. and Metallurgy* **90**(10): 257-273.

Liu, X., Liu, Y., He, C. and Li, X. (2018). Dynamic stability analysis of the bedding rock slope considering the vibration deterioration effect of the structural plane. *Bull. Eng. Geo. and Env.* **77**(1):87–103.

Li, X. Z. and Xu, Q. (2015). Application of the sspc method in the stability assessment of highway rock slopes in the yunnan province of China. *Bull.Eng.Geol.Env.* **75**(2): 551-562.

Li, Z. H., Huang, H. W., Xue, Y. D. and Yin, J. (2009). Risk assessment of rockfall hazards on highways. *Georisk* **3**(3):147–154.

Lindsay, P., Campbell, R. N., Fergusson, D. A., Gillard, G. R., and Moore, T. A. (2001). Slope stability probability classification , Waikato Coal Measures , New Zealand. *Int. J. Coal Geo.* **45**:127–145.

Lulseged Ayelew (1999). The effect of seasonal rainfall on landslides in the highlands of Ethiopia. *Bull. Eng. Geol. Env*.**58**: 9–19.

Marinos, V., Marinos, P. and Hoek, E. (2005). The geological strength index: applications and limitations. *Bull. Eng. Geo. and Env.* **64**(1): 55–65.

Mauldon, M. (1994). Intersection probabilities of impersistent joints. *Int. J. Rock Mech. and Mining Sci.* **31**(2): 107–115.

Mangesha, Tefera , Tewedros Chernet and Workneh Haro (1996). *Geological map of Ethiopia* (1:2,000,000), 2nd ed., Inst.Geo. Surv. Ethiopia, Addis Ababa, Ethiopia.

Miščević, P. and Vlastelica, G. (2014). Impact of weathering on slope stability in soft rock mass. *J. Rock Mech. and Geotech. Eng.* **6**(3):240–250.

Mogessie, A., Krenn, K., Schaflechner, J., Koch, U., Egger, T., Goritchnig, B. and Bauernfeind, D. (2002). A geological excursion to the mesozoic sediments of the Abay Basin (Blue Nile), recent volcanics of the Ethiopian Main Rift And basement rocks of the Adola Rea, Ethiopia. *Mitt.Österr.Miner.Ges.***147**:43–74.

Mulenga, C. (2015). Influence of weathering and stress relief on geotechnical properties of roadcut mass and embankment fill on St. Vincent and St. Lucia: Enschede, the Netherlands. Unpuplished Msc Thesis, Twente University, Enschede, Netherland, 96 PP.

Palmstrom, A. (1982). The volumetric joint count – a useful and simple measure of the degree of jointing. **In**: *Proceedings of the 4th Int.Cong,* pp. 221–228. IAEG, New Delhi, India.

Palmstrom, A. (1995). Rmi – a rock mass characterization system for rock engineering purposes.Unpublished Phd Thesis, University Of Oslo, Norway, 400pp.

Palmström, A. (1995). Rmi - a system for chøracterizing rock mass strength for use in rock engineering. *J. Rock Mech. and Tunnelling Tech.***1**(2):1–40.

Pantelidis, L. (2009). Rock slope stability assessment through rock mass classification systems. *Int. J. Rock Mech. and Min. Sci*. **46**:315–325.

Pantelidis, L. (2010). An alternative rock mass classification system for rock slopes. *Bull. Eng. Geol. Env.* **69**:29–39.

Patel, A. (2017). Classification of weathering in rocks and its engineering implications. *Civil Eng. Res. J, India* **2**(3):20–23.

Pathak, S., Poudel, R. K. and Kansakar, B. R. (2006). Application of probabilistic approach in rock slope stability analysis — an experience from Nepal. Disaster mitigation of debris flows, slope failures and landslides application. 797–802.

Pernito, M. A. E. (2008). Rock mass slope stability analysis based on 3d terrestrial laser scanning and ground penetrating radar rock mass slope stability analysis based on 3d terrestrial laser scanning and ground penetrating radar. Unpuplished Msc Thesis, ITC, Enschede, The Netherlands, 112 PP.

Poppe, L., Frankl, A., Poesen, J., Teshageradmasu, Dessie, M., Adgo, E. and Nyssen, J. (2013). geomorphology of the lake Tana Basin, Ethiopia. *J. Maps* **9**(3):431–437.

Price, D. G. (2009). *Engineering geology principles and practice*. Springer-Verlag, Berlin Heidelberg, Germany, 450 PP.

Raghuvanshi, T. K. (2017). Plane failure in rock slopes – a review on stability analysis techniques. *J. K. Saud Uni. - Sci.* **xxx**:xxx-xxx.

Raghuvanshi, T. K., Ibrahim, J.and Ayalew, D. (2014). Slope stability susceptibility evaluation parameter (SSEP) rating scheme – an approach for landslide hazard zonation. *J. Afr. Earth Sci.* **99**:595–612.

Rahim, I. A. (2015). Geomechanical classification scheme for heterogeneous crocker formation in Kota Kinabalu , Sabah , Malaysia : An Update. *Bull. Geo.Soc. Malaysia* **61**:85–89.

Razmi, Z. N., Lashkaripour, G. and Ghafoori, M. (2014). Geotechnical assessment and classification of ultrabasic rock masses in the south of mashhad based on GSI and RMi classification systems. *Int. J. Adv. Earth Sci.* **3**(2):61–72.

Romana M. (1985). New adjustment rating for application of the bieniawski classification to slopes. **In**: *Proc. Int. Symp. Rock Mechanics Mining Civ. Works. ISRM,* pp. 59-63. Zacatecas, Mexico.

Romana, M., Serón, J. B. and Montalar, E. (2003). SMR geomechanics classification : application , experience and validation. **In**: P*roceedings of the 10th Congress of the International, ISRM 2003–Technology Roadmap For Rock Mechanics,*pp. 1–4. South African Institute Of Mining And Metallurgy, South African.

Russo, A., Getaneh Assefa and Balemwal Atinafu. (1994). Sedimentary evolution of the Abay River (Blue Nile) basine, Ethiopia. *N.Jb.Geol.Palaont.Mh.* 291–308.

Salmi, E. F. and Hosseinzadeh, S. (2014). Slope stability assessment using both empirical and numerical methods: A case study. *Bull. Eng. Geo. and Env.*13–25.

Samuel Kinde, Samson Engeda, Asnake Kebede and Eyob Tessema (2009). Notes and proposed guidelines on updated seismic codes in Ethiopia - implications for large-scale infrastructures.Unpublished technical report, San Diego State University, San Diego, CA, USA, 36 PP.

Seifu Kebede, Travi, Y., Tamiru Alemayehu and Tenalem Ayenew (2005). Groundwater recharge , circulation and geochemical evolution in the source region of the Blue Nile River , Ethiopia. *App. Geoch.* **20**:1658–1676.

Singh, J. L. and Tamrakar, N. K. (2013). Rock mass rating and geological strength index of rock masses of Thopal-Malekhu River Areas , Central Nepal Lesser Himalaya. *Bull. Dep. Geo.* **16**: 29–42.

Smith, J. V. and Arnhardt, C. (2016). A new assessment method for structural-control failure mechanisms in rock slopes — case examples. *Aims Geosci.* **2**(3):214–230.

Sonmez, H. and Ulusay, R. (1999). Modifications to the geological strength index (GSI) and their applicability to stability of slopes. *Int. J. Rock Mech. and Min. Sci.* **36**(6):743–760.

Stead, D., Eberhardt, E. and Coggan, J. S. (2006). Developments in the characterization of

complex rock slope deformation and failure using numerical modelling techniques. *Eng. Geo.* **83**: 217–235.

Stead, D. and Wolter, A. (2015). A critical review of rock slope failure mechanisms: The Importance Of Structural Geology. *J. Stru. Geo*. **74**:1-23.

Suradi, M. and Fourie, A. (2014). The effect of rainfall patterns on the mechanisms of shallow slope failure. *Aceh Int. J. Sci. Technology* **3**(1):1–18.

Sygała, A., Bukowska, M. and Janoszek, T. (2014). High temperature versus geomechanical parameters of selected rocks – the present state of research. *J. Sust. Min.* **12**(4):45–51.

Taheri, A. (2012). Design of rock slopes using classification systems. *Advances in Eng. Research* **2**: 453-488.

Taylor H.W. (1980). A geomechanics classification applied to mining problems in the Shabanie Chrysotile asbestos mines, Rhodesia. M.Phil thesis, University of Rhodesia, Harare, Zimbabwe, 312 pp.

Tenalem Ayenew. (2005). Major ions composition of the groundwater and surface water systems and their geological and geochemical controls in the Ethiopian volcanic Terrain. *SINET: Ethiopian J. Sci.* **28**(2):171–188.

Tigel Belay, Ilfios Tesfay, Abiy Ayalew, Genet Yohannes, Teferi Zewdie, Henok Bekele, Melese Tadesse, Tesfaye Demisse and Tadesse Alemu. (2009). Geology of the were-ilu area. Unpublished technical report, geological survey of Ethiopia, Addis Ababa, Ethiopia, 56pp.

Tomás, R., Cuenca, A., Cano, M. and García-Barba, J. (2012). A graphical approach for slope mass rating (SMR). *Eng. Geo.* **124**: 67–76.

Trufat Hailemariam (2009). Slope rock mass characterization in tekeze hydropower reservoir : Implication to GIS based slope stability and reservoir impounding induced hazard analyses. Vienna 102–113.

Tsion Aragaw. (2017). An integrated expert evaluation and statistical approach for landslide hazard evaluation and zonation – a case along Alem Ketema – Fetra route corridor, Northern Showa Zone, Central Ethiopia. Unpublished MSc Thesis, Addis Ababa University, Addis Ababa, Ethiopia, 97pp.

Umrao, R. K., Singh, R., Ahmad, M. and Singh, T. N. (2011). Stability analysis of cut slopes using continuous slope mass rating and kinematic analysis in rudraprayag district , uttarakhand. *Geomaterials* **1**:79–87.

Wang, C., Mao, Y., Hu, B., Deng, Z., and Shin, J. G. (2016). Study on the safety factors of the bedding rock slope under dynamic loading. *J.Eng. Sci. and Tech. Review* **9**(3): 161–175.

Wolela Ahmed. (2008). Sedimentation Of The Triassic – Jurassic Adigrat Sandstone Formation , Blue Nile (Abay) Basin , Ethiopia. J.Afr. Earth Sci.52:30–42.

Wolela Ahmed (2009). Sedimentation and depositional environments of the barremian-cenomanian Debre Libanose Sandstone , Blue Nile (Abay) Basin , Ethiopia. *Cretaceous Research* **30**(5):1133–1145.

Wolela Ahmed. (2010). Diagenetic evolution of the ansian – pliensbachian adigrat sandstone , Blue Nile Basin , Ethiopia. *J. Afr. Earth Sci.* **56**(1):29–42.

Wolfenden, E., Ebinger, C., Yirgu, G., Deino, A. and Dereje Ayalew (2004). Evolution of the Northern Main Ethiopian Rift: Birth of a triple junction. *Earth And Planetary Sci. Let*. **224**(1–2):213–228.

Xiaohu, H., Changming, W., Tianzuo, W. and Zhiming, Z. (2015). Quantification of geological strength index based on discontinuity volume density of rock masses. *Int. J. Heat And Tech.* **33**(4): 255–261.

Yoon, W. S., Jeong, U. J. and Kim, J. H. (2002). Kinematic analysis for sliding failure of multi-faced rock slopes. *Eng. Geo.* **67**:51–61.

Youssef, A. M., Maerz, N. H. and Al-Otaibi, A. A. (2012). Stability of rock slopes along Raidah Escarpment road , Asir Area , Kingdom Of Saudi Arabia. *J.Geog. and Geo.***4**(2): 48–70.

Zare, M., Jimenez, R., Khalokakaie, R. and Jalali, S. E. (2011). A probabilistic systems methodology to analyze the importance of factors affecting the stability of rock slopes. *Eng. Geo.* **118**(3–4):82–92.

Zelalem Shiferaw. (2005). Lithological and structural mapping of the central and North Western part of Ethiopia in view of petroleum exploration. Unpublished MSc Thesis, Addis Ababa University, Addis Ababa, Ethiopia, 82 pp.

Zhang, L. and Guilbert, E. (2016). Evaluation of river network generalization methods for preserving the drainage pattern. *Isprs Int. J. Geo-Inf.* **5**: 1–22.

Zhao, L., Cao, J., Zhang, Y. and Luo, Q. (2015). Effect of hydraulic distribution on the stability of a plane slide rock slope under the nonlinear barton-bandis failure criterion. *Geomech. and Eng*. **8**(3):391–414.

Zhu, L., Huang, R. Qiu, Yan, M. and Chen, G. Qing. (2017). Geological analysis of gravitational rock slope deformation: A case from Nujiang River, China. *J. Mountain Sci.* **14**(10): 2122–2133.

IX. Annex

8.1 SSPC exposure rock mass (ERM) characterizations, calculated values

Collected discontinuities data used in exposure rock mass characterizations, which are calculated to define the discontinuity condition (TC), spacing factors for discontinuity sets and apparent angle of the dip of discontinuity of in the direction of slope dip (AP) in SSPC classification system.

8.1.1 Karst condition (ka), degree of weathering (WE), excavation method (ME), intact rock strength (IRS), larg scale roughness (RL) and small scale roughness (RS)

Slope sec.	karst(Ka)	WE	ME(natural slope)	IRS	RL			RS		
					J1	J2	J3	J1	J2	J3
1	1	0.90	1	31.25	0.75	0.75	0.80	0.60	0.60	0.80
2	,,	0.95	,,	75	0.75	0.95	0.75	0.80	0.60	0.65
3	,,	0.90	,,	75	0.80	0.75	0.95	0.80	0.65	0.80
4	,,	0.95	,,	75	0.80	0.75	0.75	0.80	0.80	0.80
5	,,	0.90	,,	31.25	0.75	0.75	0.80	0.65	0.65	0.60
6	,,	0.95	,,	75	0.80	0.75	0.75	0.80	0.60	0.80
7	,,	0.90	,,	31.25	0.95	0.80	0.75	0.80	0.80	0.60
8	,,	0.90	,,	75	0.80	0.75	0.75	0.75	0.80	0.60
9	,,	0.90	,,	132	0.75	0.75	0.80	0.75	0.60	0.80
10	,,	0.90	,,	75	0.80	0.80	0.75	0.80	0.80	0.80
11	,,	0.90	,,	31.25	0.75	0.80	0.80	0.60	0.80	0.75
12	,,	0.90	,,	31.25	0.75	0.75	0.95	0.60	0.65	0.80
13	,,	0.90	,,	75	0.85	0.75	0.75	0.60	0.65	0.80
14	,,	0.90	,,	132	0.75	0.95	0.80	0.80	0.80	0.80
15	,,	0.90	,,	31.25	0.80	0.80	0.75	0.80	0.80	0.75
16	,,	0.90	,,	31.25	0.75	0.75	0.95	0.80	0.75	0.80
17	,,	0.95	,,	75	0.75	0.95	0.75	0.80	0.75	0.80
18	,,	0.90	,,	132	0.80	0.80	0.95	0.75	0.80	0.75
19	,,	0.90	,,	31.25	0.95	0.75	0.80	0.65	0.80	0.80
20	,,	0.90	,,	31.25	0.75	0.95	0.75	0.80	0.65	0.55
21	,,	0.90	,,	31.25	0.85	0.75	0.80	0.80	0.80	0.65
22	,,	0.90	,,	31.25	0.80	0.80	0.80	0.95	0.80	0.95
23	,,	0.90	,,	31.25	0.75	0.95	0.95	0.60	0.60	0.95
24	,,	0.95	,,	75	0.75	0.75	0.75	0.80	0.60	0.80

25	,,	0.90	,,	132	0.95	0.95	0.75	0.65	0.80	0.65
26	,,	0.95	,,	132	0.95	0.75	0.80	0.80	0.60	0.80
27	,,	0.90	,,	75	0.80	0.75	0.85	0.80	0.80	0.80
28	,,	0.90	,,	31.25	1.00	0.80	0.75	0.80	0.80	0.60
29	,,	0.90	,,	31.25	0.80	0.75	0.75	0.60	0.80	0.80
30	,,	0.90	,,	132	0.75	0.75	0.85	0.60	0.60	0.60
31	,,	0.95	,,	75	0.75	0.95	0.80	0.65	0.75	0.75
32	,,	0.95	,,	132	0.95	0.80	0.80	0.80	0.80	0.80
33	,,	0.90	,,	31.25	0.80	0.75	0.75	0.75	0.80	0.80
34	,,	0.95	,,	75	0.80	0.80	0.75	0.80	0.75	0.75
35	,,	0.95	,,	132	1.00	0.95	0.95	0.75	0.80	0.80
36	,,	0.90	,,	75	0.75	0.80	0.95	0.60	0.75	0.65
37	,,	0.95	,,	132	0.80	0.75	0.95	0.80	0.80	0.80
38	,,	0.90	,,	132	0.75	0.95	0.80	0.80	0.80	0.80
39	,,	0.90	,,	75	0.75	0.95	0.75	0.80	0.80	0.80
40	,,	0.95	,,	132	0.75	0.75	0.75	0.65	0.65	0.80
41	,,	0.90	,,	132	0.75	0.75	0.75	0.80	0.60	0.80
42	,,	0.90	,,	31.25	0.95	0.80	0.80	0.80	0.80	0.80
43	,,	0.90	,,	31.25	0.80	0.75	0.75	0.80	0.75	0.80
44	,,	0.95	,,	75	0.95	0.95	0.95	0.80	0.80	0.95
45	,,	0.90	,,	31.25	0.80	0.95	0.75	0.80	0.80	0.75
46	,,	0.95	,,	75	1.00	0.75	0.95	0.60	0.75	0.80
47	,,	0.95	,,	132	0.75	0.75	0.80	0.60	0.60	0.65
48	,,	0.95	,,	75	0.95	0.75	0.80	0.80	0.65	0.80
49	,,	0.90	,,	31.25	0.95	0.80	0.75	0.75	0.80	0.80
50	,,	0.90	,,	31.25	0.80	0.75	0.80	0.80	0.75	0.60
51	,,	0.90	,,	75	0.75	0.75	0.75	0.80	0.80	0.80
52	,,	0.90	,,	31.25	0.75	0.75	0.80	0.65	0.75	0.80
53	,,	0.95	,,	75	1.00	0.75	0.95	0.80	0.80	0.80
54	,,	0.95	,,	75	0.75	0.95	0.80	0.80	0.80	0.80
55	,,	0.90	,,	75	0.80	0.75	0.75	0.80	0.80	0.80
56	,,	0.62	,,	8.75	0.80	0.80	0.80	0.80	0.80	0.80
57	,,	0.62	,,	8.75	0.80	0.75	0.75	0.60	0.65	0.60
58	,,	0.62	,,	31.25	0.80	1.00	0.80	0.65	0.80	0.75
59	,,	0.62	,,	31.25	0.85	0.85	0.80	0.80	0.80	0.80
60	,,	0.62	,,	31.25	0.75	0.80	0.75	0.80	0.80	0.80
61	,,	0.90	,,	31.25	0.80	0.75	0.75	0.90	0.80	0.90
62	,,	0.90	,,	75	0.75	0.80	0.75	0.75	0.90	0.80
63	,,	0.95	,,	75	0.75	0.80	0.75	0.80	0.65	0.80
64	,,	0.90	,,	132	0.75	0.95	0.75	0.75	0.75	0.75
65	,,	0.90	,,	75	0.85	0.75	0.85	0.80	0.80	0.80

66	,,	0.90	,,	31.25	0.75	0.80	0.85	0.95	0.65	0.60
67	,,	0.95	,,	132	0.75	0.75	0.80	0.80	0.95	0.80
68	,,	0.95	,,	75	0.75	0.75	0.75	0.60	0.60	0.90
69	,,	0.90	,,	75	0.75	0.75	0.75	0.60	0.60	0.60
70	,,	0.95	,,	75	0.75	0.75	0.75	0.60	0.60	0.60
71	,,	0.62	,,	31.25	0.80	0.80	0.80	0.95	0.95	0.80
72	,,	0.62	,,	8.75	0.85	0.80	0.75	0.80	0.75	0.80
73	,,	0.62	,,	1.25	1.00	0.95	1.00	0.75	0.75	0.75
74	,,	0.62	,,	1.25	0.75	0.95	0.75	0.75	0.60	0.60
75	,,	0.62	,,	3.12	0.80	0.75	0.80	0.75	0.75	0.75
76	,,	0.62	,,	31.25	0.80	0.75	0.80	0.80	0.95	0.80
77	,,	0.62	,,	8.75	0.75	0.75	0.80	0.60	0.60	0.60
78	,,	0.90	,,	75	0.75	0.95	0.75	0.60	0.60	0.60
79	,,	0.62	,,	1.25	1.00	0.95	1.00	0.75	0.75	0.75
80	,,	0.62	,,	3.12	0.80	0.95	0.80	0.80	0.80	0.80
81	,,	0.62	,,	3.12	0.75	0.75	0.80	0.75	0.80	0.80
82	,,	0.62	,,	1.25	0.95	1.00	0.95	0.75	0.75	0.75
83	,,	0.90	,,	31.25	0.75	0.80	0.80	0.80	0.80	0.80
84	,,	0.90	,,	31.25	0.75	0.75	0.80	0.80	0.80	0.80
85	,,	0.90	,,	31.25	0.75	0.80	0.80	0.80	0.60	0.80
86	,,	0.90	,,	31.25	0.75	0.75	0.80	0.80	0.80	0.80
87	,,	0.90	,,	31.25	0.85	0.80	0.80	0.80	0.80	0.80
88	,,	0.95	,,	132	0.75	0.80	0.75	0.80	0.80	0.80
89	,,	0.90	,,	75	0.75	0.75	0.80	0.80	0.65	0.80
90	,,	0.95	,,	75	0.75	0.75	0.85	0.60	0.60	0.80
91	,,	0.90	,,	1.25	0.95	0.75	0.95	0.75	0.75	0.75
92	,,	0.90	,,	31.25	0.75	0.75	0.75	0.60	0.60	0.60
		0.90								

8.1.2 Spacing factors (F1, F2, and F3) and Discontinuity condition (TC)

$$Factor1 = 0.30 + 0.259 * \log10^{(DS\text{-}minimum)}$$

$$Factor2 = 0.20 + 0.296 * \log10^{(DS\text{-}intermediat)}$$

$$Factor3 = 0.1 + 0.333 * \log10^{(DS\text{-}maximum)}$$

Slope sec.	Discontinuity spacing(cm)			Factor			Infill			TC		
	DS1	DS2	DS3	F1	F2	F3	J1	J2	J3	TC1	TC2	TC3
1	50	35	26	0.666	0.657	0.666	1.00	1.00	0.85	0.45	0.45	0.38

2	95	67	30	0.683	0.741	0.759	0.90	0.85	1.00	0.54	0.48	0.49
3	85	40	25	0.662	0.674	0.742	0.85	1.00	0.85	0.54	0.49	0.65
4	60	52	35	0.700	0.708	0.692	0.90	0.85	0.85	0.58	0.51	0.51
5	100	66	38	0.709	0.739	0.766	0.95	0.90	0.85	0.46	0.44	0.39
6	90	50	26	0.666	0.703	0.751	0.90	1.00	0.85	0.58	0.45	0.51
7	85	34	22	0.648	0.653	0.742	0.95	0.95	1.00	0.72	0.61	0.45
8	105	70	40	0.715	0.746	0.773	0.85	0.95	1.00	0.51	0.57	0.45
9	60	37	20	0.637	0.664	0.692	1.00	0.85	0.85	0.56	0.38	0.54
10	70	45	25	0.662	0.689	0.714	0.95	0.90	0.90	0.61	0.58	0.36
11	88	50	36	0.703	0.703	0.748	1.00	0.90	1.07	0.45	0.58	0.53
12	100	66	30	0.683	0.739	0.766	1.07	0.95	0.85	0.48	0.46	0.65
13	65	44	40	0.715	0.686	0.704	0.85	0.95	1.00	0.43	0.46	0.60
14	80	45	36	0.703	0.689	0.734	0.90	0.90	0.90	0.54	0.68	0.58
15	95	55	20	0.637	0.715	0.759	0.90	0.85	0.85	0.58	0.54	0.48
16	110	38	24	0.657	0.668	0.780	0.85	1.00	0.85	0.51	0.56	0.65
17	65	30	25	0.662	0.637	0.704	0.85	0.85	1.00	0.51	0.61	0.60
18	90	75	48	0.735	0.755	0.751	1.00	0.85	0.90	0.60	0.43	0.64
19	95	70	40	0.715	0.746	0.759	0.95	0.85	0.90	0.59	0.51	0.58
20	85	47	36	0.703	0.695	0.742	0.90	1.00	1.07	0.54	0.62	0.44
21	100	63	30	0.683	0.733	0.766	0.95	0.95	0.85	0.65	0.57	0.44
22	80	60	40	0.715	0.726	0.734	0.95	0.95	0.90	0.78	0.61	0.68
23	82	55	25	0.662	0.715	0.737	0.90	0.85	0.85	0.41	0.48	0.79
24	111	60	50	0.740	0.726	0.781	0.95	1.00	0.90	0.57	0.45	0.54
25	85	74	45	0.728	0.753	0.742	1.00	0.85	0.90	0.62	0.65	0.44
26	95	36	20	0.637	0.661	0.759	0.85	0.90	1.00	0.78	0.41	0.64
27	80	40	30	0.683	0.674	0.734	0.85	1.00	0.85	0.54	0.60	0.58
28	100	50	35	0.700	0.703	0.766	1.00	0.85	0.85	0.80	0.54	0.38
29	75	46	27	0.671	0.692	0.724	1.00	0.90	0.90	0.48	0.54	0.54
30	56	34	45	0.697	0.689	0.682	1.00	1.00	1.00	0.45	0.45	0.51
31	90	80	60	0.761	0.763	0.751	0.85	0.85	0.85	0.41	0.61	0.51
32	78	40	10	0.559	0.674	0.730	1.00	0.85	0.85	0.40	0.54	0.54
33	52	38	25	0.662	0.668	0.671	0.85	0.85	0.85	0.51	0.51	0.51
34	70	44	30	0.683	0.686	0.714	1.00	0.90	0.95	0.64	0.54	0.53
35	66	54	28	0.675	0.713	0.706	0.85	0.85	0.85	0.78	0.65	0.65
36	98	76	42	0.720	0.757	0.763	0.90	0.90	1.00	0.41	0.54	0.62
37	86	53	30	0.683	0.710	0.744	1.00	0.85	1.00	0.38	0.51	0.76
38	72	68	47	0.733	0.742	0.718	0.85	0.85	0.85	0.51	0.42	0.54
39	86	60	35	0.700	0.726	0.744	1.00	0.85	1.00	0.60	0.43	0.60
40	105	78	26	0.666	0.760	0.773	0.95	0.90	0.85	0.46	0.44	0.51
41	94	50	40	0.715	0.703	0.757	0.90	0.85	0.90	0.54	0.38	0.54
42	60	46	20	0.637	0.692	0.692	0.95	0.85	0.85	0.59	0.45	0.79

43	75	61	33	0.693	0.728	0.724	0.95	0.85	0.90	0.61	0.48	0.54
44	80	70	60	0.761	0.746	0.734	0.95	0.90	0.90	0.72	0.78	0.81
45	85	40	32	0.690	0.674	0.742	0.90	0.90	0.95	0.58	0.68	0.53
46	50	30	12	0.580	0.637	0.666	0.90	0.95	0.95	0.54	0.53	0.72
47	66	52	45	0.728	0.708	0.706	0.85	0.90	0.90	0.34	0.43	0.47
48	87	58	42	0.720	0.722	0.746	0.90	0.85	0.85	0.42	0.41	0.54
49	120	85	50	0.740	0.771	0.792	0.90	1.00	0.90	0.51	0.79	0.54
50	95	75	36	0.703	0.755	0.759	1.07	0.85	1.00	0.68	0.40	0.48
51	85	33	24	0.657	0.649	0.742	0.95	0.95	0.85	0.57	0.46	0.51
52	112	60	30	0.683	0.726	0.782	0.90	0.90	0.90	0.44	0.51	0.58
53	125	80	76	0.787	0.763	0.798	0.95	1.00	0.90	0.44	0.60	0.68
54	130	54	35	0.700	0.713	0.804	1.00	0.85	0.90	0.60	0.65	0.58
55	65	45	22	0.648	0.689	0.704	0.95	1.00	0.85	0.61	0.60	0.51
56	20	10	15	0.559	0.548	0.533	0.95	0.90	0.85	0.61	0.58	0.54
57	25	14	11	0.570	0.539	0.566	0.85	0.85	0.85	0.35	0.75	0.38
58	18	10	12	0.559	0.519	0.518	0.85	0.85	1.00	0.44	0.68	0.60
59	85	50	45	0.728	0.703	0.742	0.95	0.95	0.95	0.65	0.65	0.61
60	70	58	20	0.637	0.722	0.714	0.85	1.07	0.85	0.51	0.40	0.51
61	100	40	35	0.700	0.674	0.766	0.85	0.90	0.90	0.61	0.54	0.61
62	30	25	27	0.662	0.624	0.592	0.85	0.90	1.00	0.42	0.65	0.60
63	110	80	46	0.731	0.763	0.780	0.85	0.90	0.85	0.51	0.76	0.51
64	87	64	29	0.679	0.735	0.746	0.85	1.00	1.00	0.48	0.71	0.60
65	77	65	35	0.700	0.737	0.728	0.90	0.95	0.95	0.59	0.57	0.65
66	38	34	23	0.653	0.653	0.626	0.90	0.90	0.85	0.64	0.47	0.43
67	40	32	30	0.683	0.646	0.633	0.95	0.90	0.85	0.57	0.64	0.54
68	35	24	18	0.625	0.609	0.614	0.85	0.90	0.85	0.38	0.41	0.57
69	30	26	22	0.648	0.619	0.592	0.85	1.00	0.90	0.38	0.45	0.41
70	40	30	20	0.637	0.637	0.633	1.00	0.85	1.00	0.45	0.68	0.45
71	60	45	32	0.690	0.689	0.692	0.90	0.85	0.85	0.68	0.65	0.54
72	55	36	25	0.662	0.661	0.680	0.95	0.85	0.90	0.65	0.51	0.54
73	30	17	15	0.605	0.564	0.592	0.85	0.85	0.85	0.64	0.61	0.64
74	50	35	24	0.657	0.657	0.666	0.55	0.85	1.00	0.45	0.48	0.45
75	30	25	22	0.648	0.614	0.592	0.95	0.90	1.00	0.57	0.54	0.60
76	60	38	32	0.690	0.668	0.692	0.95	0.95	0.90	0.61	0.68	0.58
77	45	34	27	0.671	0.653	0.651	0.85	0.85	0.85	0.38	0.38	0.41
78	35	30	18	0.625	0.637	0.614	0.85	0.85	0.85	0.38	0.48	0.38
79	35	28	16	0.612	0.628	0.614	0.85	0.85	0.85	0.64	0.61	0.64
80	50	45	30	0.683	0.689	0.666	0.95	0.95	0.85	0.77	0.60	0.49
81	65	30	20	0.637	0.637	0.704	0.95	0.90	0.85	0.53	0.40	0.54
82	25	18	15	0.605	0.572	0.566	0.85	0.85	0.85	0.61	0.53	0.61
83	37	24	15	0.605	0.609	0.622	1.00	0.90	0.90	0.60	0.58	0.58

84	68	40	35	0.700	0.674	0.710	0.90	0.90	0.85	0.54	0.54	0.54
85	40	30	20	0.637	0.637	0.633	0.95	0.90	0.85	0.57	0.37	0.54
86	45	32	18	0.625	0.646	0.651	0.95	0.90	0.85	0.57	0.54	0.54
87	80	65	50	0.740	0.737	0.734	0.95	0.95	0.90	0.65	0.61	0.58
88	90	65	30	0.683	0.737	0.751	1.00	0.85	0.85	0.56	0.54	0.51
89	70	60	40	0.715	0.726	0.714	0.85	0.85	0.85	0.51	0.41	0.54
90	100	85	66	0.771	0.771	0.766	0.85	0.85	1.00	0.38	0.38	0.68
91	30	25	20	0.637	0.614	0.592	0.95	0.85	0.85	0.68	0.65	0.61
92	60	52	45	0.728	0.708	0.692	0.85	0.85	0.85	0.38	0.38	0.38

8.1.3 Apparent dip angle of discontinuity (Ap)

The apparent angle of the dip of the discontinuity plane in the direction of the slope dips (AP):
$AP=\arctan(\cos(\sigma s-Tj)*\tan\beta j)$

1) If AP > 0°, AP = apparent discontinuity dip in the direction of the slope dip
2) If AP < 0°, │ AP │ = apparent discontinuity dip in the direction of opposite the slope dip

Slope sec.	slope dip	slope dip direction (σs)	Discontinuity dip direction(Tj)			Discontinuity dip(βj)			AP		
			J1	J2	J3	J1	J2	J3	J1	J2	J3
1	72	060	332	332	025	52	20	70	2.56	0.73	66.04
2	67	090	325	020	295	80	30	50	-72.91	11.17	-47.21
3	73	010	005	320	105	63	35	15	62.91	24.23	-1.34
4	77	005	083	280	079	60	25	42	19.80	2.33	13.94
5	64	025	085	025	145	72	30	56	56.98	30.00	-36.55
6	61	060	050	125	075	68	24	52	67.69	10.66	51.03
7	80	080	085	320	130	62	85	20	61.91	-80.08	13.17
8	82	085	073	280	103	74	85	26	73.66	-84.82	24.88
9	85	030	350	008	030	75	80	40	70.72	79.23	40.00
10	80	050	030	075	310	75	62	45	74.08	59.60	-9.85
11	75	025	340	335	280	32	50	66	23.84	37.45	-30.17
12	75	020	045	007	170	45	45	85	42.19	44.26	-84.23
13	82	310	300	305	350	65	75	35	64.66	74.95	28.21
14	80	315	270	355	130	15	76	85	10.73	71.97	-84.98
15	75	345	315	325	275	65	70	10	61.70	68.83	3.45
16	78	350	340	290	270	70	53	15	69.72	33.57	2.66
17	69	025	320	320	025	30	46	69	13.71	23.64	69.00
18	80	055	260	220	200	42	80	60	-39.22	-79.65	-54.82
19	78	360	275	360	190	15	78	85	1.34	78.00	-84.92

20	72	360	293	360	305	25	72	64	10.33	72.00	49.62
21	65	005	005	270	255	65	18	80	65.00	-1.62	-62.73
22	75	020	054	293	210	70	45	85	66.30	3.00	-84.92
23	70	045	108	285	045	54	80	65	32.00	-70.57	70.00
24	60	125	315	109	210	85	22	64	-84.92	21.22	10.13
25	75	045	330	275	045	67	20	75	31.37	-13.17	75.00
26	80	050	046	316	265	58	10	86	57.94	-0.70	-85.12
27	85	047	055	330	355	45	15	80	44.72	3.45	74.02
28	85	044	048	320	344	50	10	75	49.93	1.06	61.81
29	78	058	065	085	050	38	20	70	37.79	17.97	69.82
30	76	015	345	015	025	56	30	75	52.09	30.00	74.78
31	80	016	270	045	016	66	42	80	-31.76	38.22	80.00
32	85	017	290	045	017	50	34	80	3.57	30.78	80.00
33	69	028	070	017	055	55	30	70	46.70	29.54	67.78
34	73	030	085	045	030	50	26	72	34.36	25.23	72.00
35	73	040	020	235	075	73	85	25	71.98	-84.82	20.91
36	70	020	045	045	310	50	25	55	47.21	22.91	26.03
37	85	290	110	290	295	46	32	65	-46.00	32.00	64.92
38	85	291	280	070	090	75	50	85	74.73	-41.97	-84.65
39	79	292	275	065	300	61	52	75	59.90	-41.12	74.86
40	80	293	282	270	054	78	44	80	77.78	41.63	-71.10
41	75	275	058	275	058	80	65	45	-77.55	65.00	-38.61
42	70	276	067	045	270	80	55	50	-78.60	-41.95	49.84
43	80	350	350	085	303	80	30	60	80.00	-2.88	49.75
44	67	355	289	355	056	75	62	25	56.62	62.00	12.74
45	74	352	155	036	352	85	30	65	-84.77	22.55	65.00
46	76	335	045	335	279	76	45	20	53.91	45.00	11.50
47	80	336	077	336	288	60	36	18	-18.29	36.00	12.27
48	83	337	236	337	160	65	36	30	-22.25	36.00	-29.97
49	76	338	225	338	280	62	76	36	-36.31	76.00	21.06
50	84	339	339	255	296	75	70	25	75.00	16.02	18.83
51	85	340	340	210	270	80	66	52	80.00	-55.29	23.64
52	78	341	341	100	280	70	80	56	70.00	-70.01	35.71
53	81	275	025	275	095	62	45	85	-32.75	45.00	-85.00
54	75	035	230	130	035	85	30	50	-84.82	-2.88	50.00
55	70	282	225	280	225	76	56	20	65.40	55.98	11.21
56	35	195	250	170	275	16	20	10	9.34	18.26	1.75
57	30	345	265	015	350	45	57	30	9.85	53.13	29.91
58	40	340	015	260	345	25	20	30	20.91	3.62	29.91
59	65	045	240	045	045	85	35	65	-84.82	35.00	65.00
60	68	080	065	290	080	60	50	68	59.13	-45.90	68.00

61	78	350	310	350	280	66	45	80	59.83	45.00	62.73
62	80	330	090	270	125	70	50	85	-53.95	30.79	-84.49
63	65	020	218	020	088	85	65	48	-84.74	65.00	22.59
64	80	010	085	267	010	80	60	50	55.73	-21.29	50.00
65	76	005	270	005	330	74	62	30	-16.91	62.00	25.31
66	70	350	335	290	020	65	50	45	64.23	30.79	40.89
67	73	340	130	277	085	85	55	58	-84.23	32.96	-22.50
68	75	068	280	285	350	85	75	40	-84.11	-71.45	9.90
69	70	075	325	082	260	70	45	70	-43.22	44.79	-69.93
70	55	065	345	066	015	65	35	47	20.42	35.00	34.58
71	30	135	195	310	200	20	85	30	10.31	-84.98	13.71
72	40	160	225	075	095	30	48	69	13.71	5.53	47.75
73	20	165	260	115	090	25	20	6	-2.33	13.17	1.56
74	30	245	200	110	245	45	20	30	35.26	-14.43	30.00
75	45	170	250	170	135	25	45	30	4.63	45.00	25.31
76	62	250	285	260	270	39	58	35	33.56	57.60	33.34
77	75	135	220	050	105	75	15	60	18.02	1.34	56.31
78	85	157	305	278	105	10	80	69	-8.50	-71.10	58.06
79	45	015	280	280	085	26	53	35	-2.43	-6.60	13.47
80	39	060	045	230	170	56	80	62	55.07	-79.85	-32.75
81	73	150	090	269	225	44	50	60	25.77	-30.02	24.15
82	25	035	280	280	280	20	66	10	-8.74	-43.51	-4.26
83	40	075	270	015	090	80	45	30	-79.65	26.57	29.15
84	63	050	285	135	225	12	76	80	-6.95	19.27	-79.96
85	75	286	315	070	145	85	45	10	84.29	-38.97	-7.80
86	78	066	238	260	135	78	40	15	-77.89	-39.15	5.48
87	35	150	270	079	150	85	30	35	-80.08	10.65	35.00
88	80	330	086	330	250	66	85	52	-44.56	85.00	12.53
89	65	102	025	139	025	32	54	10	8.00	47.71	2.27
90	60	135	270	125	105	54	35	72	-44.22	34.59	69.43
91	25	170	095	165	225	49	46	32	16.58	45.89	19.72
92	85	025	315	125	025	75	62	45	51.92	-18.09	45.00

8.2 Slope height, maximum slope high, H_{max}/H_{slope} and $\varphi_{mass}/dip_{slope}$

For each slope faces to calculate the maximum slope height is given by:

1) If the $dip_{slope} > \varphi_{mass}$, then

   $H_{max} = 1.6*10^{-4}*coh_{mass}*(\sin(dip_{slope})*\cos(\varphi_{mass}))/(1-\cos(dip_{slope} - \varphi_{mass}))$

2) If the $dip_{slope} < \varphi_{mass}$, then H_{max}=unlimited

The maximum possible height of the slope (H_{max}) is infinite if the slope dips less than the rock mass friction (φ_{mass}). However, this condition not existed in the present study.

Slope sec.	H_{max}	H_{slope}	H_{max}/H_{slope}	$\varphi_{mass}/dip_{slope}$	Slope sec.	H_{max}	H_{slope}	H_{max}/H_{slope}	$\varphi_{mass}/dip_{slope}$
1	5.77	45	0.13	0.36	47	21.56	25	1.00	0.65
2	21.75	65	0.33	0.61	48	9.49	29	1.46	0.50
3	12.82	90	0.14	0.53	49	9.19	25	1.16	0.45
4	10.75	75	0.14	0.51	50	5.68	34	0.17	0.38
5	12.16	75	0.16	0.48	51	7.10	34	0.21	0.44
6	29.10	85	0.34	0.65	52	6.71	34	0.20	0.40
7	4.90	50	0.72	0.34	53	14.63	20	1.15	0.58
8	10.57	60	0.18	0.52	54	15.09	25	1.15	0.57
9	12.84	45	0.71	0.57	55	13.87	20	1.23	0.54
10	9.02	100	0.09	0.48	56	10.09	30	0.34	0.40
11	7.18	85	0.08	0.40	57	13.62	20	0.68	0.45
12	7.57	80	0.09	0.41	58	13.57	21	0.65	0.47
13	8.63	93	0.09	0.48	59	11.70	15	0.78	0.48
14	22.64	45	0.79	0.65	60	7.97	60	0.13	0.41
15	6.39	65	0.10	0.38	61	6.26	30	0.86	0.38
16	5.91	70	0.08	0.37	62	6.96	55	0.13	0.43
17	13.87	35	1.00	0.54	63	32.64	40	1.12	0.67
18	28.85	35	1.02	0.69	64	23.87	45	0.80	0.66
19	7.16	80	0.09	0.41	65	13.12	35	0.79	0.54
20	7.66	77	0.10	0.41	66	5.64	20	1.05	0.35
21	11.17	69	0.16	0.47	67	27.59	50	0.49	0.66
22	7.75	72	0.11	0.42	68	7.82	65	0.12	0.44
23	8.27	68	0.12	0.42	69	9.56	60	0.16	0.47
24	48.43	40	1.21	0.72	70	26.15	60	0.44	0.62
25	42.20	25	1.46	0.73	71	2151.27	95	22.64	0.94
26	19.41	25	1.10	0.63	72	19.57	26	0.64	0.52
27	7.65	27	0.28	0.46	73	91.81	35	0.57	0.72
28	5.05	21	0.24	0.35	74	33.25	40	0.83	0.59
29	5.62	30	0.19	0.36	75	7.97	15	0.53	0.36
30	25.52	19	1.07	0.64	76	10.30	15	0.69	0.45
31	12.61	22	1.17	0.55	77	3.47	5	1.00	0.26
32	12.45	24	0.48	0.56	78	5.44	6	0.91	0.39
33	6.63	24	0.28	0.38	79	8.05	12	0.67	0.36
34	12.86	24	0.54	0.53	80	21.19	25	0.85	0.53
35	38.31	25	1.33	0.71	81	3.63	8	0.45	0.26
36	21.13	23	1.09	0.61	82	28.57	12	0.67	0.56
37	16.86	15	1.26	0.62	83	24.67	15	0.60	0.57
38	17.91	20	1.16	0.63	84	10.15	14	0.65	0.45
39	11.40	20	1.10	0.52	85	4.62	10	0.46	0.32
40	24.68	21	1.05	0.67	86	4.36	11	0.40	0.31

41	35.60	28	1.11	0.71	87	878.55	60	1.46	0.91
42	6.81	28	0.24	0.38	88	23.86	30	1.00	0.66
43	5.82	26	0.22	0.37	89	23.59	25	0.94	0.62
44	29.13	20	1.46	0.66	90	61.53	28	2.20	0.75
45	6.88	38	0.18	0.39	91	44.10	30	0.68	0.63
46	8.44	30	0.28	0.46	92	4.53	20	0.23	0.33

Weighted discontinuity condition (CD), Rock mass friction and cohesion (ϕ 'mass and Coh' mass) and Discontinuity Spacing parameter (SPA) were calculated using the following expressions.

ϕ 'mass =IRS*0.2417+SPA*52.12+CD*5.779, Coh' mass =IRS*94.27+SPA*28629+CD*3593

CD =((TC1/DS1)+(TC2/DS2)+(TS3/DS3))/((1/DS1)+(1/DS2)+(1/DS3)), SPA= F1*F2*F3

Slope sec.	ϕ 'mass	*Coh' mass*	CD	SPA	Slope sec	ϕ 'mass	*Coh' mass*	CD	SPA
1	25.589	13058.50	0.492	0.292	47	53.320	24384.141	0.424	0.364
2	40.979	19830.149	0.496	0.383	48	41.422	20088.425	0.532	0.388
3	38.746	18638.188	0.579	0.331	49	34.532	18012.095	0.590	0.452
4	39.048	18782.129	0.527	0.343	50	31.553	16347.326	0.521	0.403
5	30.936	15969.242	0.428	0.401	51	37.774	18088.053	0.540	0.317
6	39.367	18947.556	0.503	0.352	52	30.864	15974.813	0.535	0.388
7	27.052	13883.022	0.541	0.314	53	47.002	23211.831	0.671	0.480
8	42.492	20661.510	0.497	0.412	54	42.517	20719.452	0.603	0.401
9	50.059	22625.641	0.501	0.293	55	37.694	18049.382	0.552	0.314
10	38.376	18428.359	0.563	0.326	56	13.945	7563.166	0.574	0.163
11	30.175	15615.900	0.583	0.369	57	13.475	7231.717	0.399	0.174
12	30.977	16051.409	0.570	0.386	58	18.841	9396.158	0.597	0.150
13	39.076	18790.381	0.510	0.345	59	31.003	16090.870	0.630	0.380
14	53.948	24806.262	0.607	0.356	60	27.838	14317.019	0.547	0.329
15	28.490	14658.388	0.506	0.346	61	29.754	15384.281	0.582	0.361
16	28.868	14906.040	0.601	0.342	62	34.221	16153.222	0.581	0.244
17	36.990	17677.005	0.587	0.297	63	43.672	21309.907	0.498	0.435
18	57.114	26543.163	0.602	0.417	64	54.668	25192.361	0.585	0.372
19	31.876	16540.667	0.559	0.405	65	41.265	20038.170	0.618	0.375
20	29.478	15207.878	0.522	0.363	66	24.350	12381.145	0.499	0.267
21	30.469	15747.305	0.511	0.383	67	49.834	22537.279	0.585	0.279
22	31.280	16258.987	0.669	0.381	68	33.046	15463.645	0.474	0.234
23	29.396	15208.599	0.631	0.349	69	32.881	15347.181	0.413	0.237
24	42.975	20933.488	0.513	0.420	70	34.010	15973.780	0.429	0.257
25	56.264	26051.138	0.542	0.407	71	28.230	14558.869	0.610	0.329
26	51.818	23619.299	0.567	0.319	72	20.801	11320.325	0.553	0.297
27	39.077	18820.237	0.580	0.338	73	14.441	8146.352	0.626	0.202

28	30.135	15563.232	0.509	0.377	74	17.775	9895.660	0.430	0.288
29	28.138	14474.426	0.529	0.336	75	16.254	9042.624	0.560	0.235
30	51.690	23508.089	0.469	0.328	76	27.743	14295.410	0.619	0.319
31	43.810	21392.247	0.513	0.436	77	19.244	10398.287	0.393	0.285
32	49.505	22347.702	0.564	0.275	78	33.256	15552.689	0.411	0.245
33	25.968	13274.761	0.510	0.297	79	16.242	9136.365	0.629	0.236
34	38.797	18657.374	0.558	0.335	80	20.625	11466.033	0.613	0.313
35	53.324	24478.784	0.644	0.340	81	18.768	10415.686	0.541	0.286
36	42.987	20955.707	0.550	0.416	82	14.051	7927.882	0.617	0.195
37	54.551	25161.029	0.664	0.361	83	22.841	11586.755	0.581	0.229
38	55.548	25667.343	0.565	0.391	84	28.151	14487.104	0.542	0.335
39	41.391	20105.500	0.613	0.378	85	23.934	12159.571	0.516	0.257
40	55.133	25406.884	0.488	0.392	86	24.403	12430.635	0.548	0.263
41	54.526	25071.944	0.483	0.380	87	31.893	16568.957	0.605	0.400
42	26.795	13757.327	0.578	0.305	88	54.673	25174.504	0.535	0.377
43	29.731	15353.513	0.538	0.366	89	40.334	19475.779	0.497	0.371
44	44.129	21664.266	0.744	0.416	90	44.787	21925.523	0.505	0.456
45	28.999	14975.866	0.597	0.345	91	15.735	8839.336	0.584	0.231
46	34.695	16442.711	0.650	0.246	92	28.360	14534.943	0.383	0.357

8.3 SSPC reference rock mass (RRM) calculated values

Rock mass parameters are determined and converted into parameters for the 'reference' rock mass by correction for local weathering in the exposure characterized and for damage due to the method of excavation used to create the exposure. These were done using the following expressions:

RIRS= IRS/WE, RSPA= SPA/WE*ME, RFRI=RIRS*0.2417+RSPA*52.12+RCD*5.779

RCOH= RIRS*94.27+RSPA*28629+RCD*3593, RCD = CD/WE,

RTC = TC / Sqrt (1.452-1.220*e $^{(-WE)}$)

Slope face	RTC			RIRS	RSPA	RFRI	RCOH	RCD
	RTC1	RTC2	RTC3					
1	0.460	0.460	0.556	34.72	0.324	28.432	14509.448	0.546
2	0.545	0.489	0.492	78.95	0.404	43.136	20873.841	0.522
3	0.549	0.492	0.652	78.95	0.349	40.785	19619.145	0.609
4	0.582	0.515	0.515	78.95	0.361	41.103	19770.662	0.555
5	0.474	0.449	0.417	34.72	0.446	34.374	17743.602	0.475
6	0.582	0.455	0.515	78.95	0.370	41.439	19944.795	0.530
7	0.738	0.622	0.460	34.72	0.349	30.058	15425.581	0.601

8	0.515	0.576	0.455	78.95	0.434	44.729	21748.958	0.523
9	0.568	0.386	0.549	132.00	0.308	51.015	23161.536	0.527
10	0.614	0.582	0.545	78.95	0.343	40.396	19398.273	0.593
11	0.460	0.589	0.657	34.72	0.410	33.528	17351.000	0.648
12	0.492	0.474	0.661	34.72	0.429	34.419	17834.899	0.634
13	0.438	0.468	0.606	78.95	0.364	41.132	19779.349	0.537
14	0.545	0.691	0.582	132.00	0.374	55.108	25456.926	0.639
15	0.589	0.556	0.489	34.72	0.384	31.656	16287.098	0.563
16	0.522	0.575	0.661	34.72	0.380	32.076	16562.267	0.668
17	0.515	0.612	0.606	78.95	0.313	38.937	18607.374	0.617
18	0.606	0.549	0.648	132.00	0.439	58.441	27285.244	0.634
19	0.600	0.522	0.589	34.72	0.450	35.418	18378.519	0.621
20	0.552	0.632	0.451	34.72	0.403	32.754	16897.642	0.580
21	0.661	0.583	0.452	34.72	0.426	33.855	17497.006	0.568
22	0.738	0.622	0.700	34.72	0.423	34.755	18065.541	0.744
23	0.414	0.496	0.785	34.72	0.388	32.663	16898.443	0.702
24	0.576	0.455	0.545	78.95	0.442	45.237	22035.251	0.540
25	0.624	0.652	0.443	132.00	0.429	57.546	26767.322	0.571
26	0.652	0.409	0.646	132.00	0.336	52.866	24207.492	0.597
27	0.549	0.606	0.584	78.95	0.355	41.134	19810.776	0.610
28	0.818	0.556	0.391	34.72	0.419	33.484	17292.480	0.565
29	0.491	0.552	0.552	34.72	0.374	31.264	16082.695	0.588
30	0.460	0.460	0.522	132.00	0.364	53.888	24737.472	0.521
31	0.419	0.612	0.515	78.95	0.459	46.116	22518.155	0.540
32	0.768	0.549	0.549	132.00	0.290	50.431	22868.968	0.594
33	0.522	0.522	0.522	34.72	0.330	28.854	14749.735	0.567
34	0.646	0.545	0.540	78.95	0.352	40.839	19639.341	0.587
35	0.644	0.652	0.652	132.00	0.357	54.451	25112.213	0.678
36	0.409	0.545	0.624	78.95	0.438	45.250	22058.638	0.579
37	0.646	0.515	0.768	132.00	0.380	55.742	25830.366	0.699
38	0.515	0.652	0.549	132.00	0.412	56.793	26363.327	0.594
39	0.606	0.652	0.606	78.95	0.398	43.569	21163.684	0.646
40	0.468	0.443	0.515	132.00	0.412	56.355	26089.160	0.513
41	0.545	0.386	0.545	132.00	0.400	55.717	25736.591	0.509
42	0.738	0.556	0.556	34.72	0.339	29.773	15285.918	0.642
43	0.622	0.489	0.552	34.72	0.406	33.035	17059.459	0.598
44	0.729	0.691	0.820	78.95	0.438	46.452	22804.491	0.783
45	0.589	0.700	0.547	34.72	0.384	32.221	16639.851	0.663
46	0.545	0.540	0.729	78.95	0.259	36.521	17308.117	0.684
47	0.386	0.409	0.473	132.00	0.383	54.447	25012.589	0.446
48	0.691	0.419	0.549	78.95	0.408	43.602	21145.711	0.560

49	0.656	0.655	0.552	34.72	0.502	38.368	20013.438	0.656
50	0.700	0.489	0.491	34.72	0.447	35.059	18163.696	0.579
51	0.576	0.576	0.515	78.95	0.334	39.762	19040.055	0.569
52	0.449	0.518	0.589	34.72	0.431	34.294	17749.793	0.595
53	0.768	0.606	0.691	78.95	0.505	49.476	24433.506	0.706
54	0.606	0.652	0.582	78.95	0.422	44.754	21809.950	0.635
55	0.614	0.606	0.515	78.95	0.331	39.678	18999.349	0.581
56	0.790	0.748	0.707	25.00	0.467	39.843	21609.045	1.639
57	0.530	0.538	0.497	25.00	0.496	38.499	20662.048	1.139
58	0.496	0.762	0.673	50.40	0.243	30.389	15155.093	0.962
59	0.724	0.724	0.682	50.40	0.613	50.006	25953.016	1.017
60	0.572	0.768	0.572	50.40	0.530	44.899	23091.965	0.882
61	0.626	0.552	0.621	34.72	0.402	33.060	17093.646	0.646
62	0.483	0.655	0.606	78.95	0.257	36.022	17003.391	0.611
63	0.515	0.473	0.515	78.95	0.458	45.970	22431.481	0.524
64	0.483	0.720	0.568	132.00	0.391	55.866	25863.347	0.616
65	0.618	0.576	0.652	78.95	0.395	43.437	21092.810	0.650
66	0.656	0.479	0.443	34.72	0.297	27.056	13756.828	0.554
67	0.576	0.648	0.549	132.00	0.294	50.778	23068.523	0.616
68	0.386	0.409	0.580	78.95	0.246	34.786	16277.521	0.499
69	0.386	0.455	0.409	78.95	0.250	34.611	16154.927	0.435
70	0.455	0.386	0.455	78.95	0.271	35.799	16814.505	0.452
71	0.767	0.724	0.610	50.40	0.531	45.533	23482.047	0.983
72	0.724	0.572	0.605	14.11	0.479	33.550	18258.589	0.891
73	0.828	0.787	0.828	3.57	0.577	41.261	23275.292	1.788
74	0.402	0.630	0.585	3.57	0.822	50.787	28273.314	1.228
75	0.741	0.658	0.780	8.91	0.672	46.441	25836.070	1.600
76	0.682	0.759	0.646	50.40	0.514	44.748	23057.113	0.998
77	0.429	0.429	0.457	14.11	0.460	31.039	16771.431	0.634
78	0.386	0.489	0.386	78.95	0.258	35.007	16371.251	0.433
79	0.828	0.787	0.828	3.57	0.675	46.405	26103.901	1.796
80	0.790	0.938	0.707	8.91	0.895	58.930	32760.093	1.752
81	0.694	0.702	0.707	8.91	0.816	53.624	29759.103	1.546
82	0.787	0.828	0.787	3.57	0.558	40.145	22651.091	1.762
83	0.614	0.589	0.589	34.72	0.254	25.379	12874.172	0.645
84	0.552	0.552	0.556	34.72	0.372	31.279	16096.782	0.602
85	0.583	0.442	0.556	34.72	0.286	26.593	13510.634	0.573
86	0.583	0.552	0.556	34.72	0.292	27.114	13811.817	0.609
87	0.661	0.622	0.589	34.72	0.444	35.437	18409.952	0.672
88	0.606	0.549	0.515	132.00	0.397	55.872	25844.549	0.564
89	0.515	0.419	0.549	78.95	0.391	42.456	20500.820	0.523

90	0.386	0.386	0.687	78.95	0.480	47.145	23079.498	0.531
91	0.880	0.621	0.787	3.57	0.661	44.958	25255.246	1.667
92	0.391	0.391	0.391	34.72	0.396	31.511	16149.936	0.425

8.4 SSPC slope rock mass (SRM) calculated values

This is derived from the 'reference rock mass' (RRM) by adjustment of the parameters of the RRM with the slope-specific parameters. These were done using the following expressions:

SCD = RCD*SWE, SIRS = RIRS*SWE, SSPA= RSPA*SWE*SME,

STC = RTC / Sqrt (1.452-1.220*e $^{(-SWE)}$), SFRI = SIRS*0.2417+SSPA*52.12+SCD*5.779,

SCOH (Pa) = SIRS*94.27+SSPA*28629+SCD*3593

Slope sec.	STC			SCD	SIRS	SSPA	SFRI	SCOH(Pa)
	STC1	STC2	STC3					
1	0.45	0.45	0.54	0.492	31.25	0.292	25.589	13058.50
2	0.54	0.48	0.49	0.496	75.00	0.383	40.979	19830.15
3	0.54	0.49	0.65	0.579	75.00	0.331	38.746	18638.19
4	0.58	0.51	0.51	0.527	75.00	0.343	39.048	18782.13
5	0.46	0.44	0.41	0.428	31.25	0.401	30.936	15969.24
6	0.58	0.45	0.51	0.503	75.00	0.352	39.367	18947.56
7	0.72	0.61	0.45	0.541	31.25	0.314	27.052	13883.02
8	0.51	0.57	0.45	0.497	75.00	0.412	42.492	20661.51
9	0.56	0.38	0.54	0.501	125.40	0.293	48.464	22003.46
10	0.61	0.58	0.54	0.563	75.00	0.326	38.376	18428.36
11	0.45	0.58	0.64	0.583	31.25	0.369	30.175	15615.90
12	0.48	0.46	0.65	0.570	31.25	0.386	30.977	16051.41
13	0.43	0.46	0.60	0.510	75.00	0.345	39.076	18790.38
14	0.54	0.68	0.58	0.607	125.40	0.356	52.353	24184.08
15	0.58	0.54	0.48	0.506	31.25	0.346	28.490	14658.39
16	0.51	0.56	0.65	0.601	31.25	0.342	28.868	14906.04
17	0.51	0.61	0.60	0.587	75.00	0.297	36.990	17677.01
18	0.60	0.54	0.64	0.602	125.40	0.417	55.519	25920.98
19	0.59	0.51	0.58	0.559	31.25	0.405	31.876	16540.67
20	0.54	0.62	0.44	0.522	31.25	0.363	29.478	15207.88

21	0.65	0.57	0.44	0.511	31.25	0.383	30.469	15747.31
22	0.72	0.61	0.68	0.669	31.25	0.381	31.280	16258.99
23	0.41	0.48	0.77	0.631	31.25	0.349	29.396	15208.60
24	0.57	0.45	0.54	0.513	75.00	0.420	42.975	20933.49
25	0.62	0.65	0.44	0.542	125.40	0.407	54.669	25428.96
26	0.65	0.41	0.64	0.567	125.40	0.319	50.223	22997.12
27	0.54	0.60	0.58	0.580	75.00	0.338	39.077	18820.24
28	0.80	0.54	0.38	0.509	31.25	0.377	30.135	15563.23
29	0.48	0.54	0.54	0.529	31.25	0.336	28.138	14474.43
30	0.45	0.45	0.51	0.469	118.80	0.328	48.500	22263.73
31	0.41	0.61	0.51	0.513	75.00	0.436	43.810	21392.25
32	0.76	0.54	0.54	0.564	125.40	0.275	47.910	21725.52
33	0.51	0.51	0.51	0.510	31.25	0.297	25.968	13274.76
34	0.64	0.54	0.53	0.558	75.00	0.335	38.797	18657.37
35	0.64	0.65	0.65	0.644	125.40	0.340	51.729	23856.60
36	0.41	0.54	0.62	0.550	75.00	0.416	42.987	20955.71
37	0.64	0.51	0.76	0.664	125.40	0.361	52.955	24538.85
38	0.51	0.65	0.54	0.565	125.40	0.391	53.953	25045.16
39	0.60	0.65	0.60	0.613	75.00	0.378	41.391	20105.50
40	0.46	0.44	0.51	0.488	125.40	0.392	53.538	24784.70
41	0.54	0.38	0.54	0.483	125.40	0.380	52.931	24449.76
42	0.72	0.54	0.54	0.578	31.25	0.305	26.795	13757.33
43	0.61	0.48	0.54	0.538	31.25	0.366	29.731	15353.51
44	0.72	0.68	0.81	0.744	75.00	0.416	44.129	21664.27
45	0.58	0.68	0.53	0.597	31.25	0.345	28.999	14975.87
46	0.54	0.53	0.72	0.650	75.00	0.246	34.695	16442.71
47	0.38	0.41	0.47	0.424	125.40	0.364	51.724	23761.96
48	0.68	0.41	0.54	0.532	75.00	0.388	41.422	20088.43
49	0.64	0.64	0.54	0.590	31.25	0.452	34.532	18012.09
50	0.68	0.48	0.48	0.521	31.25	0.403	31.553	16347.33
51	0.57	0.57	0.51	0.540	75.00	0.317	37.774	18088.05
52	0.44	0.51	0.58	0.535	31.25	0.388	30.864	15974.81
53	0.76	0.60	0.68	0.671	75.00	0.480	47.002	23211.83
54	0.60	0.65	0.58	0.603	75.00	0.401	42.517	20719.45
55	0.61	0.60	0.51	0.552	75.00	0.314	37.694	18049.38
56	0.61	0.58	0.54	0.574	8.75	0.163	13.945	7563.17
57	0.41	0.41	0.38	0.399	8.75	0.174	13.475	7231.72
58	0.44	0.68	0.60	0.597	31.25	0.150	18.841	9396.16
59	0.65	0.65	0.61	0.630	31.25	0.380	31.003	16090.87
60	0.51	0.68	0.51	0.547	31.25	0.329	27.838	14317.02
61	0.61	0.54	0.61	0.582	31.25	0.361	29.754	15384.28

62	0.48	0.65	0.60	0.581	75.00	0.244	34.221	16153.22
63	0.51	0.47	0.51	0.498	75.00	0.435	43.672	21309.91
64	0.48	0.71	0.56	0.585	125.40	0.372	53.073	24570.18
65	0.61	0.57	0.65	0.618	75.00	0.375	41.265	20038.17
66	0.64	0.47	0.43	0.499	31.25	0.267	24.350	12381.15
67	0.57	0.64	0.54	0.585	125.40	0.279	48.239	21915.10
68	0.38	0.41	0.57	0.474	75.00	0.234	33.046	15463.65
69	0.38	0.45	0.41	0.413	75.00	0.237	32.881	15347.18
70	0.45	0.38	0.45	0.429	75.00	0.257	34.010	15973.78
71	0.68	0.65	0.54	0.610	31.25	0.329	28.230	14558.87
72	0.65	0.51	0.54	0.553	8.75	0.297	20.801	11320.33
73	0.64	0.61	0.64	0.626	1.25	0.202	14.441	8146.35
74	0.31	0.48	0.45	0.430	1.25	0.288	17.775	9895.66
75	0.57	0.51	0.60	0.560	3.12	0.235	16.254	9042.62
76	0.61	0.68	0.58	0.619	31.25	0.319	27.743	14295.41
77	0.38	0.38	0.41	0.393	8.75	0.285	19.244	10398.29
78	0.38	0.48	0.38	0.411	75.00	0.245	33.256	15552.69
79	0.64	0.61	0.64	0.629	1.25	0.236	16.242	9136.37
80	0.61	0.72	0.54	0.613	3.12	0.313	20.625	11466.03
81	0.53	0.54	0.54	0.541	3.12	0.286	18.768	10415.69
82	0.61	0.64	0.61	0.617	1.25	0.195	14.051	7927.88
83	0.60	0.58	0.58	0.581	31.25	0.229	22.841	11586.76
84	0.54	0.54	0.54	0.542	31.25	0.335	28.151	14487.10
85	0.57	0.43	0.54	0.516	31.25	0.257	23.934	12159.57
86	0.57	0.54	0.54	0.548	31.25	0.263	24.403	12430.64
87	0.65	0.61	0.58	0.605	31.25	0.400	31.893	16568.96
88	0.60	0.54	0.51	0.535	125.40	0.377	53.078	24552.32
89	0.51	0.41	0.54	0.497	75.00	0.371	40.334	19475.78
90	0.38	0.38	0.68	0.505	75.00	0.456	44.787	21925.52
91	0.68	0.48	0.61	0.584	1.25	0.231	15.735	8839.34
92	0.38	0.38	0.38	0.383	31.25	0.357	28.360	14534.94

8.5 GSI value estimation

All slope faces, after calculating the mean structure rating (SR) based on volumetric joint count (Jv) and surface condition rating (SCR) based on weathering rating (Rw), rough rating (Rr), infile and rating (Rf). And also joint condition factor (Jc) and Block volume (Vb) was calculated using the following expressions.

Jc $= \frac{JwJs}{Ja}$, where, large-scale waviness (Jw) and small-scale smoothness (Js) and joint alteration factor (Ja)

$Jv = \frac{1}{S1} + \frac{1}{S2} + \frac{1}{S3}$, Where, S1, S2 and S3 are the average discontinuity spacing the joints sets

SR= -17.5ln (Jv) +79.8, SCR=Rr+ Rw + Rf,

$Vb = S1 * S2 * S3$ Where, S1, S2 and S3 are the average discontinuity spacing the joints sets

8.5.1 Structure rating (SR) surface condition rating (SCR) volumetric, joint count (Jv) and others input parameters and results

Slope sec.	Mean SCR	Mean SR	Mean Jv	Range GSI value	GSI Estimated	Js	Jw	Ja	Vb (cm3)	Jc
1	12.00	41.94	8.70	45-50	48	1.33	1.67	2.00	45,500	1.44
2	12.67	48.80	5.88	50-55	54	1.50	1.17	2.00	190,950	0.83
3	14.00	44.13	7.68	55	55	1.83	1.83	1.67	85,000	2.25
4	13.33	47.19	6.45	55-60	54	2.00	1.67	2.33	109,200	1.33
5	8.67	51.13	5.15	45	45	1.33	1.17	2.00	250,800	0.75
6	13.33	45.85	6.96	55	55	1.67	1.67	1.67	117,000	2.50
7	11.00	42.02	8.66	45-50	46	1.67	1.83	2.00	63,580	1.67
8	12.67	52.06	4.88	55	55	1.33	1.33	1.67	294,000	1.42
9	13.33	40.64	9.37	50-55	52	1.33	1.67	1.67	44,400	1.50
10	12.00	44.19	7.65	50	50	2.00	2.33	2.00	78,750	2.33
11	10.67	48.70	5.91	45-50	48	1.33	1.83	2.67	158,400	1.03
12	10.00	48.89	5.85	45-50	48	1.50	1.33	2.00	198,000	1.00
13	13.33	47.56	6.31	55	55	1.50	1.17	1.67	114,400	1.08
14	12.33	47.73	6.25	50-55	52	2.00	1.83	2.00	129,600	1.83
15	11.00	43.69	7.87	45-50	47	1.67	2.33	2.33	104,500	2.11
16	12.00	44.06	7.71	50	50	1.67	1.17	2.00	100,320	1.00
17	15.00	41.60	8.87	55-60	58	1.67	1.17	1.33	48,750	1.50
18	13.33	53.37	4.53	60-65	62	1.33	2.00	2.00	324,000	1.50
19	10.00	51.70	4.98	45-50	48	1.83	1.83	2.33	266,000	1.60
20	11.00	48.21	6.08	45-50	48	2.17	1.33	2.67	143,820	1.08
21	10.33	48.68	5.92	45-50	47	1.83	1.83	2.00	189,000	1.71
22	10.67	50.23	5.42	50	50	2.67	2.67	2.00	192,000	3.50
23	10.33	45.65	7.04	45-50	46	1.67	1.33	2.00	112,750	1.17
24	12.67	53.22	4.57	55-60	57	1.67	1.50	1.67	333,000	1.75
25	14.33	52.53	4.75	60	60	1.67	1.33	2.00	283,050	1.13
26	13.33	41.68	8.83	50-55	52	1.67	1.83	2.00	68,400	1.67

27	15.00	45.54	7.08	55-60	58	2.00	2.33	2.00	96,000	2.33
28	12.00	48.87	5.86	50-55	54	1.67	1.83	2.00	175,000	1.67
29	10.67	45.23	7.21	45-50	47	1.67	1.33	3.33	93,150	0.79
30	13.33	45.87	6.95	50-55	53	1.00	1.33	2.00	85,680	0.67
31	13.33	55.42	4.03	55-60	58	1.17	1.50	2.00	432,000	0.88
32	14.00	33.89	13.78	50-55	52	2.00	2.50	2.00	31,200	2.50
33	11.33	42.24	8.55	45-50	47	1.67	1.33	2.33	49,400	1.00
34	12.00	45.66	7.03	50	50	1.33	1.83	2.00	92,400	1.42
35	11.33	45.90	6.94	45-50	48	1.67	1.83	2.00	99,792	1.58
36	11.33	52.65	4.72	50-55	52	1.17	1.33	2.00	312,816	0.79
37	15.67	47.36	6.38	60-65	62	2.00	1.83	2.00	136,740	1.83
38	14.33	51.68	4.99	60	60	2.00	2.00	2.67	230,112	1.75
39	15.33	49.38	5.69	60	60	2.00	1.33	2.00	180,600	1.33
40	11.33	48.21	6.08	45-50	48	1.67	1.50	2.67	212,940	1.06
41	12.67	49.76	5.56	50-55	54	1.67	1.50	2.00	188,000	1.25
42	11.67	41.66	8.84	45-50	48	2.00	2.50	3.00	55,200	1.83
43	10.00	48.44	6.00	45-50	47	1.67	1.83	2.33	150,975	1.50
44	12.33	54.09	4.35	55	55	2.33	2.00	2.00	336,000	2.25
45	9.33	46.25	6.80	35	35	1.67	1.83	3.33	108,800	0.92
46	10.67	34.04	13.67	40	40	1.33	1.17	2.00	18,000	0.75
47	10.67	49.46	5.66	45-50	48	1.17	1.50	2.67	154,440	0.75
48	12.67	50.77	5.25	60	60	1.83	2.33	2.00	211,932	2.25
49	10.67	55.50	4.01	60-65	62	1.67	1.67	2.33	510,000	1.44
50	12.00	51.07	5.16	55-60	58	1.33	1.83	3.00	256,500	1.00
51	13.33	42.61	8.37	50-55	54	2.00	1.33	2.00	67,320	1.33
52	8.67	48.76	5.89	40-45	42	1.50	1.83	3.33	201,600	0.85
53	13.00	58.56	3.37	60	60	2.00	1.83	2.67	760,000	1.67
54	14.00	50.04	5.48	55-60	58	2.00	2.00	3.33	245,700	1.50
55	14.00	42.75	8.31	55	55	2.00	1.67	2.00	64,350	1.67
56	6.67	25.97	21.67	30	30	2.00	3.00	3.00	3,000	2.00
57	4.67	27.17	20.23	25	25	1.17	1.50	3.00	3,850	0.58
58	6.00	24.27	23.89	25-30	28	1.50	2.00	3.00	2,160	1.08
59	7.33	50.29	5.40	35	35	2.00	3.00	3.00	191,250	2.00
60	10.00	43.08	8.15	35-40	38	2.00	1.67	3.00	81,200	1.11
61	11.33	47.43	6.36	55-60	58	1.33	1.17	2.00	140,000	0.75
62	13.67	37.78	11.04	50	50	1.33	1.33	2.00	20,250	0.83
63	12.67	54.14	4.33	55-60	56	1.83	1.33	1.67	404,800	1.71
64	15.67	47.98	6.16	60-65	62	1.00	1.17	2.00	161,472	0.58
65	12.33	49.36	5.69	55-60	56	2.00	2.00	2.00	175,175	2.00
66	11.00	39.64	9.92	45	45	1.83	1.33	2.67	29,716	0.88
67	13.00	41.43	8.96	50-55	52	2.33	1.83	2.00	38,400	2.00
68	13.67	35.49	12.58	45-50	48	1.00	1.50	2.00	15,120	0.75
69	14.33	36.72	11.72	50-55	54	1.00	1.17	2.00	17,160	0.58
70	14.67	38.10	10.83	50-55	53	1.00	1.17	2.00	24,000	0.58
71	10.00	45.71	7.01	35-40	36	2.67	2.67	3.33	86,400	2.13
72	8.67	42.15	8.60	30-35	33	1.67	1.83	3.33	49,500	1.00

73	4.67	31.41	15.88	25-30	27	1.00	1.83	7.33	7,650	0.38
74	6.00	41.30	9.02	30-35	42	1.00	1.17	10.0	42,000	0.12
75	7.33	36.49	11.88	35-40	38	1.00	1.50	10.0	16,500	0.15
76	8.33	44.72	7.42	30-35	33	2.33	2.33	3.33	72,960	1.50
77	7.33	41.61	8.87	35-40	38	1.00	1.33	3.33	41,310	0.42
78	9.33	36.69	11.75	40	40	1.00	1.33	3.33	18,900	0.46
79	6.67	35.35	12.68	30-35	34	1.00	1.83	10.0	15,680	0.18
80	7.33	44.41	7.56	35-40	39	2.00	2.50	10.0	67,500	0.50
81	6.67	39.73	9.87	35	35	1.67	1.67	3.67	39,000	0.81
82	8.00	31.04	16.22	30-35	32	1.00	1.67	10.0	6,750	0.17
83	10.67	34.21	13.54	40-45	43	2.00	2.50	10.0	13,320	0.50
84	9.67	46.18	6.83	45	45	2.00	1.67	4.00	95,200	0.83
85	10.00	38.10	10.83	40-45	43	1.67	2.00	3.00	24,000	2.38
86	10.00	37.99	10.90	40-45	43	2.00	1.67	4.00	25,920	0.83
87	10.33	52.39	4.79	45-50	49	2.00	3.00	2.00	260,000	3.00
88	14.67	48.49	5.98	55-60	58	2.00	1.67	1.67	175,500	2.00
89	13.33	49.67	5.60	55	55	1.83	1.67	1.67	168,000	1.92
90	14.00	56.94	3.69	60-65	63	1.33	1.67	2.00	561,000	1.33
91	6.00	35.83	12.33	30-35	33	1.00	1.33	10.0	15,000	0.13
92	10.00	49.00	5.81	45-50	47	1.00	1.00	1.67	140,400	0.67

8.5.2 Weathering rating (Rw), Rough rating (Rr), infile rating (Rf)

Slope sec.	R w	Rr	Rf	Slope Sec.	R w	Rr	Rf	Slope sec.	R w	Rr	Rf	Slope sec.	Rw	Rr	Rf
1	3	3.67	5.33	24	5	4.33	3.33	47	5	3.00	2.67	70	5	4.33	5.33
2	5	3.67	4.00	25	5	5.33	4.00	48	5	4.33	3.33	71	1	5.67	3.33
3	5	4.33	4.67	26	5	4.33	4.00	49	3	4.33	3.33	72	1	5.00	2.67
4	5	5.00	3.33	27	5	5.33	4.67	50	3	4.33	4.67	73	1	1.67	2.00
5	3	3.00	2.67	28	3	4.33	4.67	51	5	5.67	2.67	74	1	1.67	3.33
6	5	4.33	4.00	29	3	4.33	3.33	52	3	3.67	2.00	75	1	3.00	3.33
7	3	4.67	3.33	30	3	4.33	6.00	53	5	5.33	2.67	76	1	5.33	2.00
8	5	3.67	4.00	31	5	4.33	4.00	54	5	5.00	4.00	77	1	3.00	3.33
9	5	3.67	4.67	32	5	4.33	4.67	55	5	5.00	4.00	78	5	2.33	2.00
10	5	5.00	2.00	33	3	4.33	4.00	56	1	3.00	2.67	79	1	3.67	2.00
11	3	3.67	4.00	34	5	3.67	3.33	57	1	1.67	2.00	80	1	3.67	2.67
12	3	3.67	3.33	35	5	4.33	2.00	58	1	1.67	3.33	81	1	3.67	2.00
13	5	4.33	4.00	36	5	3.00	3.33	59	1	4.33	2.00	82	1	3.00	4.00
14	5	5.33	2.00	37	5	5.33	5.33	60	1	5.00	4.00	83	3	4.33	3.33
15	3	4.67	3.33	38	5	5.33	4.00	61	3	5.67	2.67	84	3	4.67	2.00
16	3	4.33	4.67	39	5	5.00	5.33	62	5	4.67	4.00	85	3	4.33	2.67
17	5	5.33	4.67	40	5	3.67	2.67	63	5	4.33	3.33	86	3	4.33	2.67
18	5	4.33	4.00	41	5	4.33	3.33	64	5	5.33	5.33	87	3	5.33	2.00
19	3	4.33	2.67	42	3	5.33	3.33	65	5	5.33	2.00	88	5	5.67	4.00
20	3	4.00	4.00	43	3	4.33	2.67	66	3	5.33	2.67	89	5	4.33	4.00

21	3	4.67	2.67	44	5	5.33	2.00	67	5	5.33	2.67	90	5	5.00	4.00
22	3	5.67	2.00	45	3	4.33	2.00	68	5	5.33	3.33	91	1	3.00	2.00
23	3	4.00	3.33	46	5	3.67	2.00	69	5	5.33	4.00	92	3	3.67	3.33

Weathering rating (Rw), Rough rating (Rr), infile rating (Rf)

8.6 Sliding criteria and toppling criteria

Slope sec.	Sliding criteria sliding if: TC<0.0113*(AP)			Toppling criteria Toppling if: TC < 0.0087(-90-AP+dip discontinuity)		
	0.0113*(AP)			0.0087(-90-AP+dip discontinuity)		
	J1	J2	J3	J1	J2	J3
1	0.03	0.01	0.75	-0.35	-0.62	-0.75
2	-0.82	0.13	-0.53	0.55	-0.62	0.06
3	0.71	0.27	-0.02	-0.78	-0.69	-0.64
4	0.22	0.03	0.16	-0.43	-0.59	-0.54
5	0.64	0.34	-0.41	-0.65	-0.78	0.02
6	0.76	0.12	0.58	-0.78	-0.67	-0.77
7	0.70	-0.90	0.15	-0.78	0.65	-0.72
8	0.83	-0.96	0.28	-0.78	0.69	-0.77
9	0.80	0.90	0.45	-0.75	-0.78	-0.78
10	0.84	0.67	-0.11	-0.78	-0.76	-0.31
11	0.27	0.42	-0.34	-0.71	-0.67	0.05
12	0.48	0.50	-0.95	-0.76	-0.78	0.69
13	0.73	0.85	0.32	-0.78	-0.78	-0.72
14	0.12	0.81	-0.96	-0.75	-0.75	0.70
15	0.70	0.78	0.04	-0.75	-0.77	-0.73
16	0.79	0.38	0.03	-0.78	-0.61	-0.68
17	0.15	0.27	0.78	-0.64	-0.59	-0.78
18	-0.44	-0.90	-0.62	-0.08	0.61	0.22
19	0.02	0.88	-0.96	-0.66	-0.78	0.70
20	0.12	0.81	0.56	-0.66	-0.78	-0.66
21	0.73	-0.02	-0.71	-0.78	-0.61	0.46
22	0.75	0.03	-0.96	-0.75	-0.42	0.70
23	0.36	-0.80	0.79	-0.59	0.53	-0.78
24	-0.96	0.24	0.11	0.70	-0.78	-0.31
25	0.35	-0.15	0.85	-0.47	-0.49	-0.78
26	0.65	-0.01	-0.96	-0.78	-0.69	0.71
27	0.51	0.04	0.84	-0.78	-0.68	-0.73
28	0.56	0.01	0.70	-0.78	-0.71	-0.67

29	0.43	0.20	0.79	-0.78	-0.77	-0.78
30	0.59	0.34	0.85	-0.75	-0.78	-0.78
31	-0.36	0.43	0.90	0.07	-0.75	-0.78
32	0.04	0.35	0.90	-0.38	-0.75	-0.78
33	0.53	0.33	0.77	-0.71	-0.78	-0.76
34	0.39	0.29	0.81	-0.65	-0.78	-0.78
35	0.81	-0.96	0.24	-0.77	0.69	-0.75
36	0.53	0.26	0.29	-0.76	-0.76	-0.53
37	-0.52	0.36	0.73	0.02	-0.78	-0.78
38	0.84	-0.47	-0.96	-0.78	0.02	0.69
39	0.68	-0.46	0.85	-0.77	0.03	-0.78
40	0.88	0.47	-0.80	-0.78	-0.76	0.53
41	-0.88	0.73	-0.44	0.59	-0.78	-0.06
42	-0.89	-0.47	0.56	0.60	0.06	-0.78
43	0.90	-0.03	0.56	-0.78	-0.50	-0.69
44	0.64	0.70	0.14	-0.62	-0.78	-0.68
45	-0.96	0.25	0.73	0.69	-0.72	-0.78
46	0.61	0.51	0.13	-0.59	-0.78	-0.71
47	-0.21	0.41	0.14	-0.10	-0.78	-0.73
48	-0.25	0.41	-0.34	-0.02	-0.78	-0.26
49	-0.41	0.86	0.24	0.07	-0.78	-0.65
50	0.85	0.18	0.21	-0.78	-0.31	-0.73
51	0.90	-0.62	0.27	-0.78	0.27	-0.54
52	0.79	-0.79	0.40	-0.78	0.52	-0.61
53	-0.37	0.51	-0.96	0.04	-0.78	0.70
54	-0.96	-0.03	0.57	0.69	-0.50	-0.78
55	0.74	0.63	0.13	-0.69	-0.78	-0.71
56	0.11	0.21	0.02	-0.73	-0.77	-0.71
57	0.11	0.60	0.34	-0.48	-0.75	-0.78
58	0.24	0.04	0.34	-0.75	-0.64	-0.78
59	-0.96	0.40	0.73	0.69	-0.78	-0.78
60	0.67	-0.52	0.77	-0.78	0.05	-0.78
61	0.68	0.51	0.71	-0.73	-0.78	-0.63
62	-0.61	0.35	-0.95	0.30	-0.62	0.69
63	-0.96	0.73	0.26	0.69	-0.78	-0.56
64	0.63	-0.24	0.57	-0.57	-0.08	-0.78
65	-0.19	0.70	0.29	0.01	-0.78	-0.74
66	0.73	0.35	0.46	-0.78	-0.62	-0.75
67	-0.95	0.37	-0.25	0.69	-0.59	-0.08
68	-0.95	-0.81	0.11	0.69	0.49	-0.52
69	-0.49	0.51	-0.79	0.20	-0.78	0.43

70	0.23	0.40	0.39	-0.40	-0.78	-0.67
71	0.12	-0.96	0.15	-0.70	0.70	-0.64
72	0.15	0.06	0.54	-0.64	-0.41	-0.60
73	-0.03	0.15	0.02	-0.55	-0.72	-0.74
74	0.40	-0.16	0.34	-0.70	-0.48	-0.78
75	0.05	0.51	0.29	-0.61	-0.78	-0.74
76	0.38	0.65	0.38	-0.74	-0.78	-0.77
77	0.20	0.02	0.64	-0.29	-0.66	-0.75
78	-0.10	-0.80	0.66	-0.62	0.53	-0.69
79	-0.03	-0.07	0.15	-0.54	-0.26	-0.60
80	0.62	-0.90	-0.37	-0.77	0.61	0.04
81	0.29	-0.34	0.27	-0.62	-0.09	-0.47
82	-0.10	-0.49	-0.05	-0.53	0.17	-0.66
83	-0.90	0.30	0.33	0.61	-0.62	-0.78
84	-0.08	0.22	-0.90	-0.62	-0.29	0.61
85	0.95	-0.44	-0.09	-0.78	-0.05	-0.63
86	-0.88	-0.44	0.06	0.57	-0.09	-0.70
87	-0.90	0.12	0.40	0.65	-0.61	-0.78
88	-0.50	0.96	0.14	0.18	-0.78	-0.44
89	0.09	0.54	0.03	-0.57	-0.73	-0.72
90	-0.50	0.39	0.78	0.07	-0.78	-0.76
91	0.19	0.52	0.22	-0.50	-0.78	-0.68
92	0.59	-0.20	0.51	-0.58	-0.09	-0.78

8.7 Standards

8.7.1 Weathering standards

Scale of weathering grades classification for uniform materials, according to BS5930 (1981), incorporating SSPC system (Hack, 1998).

No.	Degree of weathering	Description	WE
1	Un weathered	No visible sign of rock material weathering; perhaps slight discoloration on major discontinuity surfaces.	1.00
2	Slightly	Discoloration indicates weathering of rock material and discontinuity surfaces. All the rock material may be discolored by weathering.	0.95
3	Moderately weathered	Less than half of the rock material is decomposed or disintegrated to a soil. Fresh or discolored rock is present either as a continuous framework or as core stones.	0.90
4	Highly	More than half of the rock material is decomposed or disintegrated to a	0.62

	weathered	soil. Fresh or discolored rock is present either as a discontinuous framework or as core stones.	
5	Completely weathered	All rock material is decomposed and/or disintegrated to soil. The original mass structure is still largely intact.	0.35

8.7.2 Classification of Intact rock strength based on BS 5930(1981) (after Hack and Huisman, 2002)

No.	term	Field description	UCS(MN/m2)
1	Very weak	Crumbles in hand	<1.25 MPa
2	Weak	Thin slabs break easy in hand	1.25-5 MPa
3	Moderately weak	Thin slabs broken by heavy hand pressure	5-12.5 MPa
4	Moderately strong	Lumps broken by light hammer blows	12.5-50 MPa
5	strong	Lumps broken by heavy hammer blows	50-100 MPa
6	Very strong	Lumps only chip by heavy hammer blows	100-200 MPa
7	Extremely strong	Rocks ring on hammer blows	>200 MPa

8.7.3 Method of excavation used, according to SSPC system (Hack, 1998)

No.	Excavation Method (ME)	
1	Natural/hand-made	1.00
2	Pneumatic hammer excavation	0.76
3	Pre-splitting/smooth wall blasting	0.99
Conventional blasting with result		
4	Good	0.77
5	Open discontinuities	0.75
6	Dislodged blocks	0.72
7	Fractured intact rock	0.67
8	Crushed intact rock	0.62

8.7.4 Roughness and infill material (after Hack, 1998; Hack and Price, 1995)

	Discontinuity condition			
	Large scale roughness(RL)	Wavy		1.00
		Slightly wavy		0.95
		curved		0.85
		Slightly curved		0.80
		straight		0.75
	Small scale	Rough	stepped	0.95

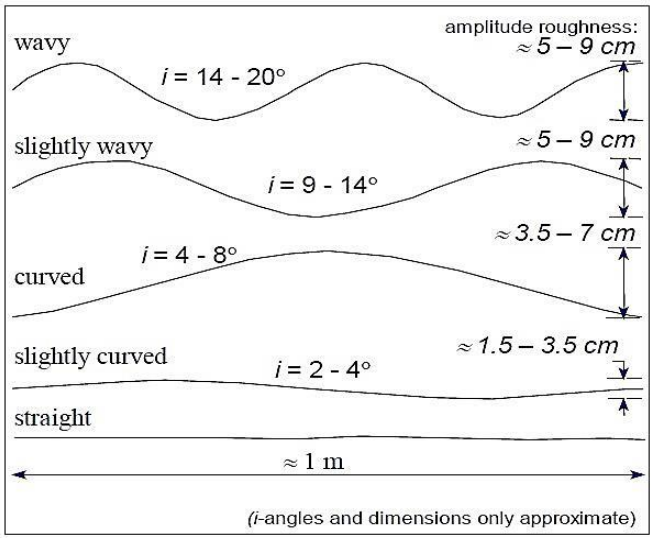

Large scale roughness profile

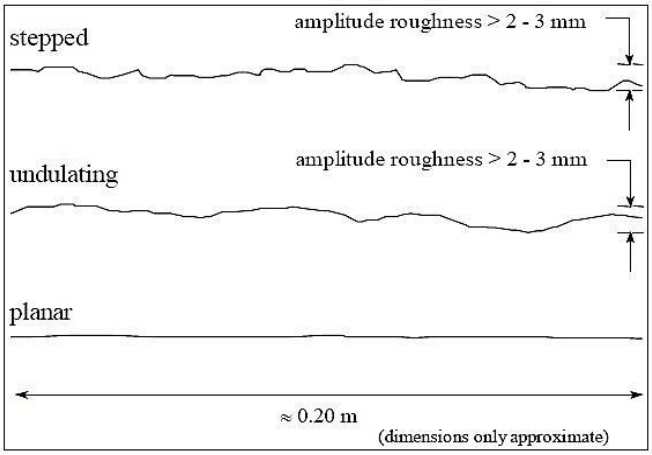

Small scale roughness profile

roughness(RS)	Smooth	stepped	0.90
	Polished	stepped	0.85
	Rough	undulating	0.80
	Smooth	undulating	0.75
	Polished	undulating	0.70
	Rough	planar	0.65
	Smooth	planar	0.60
	Polished	planar	0.55
Infill material(lm)	Cemented / cemented infill		1.07
	No infill - surface staining		1.00
	Non softening & sheared material	coarse	0.95
		medium	0.90
		fine	0.85
	soft sheared material	coarse	0.75
		medium	0.65
		fine	0.55
	Gouge < irregularities		0.42
	Gouge > irregularities		0.17
	Flowing material		0.05
Karst (ka)	None		1.00
	Karst		0.92

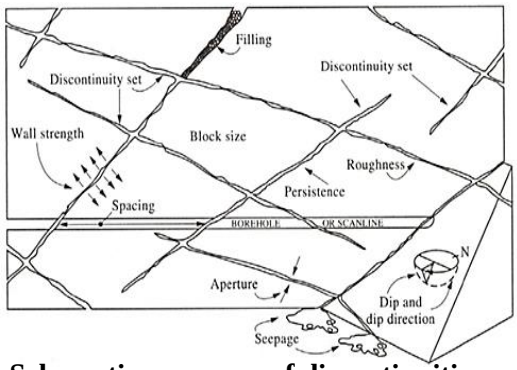

Schematic summery of discontinuities properties in slope rock mass (After Hudson and Harrison, 2000)

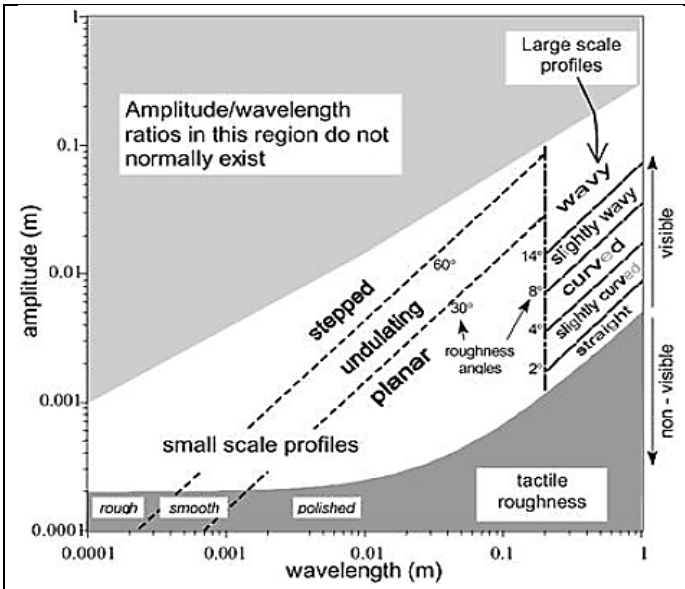

Interpretation of roughness as a function of wave length and amplitude

8.7.5 Joint alteration factor (Ja) (After Cai et al. 2004)

	Term	Description	Ja
Rock wall contact	Clear joints Healed or ‘‘welded’’ joints (unweathered)	Softening, impermeable filling (quartz, epidote, etc.)	0.75
	Fresh rock walls (unweathered)	No coating or filling on joint surface, except for staining	1
	Alteration of joint wall: slightly to moderately weathered	The joint surface exhibits one class higher alteration than the rock	2
	Alteration of joint wall: highly Weathered	The joint surface exhibits two classes higher alteration than the rock	4
	Coating or thin filling Sand, silt, calcite, etc.	Coating of frictional material without clay	3
	Clay, chlorite, talc, etc.	Coating of softening and cohesive minerals	4
Filled joints with partial or no contact between the rock wall surfaces	Sand, silt, calcite, etc.	Filling of frictional material without clay	4
	Compacted clay materials	Hard filling of softening and cohesive materials	6
	Soft clay materials	Medium to low over-consolidation of filling	8
	Swelling clay materials	Filling material exhibits swelling properties	8-12

8.7.6 Terms to describe small-scale smoothness (After Cai et al. 2004)

Smoothness terms	Description	Rating for smoothness(Js)
Very rough	Near vertical steps and ridges occur with interlocking effect on the joint surface	3
Rough	Some ridge and side-angle are evident; asperities are clearly visible; discontinuity surface feels very abrasive (rougher than sandpaper grade 30)	2
Slightly rough	Asperities on the discontinuity surfaces are distinguishable and can be felt (like sandpaper grade 30–300)	1.5
Smooth	Smooth Surface appear smooth and feels so to touch (smoother than sandpaper grade 300)	1
Polished	Visual evidence of polishing exists. This is often seen in coating of chlorite and specially talc	0.75
Slickensided	Polished and striated surface that results from sliding along a fault surface or other movement Surface	0.6–1.5

8.7.7 Terms to describe large-scale waviness (After Cai et al. 2004)

Waviness terms	Rating for waviness Jw
Interlocking (large-scale)	3
Stepped	2.5
Large undulation	2
Small to moderate undulation	1.5
Planar	1

8.7.8 Roughness rating, infilling rating and weathering rating (after Sonmez et al., 2003; Cai et al. 2004

Roughness	Very rough	Rough	Slightly rough	smooth	Slickenside
Rating	6	5	3	1	0
Infilling	none	Hard(<5mm)	Hard(>5mm)	Soft(<5mm)	Soft(>5mm)
rating	6	4	2	2	0
Weathering rating	none	Slightly weathered	Moderately weathered	Highly weathered	decomposed
Rating	6	5	3	1	0

8.7.9 The quality of the rock mass classification RMR (Bieniawski, 1989)

Value of GSI	76 – 95	56 – 75	36 - 55	21 - 35	< 20
Description Rock Mass Quality	Very good rock	Good rock	Fair rock	Poor rock	Very poor rock

8.8. Stability probability of discontinuities in sliding and toppling criterion

orientation dependent										
Slope sec.	Sliding for discontinuities and slopes				Toppling for discontinuities and slopes				Orientation dependent SSPC	Visual estimation
	J1	J2	J3	Slope	J1	J2	J3	Slope		
1	>95%	>95%	<5%	<5%	100%	100%	100%	100%	<5%	class 3
2	100%	>95%	100%	>95%	80%	100%	>95%	80%	80%	class 2
3	<5%	>95%	100%	<5%	100%	100%	100%	100%	<5%	class 2
4	>95%	>95%	>95%	>95%	100%	100%	100%	100%	>95%	class 1
5	<5%	>95%	100%	<5%	100%	100%	>95%	>95%	<5%	class 3
6	<5%	>95%	50%	<5%	100%	100%	100%	100%	<5%	class 2
7	>95%	100%	>95%	>95%	100%	25%	100%	25%	25%	class 1
8	<5%	>95%	100%	<5%	100%	<5%	100%	<5%	<5%	class 2
9	<5%	<5%	>95%	<5%	100%	100%	100%	100%	<5%	class 3
10	<5%	80%	100%	<5%	100%	100%	100%	100%	<5%	class 3
11	>95%	>95%	100%	>95%	100%	100%	<5%	<5%	<5%	class 2
12	80%	75%	100%	75%	100%	100%	85%	85%	75%	class 2
13	<5%	<5%	<5%	<5%	100%	100%	100%	100%	<5%	class 3
14	>95%	<5%	100%	<5%	100%	100%	<5%	<5%	<5%	class 3
15	<5%	<5%	<5%	<5%	100%	100%	100%	100%	<5%	class 2
16	<5%	>95%	>95%	<5%	100%	100%	100%	100%	<5%	class 2
17	>95%	>95%	<5%	<5%	100%	100%	100%	100%	<5%	class 2
18	100%	100%	100%	100%	>95%	<5%	>95%	<5%	<5%	class 1
19	>95%	<5%	100%	<5%	100%	100%	<5%	<5%	<5%	class 3
20	>95%	<5%	<5%	<5%	100%	100%	100%	100%	<5%	class 3
21	50%	100%	100%	50%	100%	100%	>95%	>95%	50%	class 3
22	8%	>95%	100%	8%	100%	100%	60%	60%	8%	class 2
23	>95%	100%	60%	60%	100%	15%	100%	15%	15 %	class 2
24	100%	>95%	>95%	>95%	75%	100%	100%	75%	75%	class 1
25	>95%	100%	<5%	<5%	100%	100%	100%	100%	<5%	class 2
26	>95%	100%	100%	>95%	100%	100%	40%	40%	40%	class 2
27	>95%	>95%	<5%	<5%	100%	100%	100%	100%	<5%	class 2
28	>95%	>95%	<5%	<5%	100%	100%	100%	100%	<5%	class 2
29	>95%	>95%	<5%	<5%	100%	100%	100%	100%	<5%	class 3
30	10%	>95%	<5%	<5%	100%	100%	100%	100%	<5%	class 2
31	100%	>95%	<5%	<5%	>95%	100%	100%	100%	<5%	class 3
32	>95%	>95%	<5%	<5%	100%	100%	100%	100%	<5%	class 3
33	75%	>95%	<5%	<5%	100%	100%	100%	100%	<5%	class 3
34	>95%	>95%	<5%	<5%	100%	100%	100%	100%	<5%	class 2
35	<5%	100%	>95%	<5%	100%	80%	100%	80%	<5%	class 1
36	10%	>95%	>95%	10%	100%	100%	100%	100%	10%	class 1
37	100%	>95%	>95%	<95%	>95%	100%	100%	>95%	>95%	class 1
38	<5%	100%	100%	<5%	100%	>95%	<5%	<5%	<5%	class 2
39	10%	100%	<5%	<5%	100%	>95%	100%	>95%	<5%	class 2
40	<5%	50%	100%	<5%	100%	100%	20%	20%	<5%	class 1

41	100%	<5%	100%	<5%	25%	100%	>95%	25%	<5%	class 2
42	100%	100%	65%	65%	>95%	>95%	100%	>95%	65%	class 3
43	<5%	100%	65%	<5%	100%	100%	100%	100%	<5%	class 2
44	>95%	80%	>95%	80%	100%	100%	100%	100%	80%	class 1
45	100%	>95%	<5%	<5%	15%	100%	100%	15%	<5%	class 2
46	20%	>95%	>95%	20%	100%	100%	100%	100%	20%	class 3
47	100%	75%	>95%	75%	>95%	100%	100%	>95%	75%	class 2
48	100%	75%	100%	75%	>95%	100%	>95%	>95%	75%	class 1
49	100%	<5%	>95%	<5%	>95%	100%	100%	>95%	<5%	class 1
50	<5%	>95%	>95%	<5%	100%	100%	100%	<5%	<5%	class 2
51	<5%	100%	>95%	<5%	100%	>95%	100%	<5%	<5%	class 2
52	<5%	100%	>95%	<5%	100%	10%	100%	10%	<5%	class 3
53	100%	>95%	100%	>95%	>95%	100%	55%	55%	55%	class 1
54	100%	100%	75%	75%	15%	100%	100%	15%	15%	class 2
55	50%	50%	>95%	50%	100%	100%	100%	100%	50%	class 2
56	<5%	>95%	>95%	<5%	100%	100%	100%	100%	<5%	class 3
57	<5%	<5%	85%	<5%	100%	100%	100%	100%	<5%	class 3
58	<5%	>95%	>95%	<5%	100%	100%	100%	100%	<5%	class 2
59	100%	>95%	<5%	<5%	>95%	100%	100%	>95%	<5%	class 3
60	<5%	100%	<5%	<5%	100%	>95%	100%	>95%	<5%	class 3
61	30%	85%	10%	10%	100%	100%	100%	100%	10%	class 1
62	100%	>95%	100%	>95%	85%	100%	8%	8%	8%	class 3
63	100%	<5%	>95%	<5%	10%	100%	100%	10%	10%	class 1
64	10%	100%	55%	10%	100%	>95%	100%	>95%	10%	class 1
65	100%	<5%	>95%	<5%	>95%	100%	100%	>95%	<5%	class 2
66	25%	>95%	75%	25%	100%	100%	100%	100%	25%	class 3
67	100%	>95%	100%	>95%	<5%	100%	>95%	<5%	<5%	class 2
68	100%	100%	>95%	>95%	<5%	<5%	100%	<5%	<5%	class 3
69	100%	70%	100%	70%	>95%	100%	50%	>95%	70%	class 2
70	>95%	65%	>95%	65%	100%	100%	100%	100%	70%	class 2
71	>95%	100%	>95%	>95%	100%	>95%	100%	>95%	>95%	class 2
72	>95%	>95%	85%	85%	100%	100%	100%	100%	85%	class 2
73	100%	>95%	>95%	>95%	100%	100%	100%	100%	>95%	class 2
74	45%	100%	>95%	45%	100%	100%	100%	100%	45%	class 1
75	>95%	80%	>95%	80%	100%	100%	100%	100%	80%	class 2
76	>95%	>95%	>95%	>95%	100%	100%	100%	100%	>95%	class 2
77	>95%	>95%	<5%	<5%	100%	100%	100%	100%	<5%	class 3
78	100%	100%	<5%	<5%	>95%	<5%	100%	<5%	<5%	class 3
79	100%	100%	>95%	>95%	100%	100%	100%	100%	>95%	class 2
80	80%	100%	100%	80%	100%	>95%	100%	>95%	80%	class 3
81	>95%	100%	>95%	>95%	100%	>95%	100%	>95%	>95%	class 2
82	100%	100%	100%	100%	100%	100%	100%	100%	100%	class 3
83	100%	>95%	>95%	>95%	>95%	100%	100%	>95%	>95%	class 2
84	100%	>95%	100%	>95%	100%	100%	75%	75%	75%	class 2
85	<5%	100%	100%	<5%	100%	>95%	100%	>95%	<5%	class 3
86	100%	100%	>95%	>95%	10%	>95%	100%	10%	10%	class 3
87	100%	<5%	>95%	<5%	>95%	100%	100%	>95%	<5%	class 1
88	100%	<5%	>95%	<5%	>95%	100%	100%	>95%	<5%	class 1

89	>95%	20%	>95%	20%	100%	100%	100%	100%	<5%	class 2
90	100%	70%	60%	60%	>95%	100%	100%	>95%	60%	class 1
91	>95%	75%	>95%	75%	100%	100%	100%	100%	50%	class 2
92	<5%	100%	<5%	<5%	100%	>95%	100%	>95%	<5%	class 3

8.9 Geographic coordinates of rock slopes sections

Slope face	Coordination		Slope face	Coordination	
	Northing	Easting		Northing	Easting
1	10°04’12.2”	038°59’49.2”	47	10°04’06.2”	038°59’28.4”
2	10°04’10.7”	038°59’49.1”	48	10°04’04.7”	038°59’25.9”
3	10°04’8.8”	038°59’49.4”	49	10°04’02.9”	038°59’24.5”
4	10°04’06.8”	038°59’49.6”	50	10°04’01.9”	038°59’23.4”
5	10°04’04.6”	038°59’50.2”	51	10°04’00.5”	038°59’22.1”
6	10°04’02.8”	038°59’50.4”	52	10°03’58.8”	038°59’22.0”
7	10°04’00.6”	038°59’50.9”	53	10°03’56.6”	038°59’20.3”
8	10°03’58.1”	038°59’52.4”	54	10°03’55.2”	038°59’10.1”
9	10°03’56.4”	038°59’55.8”	55	10°03’54.8”	038°59’06.5”
10	10°03’55”	038°59’58.1”	56	10°03’54.3”	038°59’00.8”
11	10°03’53.8”	038°59’58.3”	57	10°03’59”	038°58’53.3”
12	10°03’51.4”	039°00’00.8”	58	10°03’58.6”	038°58’41.2”
13	10°03’51.3”	039°00'03.0”	59	10°03’58.7”	038°58’40.1”
14	10°03’51.6”	039°00’05.2”	60	10°03’59”	038°58’38.9”
15	10°03’50.2”	039°00’11.0”	61	10°03’59.6”	038°58’37.7”
16	10°03’52.8”	039°00’17.4”	62	10°03’59.8”	038°58’36.7”
17	10°03’51.9”	039°00’21.8”	63	10°04’00.1”	038°58’35.9”
18	10°03’45.3”	039°00’26.7”	64	10°04’00.4”	038°58’34.6”
19	10°03’44.2”	039°00’32.5”	65	10°04’08.25”	038°58’27.32”
20	10°03’44.0”	039°00’35.4”	66	10°04’18.2”	038°58’09.3”
21	10°03’44.1”	039°00’39.6”	67	10°04’17.1”	038°58’06.5”
22	10°03’43.9”	039°00’42.5”	68	10°04’16.6”	038°58’04.1”
23	10°03’41.1”	039°00’47.4”	69	10°04’16.5”	038°58’02”
24	10°03’38.3”	039°00’51.1”	70	10°04’17.0”	038°58’00.7”
25	10°04’13.1”	038°59’48.5”	71	10°03’28.0”	038°59’20.8”
26	10°04’13.9”	038°59’47.4”	72	10°03’27.9”	038°59’20.0”
27	10°04’14.2”	038°59’46.3”	73	10°03’26”	038°59’13.5”
28	10°04’14.5”	038°59’45.1”	74	10°03’24.5”	038°59’13”
29	10°04’14.9”	038°59’43.9”	75	10°03’21.5”	038°59’09.9”
30	10°04’15.9”	038°59’42.7”	76	10°03’20.8”	038°59’20.8”
31	10°04’16.8”	038°59’41.3”	77	10°03’21.6”	038°59’44.9”
32	10°04’17.9”	038°59’40”	78	10°03’14.3”	038°59’57.3”
33	10°04’18.6”	038°59’38.8”	79	10°03’22.0”	039°00’25.0”

34	10°04’19.2”	038°59’37.6”	80	10°03’21.3”	039°00’32.4”
35	10°04’19.8”	038°59’36.6”	81	10°03’19.8”	039°00’31.9”
36	10°04’20.5”	038°59’35.7”	82	10°03’19.3”	039°00’31.3”
37	10°04’20.8”	038°59’34.5”	83	10°03’18.8”	039°00’32”
38	10°04’19.8”	038°59’33.7”	84	10°03’18.9”	039°00’31.4”
39	10°04’18.6”	038°59’33.4”	85	10°03’18.5”	039°00’31.9”
40	10°04’17.5”	038°59’33.3”	86	10°03’18.1”	039°00’32.8”
41	10°04’16.4”	038°59’32.5”	87	10°02’54.4”	038°59’35.4”
42	10°04’13.3”	038°59’32.2”	88	10°02’43.3”	038°59’30.1”
43	10°04’11.9”	038°59’32”	89	10°02’51.0”	038°59’15.5”
44	10°04’10.3”	038°59’31.4”	90	10°02’48.3”	038°59’15.6”
45	10°04’08.5”	038°59’30.5”	91	10°03’00.7”	038°59’08.7”
46	10°04’07.3”	038°59’29.8”	92	10°03’49.1”	039°00’07.3”